



Cite this: *Mol. Syst. Des. Eng.*, 2023, **8**, 1097

# Stimuli-responsive structure–property switchable polymer materials

Zhuang Mao Png,<sup>a</sup> Chen-Gang Wang,<sup>†a</sup> Jayven Chee Chuan Yeo,<sup>bc</sup> Johnathan Joo Cheng Lee,<sup>b</sup> Nayli Erdeanna Surat'man,<sup>a</sup> Yee Lin Tan,<sup>bd</sup> Hongfei Liu,<sup>b</sup> Pei Wang,<sup>b</sup> Beng Hoon Tan,<sup>b</sup> Jian Wei Xu,<sup>id\*abc</sup> Xian Jun Loh<sup>id\*ab</sup> and Qiang Zhu<sup>id\*abe</sup>

The development of polymeric materials with switchable properties upon exposure to external stimuli such as light, heat, force, acids/bases, and chemicals has attracted much attention due to their potential applications in smart coatings, drug carriers, soft robotics, etc. Thus, a systematic understanding of the relationship between the chemical structures and stimuli-responsive properties as well as the corresponding mechanisms of switchable stimuli-responsive polymers is important to guide the sophisticated design of functional macromolecules for specific applications. In this review, we outline the representative chemical structures that enable reversible structural switching to be achieved under photo-, mechano-, CO<sub>2</sub>- and chemo-stimuli, with a brief discussion on thermo- and pH-activation. Polymer materials containing these chemical moieties exhibit unique behaviours on changing their mechanical, thermal or photochemical property in a switchable manner, and their applications in healing materials, rewritable surfaces, drug delivery carriers, conductive hydrogels and luminescent materials are highlighted. Based on the comprehensive summary of structural switchable moieties and applications of polymer materials, this review gives insight into how bottom-up approaches can be used to inspire the future design of switchable multi-stimuli-responsive polymer materials.

Received 6th January 2023,  
Accepted 20th March 2023

DOI: 10.1039/d3me00002h

rsc.li/molecular-engineering

## Design, System, Application

Stimuli-responsive polymers are promising materials whose properties can be controllably and predictably changed by external stimuli and have a wide range of applications including molecular sensing, drug carriers, coatings, artificial muscles, and thermoelectric materials. At the heart of these materials are the moieties that alter their chemical structure in response to an external stimuli, resulting in a change in macroscopic properties such as colour, morphology, and phase transition temperature. This review covers the design of polymers responsive to six different stimuli (light, pH, thermal, force, CO<sub>2</sub>, and redox), with a section regarding polymers responsive to multiple stimuli also included. This review is structured according to the key enabling functional groups and discusses tuning of the properties of polymers by changes in their position or chemical structure. We believe that this class of polymers will see greater utilization with the maturity of this field, with a more extensive library of stimuli-responsive moieties.

## 1 Introduction

In the past two decades, major efforts have been devoted to creating on-demand stimuli-responsive materials to mimic natural systems.<sup>1–4</sup> Stimuli-responsive polymers are a class of promising “smart” materials that are capable of altering their properties when triggered by external stimuli in a controllable manner.<sup>1,5–8</sup> Depending on the polymer structure, the triggering stimuli can be physical (temperature, light, mechanical force, magnetic field, electric interaction, etc.), chemical (pH, redox, molecules, supramolecular interaction, etc.) or biological (enzyme, etc.). Due to their versatile stimuli-responsive functions and cost-effective preparation, smart polymer materials, such as nanoparticles, films and hydrogels, are attracting great interest for extensive

<sup>a</sup> Institute of Sustainability for Chemicals, Energy and Environment (ISCE2), Agency for Science, Technology and Research (A\*STAR), 2 Fusionopolis Way, Innovis #08-03, 138634, Singapore

<sup>b</sup> Institute of Materials Research and Engineering, Agency for Science, Technology and Research (A\*STAR), 2 Fusionopolis Way, Innovis #08-03, 138634, Singapore. E-mail: zhuq@imre.a-star.edu.sg

<sup>c</sup> Department of Chemistry, National University of Singapore, 3 Science Drive 3, 117543, Singapore

<sup>d</sup> Department of Materials, Imperial College London, Royal School of Mines, Exhibition Road, London, SW7 2AZ, UK

<sup>e</sup> School of Chemistry, Chemical Engineering and Biotechnology, Nanyang Technological University, 21 Nanyang Link, 637371, Singapore

<sup>†</sup> These authors contributed equally.



applications such as drug carriers, coatings, molecular sensing, artificial muscles, and thermoelectric materials.<sup>9–14</sup>

Among the stimuli-responsive polymers, reversibly switchable smart polymer materials and surfaces can achieve reversible “on–off” switching to tune their structures and properties several times.<sup>9,15,16</sup> In nature, several creatures, *e.g.*, cuttlefish, chameleon and gray treefrog, are masters at reversibly changing their appearance such as colour and pattern in response to their surrounding environment.<sup>17–19</sup> These reversible transformation features can be attributed to pigment translocation or molecular switch in their chromatophores, allowing them to mimic their background environments. Additionally, biopolymers such as proteins and nucleic acids extensively exist in living organic systems and undergo conformational changes to modulate and maintain physiological parameters. Consequently, these stimuli-responsive creatures and biomacromolecules have inspired scientists to develop various synthetic polymeric materials to mimic their adaptive behaviours.<sup>20–22</sup>

Although pigment translocation still lacks applications in materials science, molecular switching is a promising and effective approach to endow materials with switchable physical and chemical properties. Many reversibly switchable molecules, such as photochromic molecules, host–guest molecule pairs, and mechanically interlocked molecules, have been developed and found many applications.<sup>23–28</sup> In recent years, design at the molecular level by exploiting reversibly switchable molecules has enabled the synthesis of functional monomers, and then polymers to produce novel polymeric materials with unique stimuli-responsive behaviors.<sup>9,10,16</sup> Many applications of reversibly switchable polymers have been found to control the appearance of materials or serve as a release system.

Herein, we attempt to summarize the numerous stimuli-responsive building units and how they alter their conformation or geometry reversibly in a polymer chain, and subsequently used to construct switchable polymer materials with stimuli-responsive functional groups and their reversibly conformational or geometric changes in a polymer chain to construct smart materials with switchable properties. Beyond the well-studied reversible phase transition behaviors *via* intermolecular hydrophobic interactions (*e.g.*, lower critical solution temperature (LCST) and upper critical solution temperature (UCST)) or supramolecular interactions, polymers with reversibly switchable chemical structures through isomerization, cyclization, ionization and bond cleavage are highlighted. Furthermore, structure-switchable functional groups triggered by various stimuli, including photo, mechanical, carbon dioxide (CO<sub>2</sub>) and redox, are catalogued to express their structure transformation mechanisms, while thermal- and acidic/basic (pH)-responsive polymers will be briefly discussed. Subsequently, polymeric materials containing switchable functional groups are introduced to demonstrate their state-of-the-art applications and structure–property relationships. Examples of the combination of different stimuli-responsive functional groups to develop dual- or multiple-stimuli-responsive polymeric materials and surfaces

are also introduced. Finally, we address the remaining challenges and outlook for the future development of reversibly switchable smart polymeric materials.

## 2 Polymers with switchable structures and their applications

### 2.1 Photo-responsive polymers

As representative polymers,<sup>29,30</sup> photo-responsive polymers are polymers that can respond to light, leading to a reversible change in either their conformation or chemical structure. They have a variety of potential applications ranging from drug delivery to actuators and self-healing materials. Some of the key photo-responsive chemical structures include azobenzene, diarylethenes, spiropyrans and disulfides. These moieties impart different photo-responsive properties to polymers. For instance, *cis–trans* isomerism can modulate the crystallinity and glass transition temperature ( $T_g$ ) of polymers. Meanwhile, diarylethenes and spiropyrans can change their colour and fluorescence. In this section, we review photo-responsive polymers with emphasis on how changes in their chemical structure modulate their properties.

**2.1.1 Azobenzene.** The most common light-responsive moiety is azobenzene. Its *cis* isomer and photo-induced conversion were reported in 1937,<sup>31</sup> and subsequently extensive research has focused on its properties and applications.<sup>32</sup> *Trans* azobenzene, the thermally favoured isomer, is converted to *cis* azobenzene upon exposure to UV irradiation, while the reverse can be mediated by exposure to either visible light or thermally in the dark (Fig. 1a).<sup>33</sup> It has been found that this process is highly sensitive, and both its rate and quantum yield can be influenced by the solvent, temperature, substituents on the phenyl ring, and irradiation wavelength. As many as four different mechanisms have been postulated (rotation, inversion, concerted inversion, and inversion-assisted rotation), with multiple pathways being used to explain empirical observations.<sup>34</sup> More recently, progress has also been made in achieving *trans* to *cis* conversion *via* visible light irradiation, either by direct functionalisation of the azobenzene ring,<sup>35,36</sup> extended conjugation,<sup>37</sup> or photo upconversion strategies.<sup>38</sup> This has enabled photo isomerism to be achieved without exposure to harmful UV rays, which is particularly important in the case of biological applications. Azobenzene and its derivatives are also often used because they are stable and do not exhibit significant side reactions.<sup>39</sup> Some of the azo-benzene containing polymers are shown in Fig. 1b.

The *cis–trans* transition of azobenzene has been used to modulate the fluorescence of polymers. Kuehne's group reported the preparation of a series of light-modulated monodisperse conjugated polymer particles.<sup>40</sup> Azobenzene was conjugated with fluorene *via* Suzuki–Miyaura polymerisation and grafted on a poly(vinylpyrrolidone-*co*-vinyl acetate) (PVPVA) nucleus (**P2a–c**). In the case of **P2a**, given that the *trans* to *cis* switching occurs along the polymer backbone, large-scale motion is required. In contrast, for



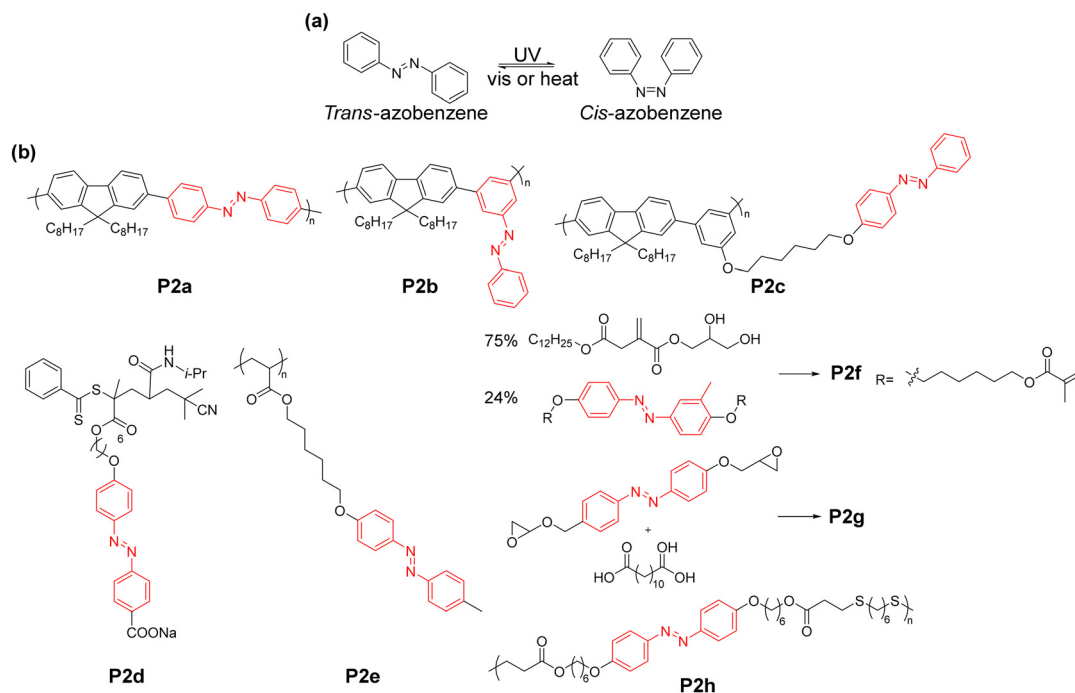


Fig. 1 (a) *Cis* and *trans* isomers of azobenzene. (b) Examples of polymers containing azobenzene units.

both **P2b** and **P2c**, the *trans* to *cis* switching only resulted in movement of their side chain, while **P2c** is completely non-conjugated with the polymer backbone as the azobenzene moiety is separated from the polymer backbone by the alkyl chain. Upon exposure to UV, the fluorescence of all three polymers shifted from about 450 nm to 600 nm (Fig. 2a). This was attributed to the non-radiative decay in the *trans*-configuration, which is significantly reduced in the *cis*-configuration, although the mechanism was not fully understood.<sup>41</sup> The fluorescence switching was significantly slower for **P2a** compared to **P2b** and **P2c** because the entire polymer backbone needed to move, which is due to the fact that the fluorescence switching of **P2a** is triggered by the conformation change of the entire **P2a** polymer backbone. Consequently, the *cis* to *trans* transition for **P2a** was not fully reversible. As another example, in the work by Ren and co-workers, they prepared an amphiphilic diblock copolymer, **P2d**.<sup>42</sup> The fluorescence of the polymer was sensitive towards pH, temperature and UV. In its neutral and basic conditions, the fluorescence of the polymer increased upon exposure to UV light, corresponding to the photo-isomerism of the azobenzene from *trans* to *cis*. Alternatively, under acidic conditions, only a slight increase in fluorescence was observed. This was due to the highly aggregated structure under acidic conditions, which inhibited the *trans* to *cis* photo-isomerism.

In principle, the *cis*–*trans* transition can lead to a change in the melting point of azobenzene and the glass transition temperature ( $T_g$ ) of polymers with azobenzene moieties. Although the melting points of the *cis* and *trans* isomers with unfunctionalized azobenzene only differed by 3 °C, (68 °C for

*trans* and 71 °C for *cis*),<sup>43</sup> polymers with azobenzene carrying long alkoxy chains can exhibit significantly higher differences

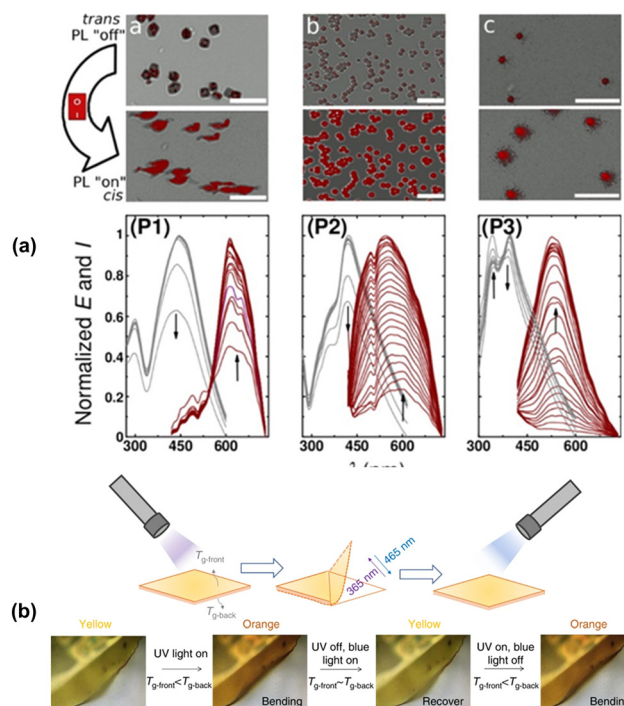


Fig. 2 (a) Photoluminescence (PL) of **P2a**–**c** upon exposure to UV light.<sup>40</sup> Reproduced from ref. 40 with permission from the American Chemical Society, Copyright 2013. (b) Actuation behavior of the acid-based azobenzene-containing epoxy polymer **P2f**.<sup>49</sup> Reproduced from ref. 49 with permission. Copyright 2018, Nature Publishing Group.



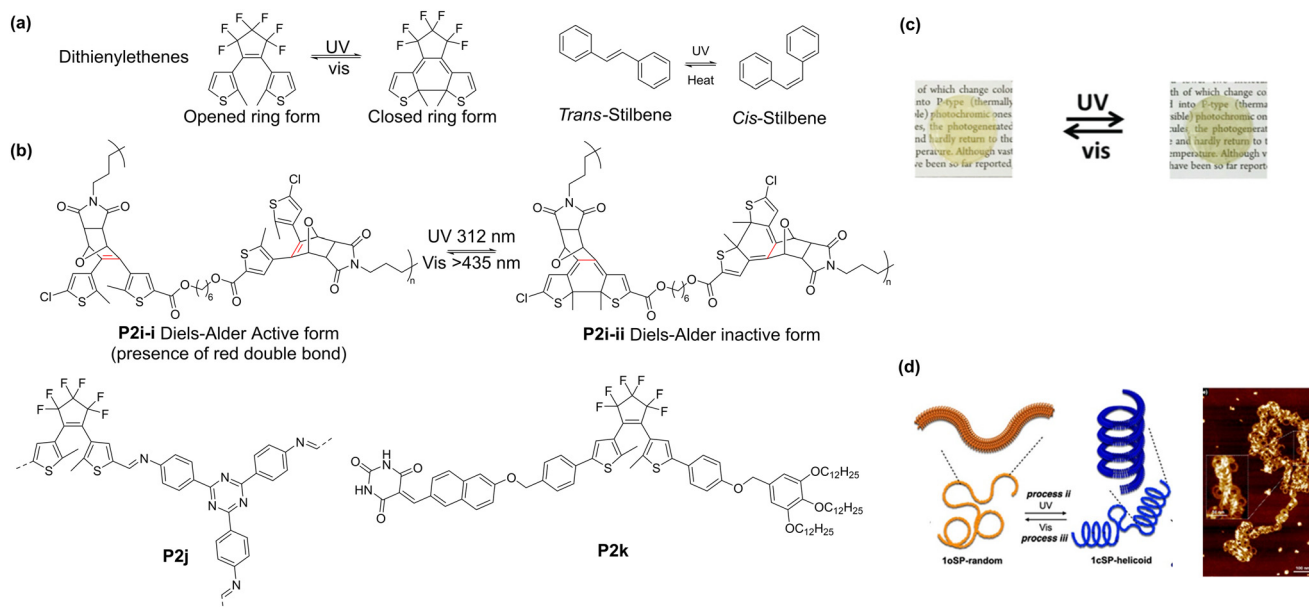
in melting point, with photo-induced liquefaction observable.<sup>44</sup> As early as the 1980s, the photo-responsive properties of azobenzene-containing polymers have been reported, and a change in viscosity upon irradiation was also noted upon exposure to UV light.<sup>45</sup> However, a change in  $T_g$  upon irradiation has only recently been reported.

Wu's group also reported the preparation of an azobenzene-containing polymer **P2e** via reversible addition-fragmentation chain-transfer (RAFT) polymerization.<sup>46</sup> **P2e** was a hard solid at room temperature with a  $T_g$  of about 48 °C. Upon exposure to UV light, the surface of the polymer liquefied despite remaining at a temperature of only 28.5 °C. The  $T_g$  of the generated *cis* isomer was measured to be around -10 °C. Upon illumination with 530 nm visible light, the liquid polymer turned back into a solid, corresponding to the *cis* to *trans* isomerism. These types of materials can possibly be useful for repairable coatings or photo-switchable adhesives. However, at present, the liquefaction of bulk materials is still difficult to achieve due to the limited penetration of UV light (molar absorptivity of azobenzene is about  $2.0 \times 10^4 \text{ mol}^{-1} \text{ L cm}^{-1}$  at 365 nm).<sup>47</sup> These polymers were also found to exhibit actuation properties, bending towards a UV light source, but returning to their original shape upon exposure to blue light.<sup>48</sup>

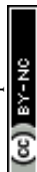
The *cis-trans* photo-isomerism of azobenzene can also produce mechanical responses. Koyama's group reported the preparation of a dodecyl glyceryl itaconate polymer crosslinked with a *meta*-methylazobenzene-containing moiety to form a liquid crystalline network, *i.e.*, **P2f**.<sup>49</sup> This polymer exhibited a  $T_g$  of 29 °C, which was reduced to 16 °C upon exposure to UV irradiation, with a corresponding decrease in

Young's modulus from 140 MPa to 65.6 MPa. However, exposure to visible light restored the  $T_g$  within 2–4 seconds, enabling efficient photomechanical actuation. Exposure to UV light (354 nm) resulted in film bending towards the light, while exposure to blue light (465 nm) restored its flatness (Fig. 2b). The light intensity was also correlated with the bending speed. The mechanism of this bending was postulated to be due to the differences in the degree of absorption of photons between the front surface of the polymer and the back surface, which resulted in a difference in  $T_g$  between the front and the back of the film, with the inner strain causing the bending. As another example, in the work by Zhao and Xia, they prepared dodecanedioic acid-based epoxy networks, **P2g**.<sup>50</sup> The networks were dynamic under high temperature in the presence of a catalyst, making them reprocessable and vitrimeric.<sup>51</sup> The UV-induced torque could drive a cylinder and a "vehicle", with no apparent degradation even after 100 rotations. Hayward's group also reported the preparation of an acrylate-thiol based polymer, **P2h**.<sup>52</sup> Actuation behaviour was observed upon illumination with UV light even at 25 °C, but was found to be reversible upon exposure to green light only at temperatures above 60 °C.

**2.1.2 Diarylethenes.** Photochromic diarylethenes (Fig. 3a), which were first reported in 1988,<sup>55</sup> are photochromic molecules that can undergo  $6\pi$ -electron cyclisation upon exposure to UV light and reversibly return to the initial opening isomer upon irradiation with visible light.<sup>56</sup> Unlike azobenzene, this transition is usually thermally irreversible. The 2-aryl position is often substituted to prevent oxidative aromatisation. This transition often leads to significantly



**Fig. 3** (a) Light-mediated ring opening and closing of diarylethenes and *cis-trans* isomerism of stilbene. (b) Examples of diarylethene-containing polymers. (c) Photochromic properties of **P2j** in PMMA matrix. Yellow (left image): ring-opened form. Green (right image): ring-closed form.<sup>53</sup> Reproduced from ref. 53 with permission from The Royal Society of Chemistry, Copyright 2019. (d) Helical folding obtained by post-polymerization irradiation of **P2k**.<sup>54</sup> Reproduced from ref. 54 with permission. Copyright 2021, the American Chemical Society.



different frontier molecular orbital levels, resulting in a change in colour, fluorescence, and even electrical conductivity and electroluminescence in the case of conjugated polymers with such diarylethene units.<sup>57</sup> Therefore, they have received significant attention in photo-tunable optoelectronics. Hetero-aryl groups, such as dithienylethenes, are also often used in place of phenyl rings to improve the stability of the closed ring form.<sup>58</sup>

The thermal stability of diarylethenes was used to control the reversibility of the Diels–Alder reaction in an adhesive material.<sup>59</sup> Polymer **P2i** (Fig. 3b), was prepared by Diels–Alder reaction between the furan and the maleimide groups, forming a dithienylethene moiety. The Diels–Alder reaction was reversible by heating the polymer to 90 °C, resulting in a decrease in adhesion strength. However, upon exposure to 312 nm UV light, 6 $\pi$ -electron cyclisation occurring, resulting in the disappearance of the double bond of the diarylethene and preventing the occurrence of the reverse Diels–Alder reaction. Consequently, even when the polymer was heated to 90 °C, the adhesion strength did not decrease. This also demonstrated the thermal stability of the closed-ring configuration. Upon exposure to visible light (>435 nm), the reverse open-ring reaction occurred, allowing the reverse Diels–Alder reaction to proceed when heated.

Another application of photochromic diarylethenes is in photochromic films. Gu's group prepared an dithienyl-containing polyimine as a conjugated polymer network (**P2j**).<sup>53</sup> The yellow polymer solid turned olive green upon exposure to UV light (365 nm) for 50 s, which was reversed by exposure to visible light (>500 nm) in about the same time. This is relatively fast compared to other polymers, which require more than 2 min to undergo the same change. Upon repeated cycling, a small amount of weight loss was observed (~5%), but the overall physical structure of the polymer film was found to be stable. The composite films prepared by dispersing **P2j** in a PMMA matrix were found to undergo the same transition as the neat polymer (Fig. 3c). Another example of photochromic polymers was demonstrated by Bianco's group.<sup>60</sup> Six different variations of diarylethenes were prepared to examine the effect of functionality, and combined with dicyclohexylmethane 4,4'-diisocyanate to form polyurethanes. Interestingly, a linear relationship was observed between the molar extinction coefficient and the peak wavelength of the closed-ring form. Recently, Yagai's group also demonstrated the potential of diarylethene to control the folding of polymers<sup>54</sup> by making use of the difference in  $\pi$ - $\pi$  stacking between the ring-closed and ring-opened form of diarylethene. Supramolecular polymers of **P2k** were prepared by cooling hot methylcyclohexane solution to obtain randomly coiled polymers. However, polymer **P2k** adopted a helical structure, as evidenced by the AFM imaging when the polymer was irradiated with UV light (293 nm), while upon cooling, AFM imaging showed that helical structures were adopted (Fig. 3d). In contrast, the polymer preferred a random supramolecular structure when exposed to visible light (620–645 nm).

Stilbenes are another class of diarylethenes that exhibit photo-responsiveness (Fig. 3a), though their mechanism differs from that of dithienylethenes given that they undergo *trans* to *cis* photo-isomerism similar to azobenzene. One example of this is in Harada's work, where they installed stilbene into a “daisy chain” crosslink.<sup>61</sup> The *trans* to *cis* transition resulted in a significant change in polymer length, allowing for muscle-like contraction and expansion of the polymer, mediated by selective photoirradiation.

**2.1.3 Spiropyran.** Photochromic spiropyrans, which were first reported by Fischer and Hirshberg in 1953,<sup>62</sup> can cleave their C–O bond upon irradiation with UV to form a ring-opened merocyanine form (Fig. 4a).<sup>63</sup> Besides a change in colour, this reversible transition upon exposure to visible light also results in a change in dipole, polarity, and even molecular volume.<sup>64</sup> There is no conjugation between the two halves of the spiral given that they are orthogonal to each other. Consequently, the spiropyran form is neutral, non-polar and can absorb light typically in the UV region. Meanwhile, the merocyanine form is conjugated and has a significant dipole moment, which can be changed in

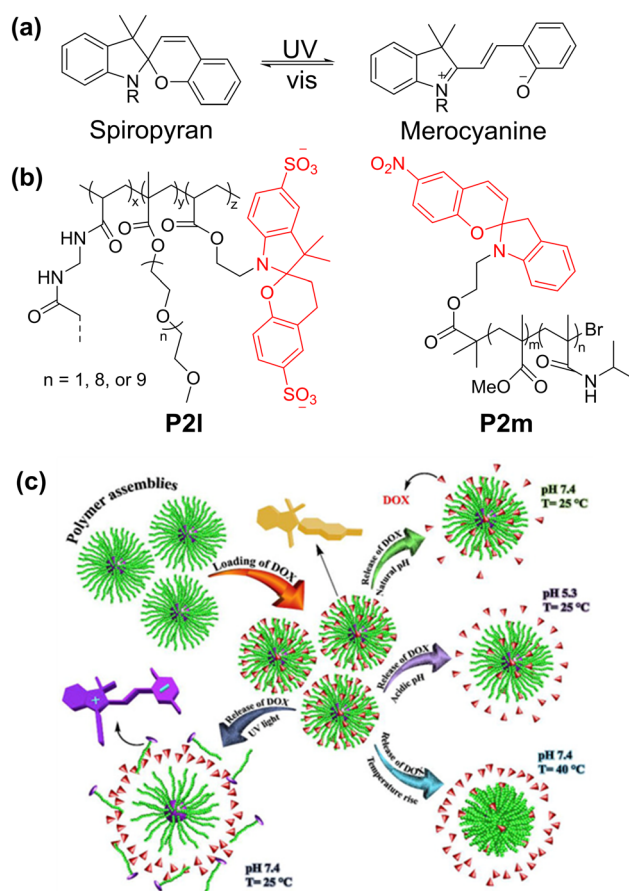


Fig. 4 (a) Light-driven conversion between spiropyran and merocyanine forms. (b) Light-responsive spiropyran-containing polymers. (c) Effect of pH, UV and elevated temperature on release of doxorubicin from polymer **P2k** micelles.<sup>70</sup> Reproduced from ref. 70 with permission. Copyright 2020, Elsevier.



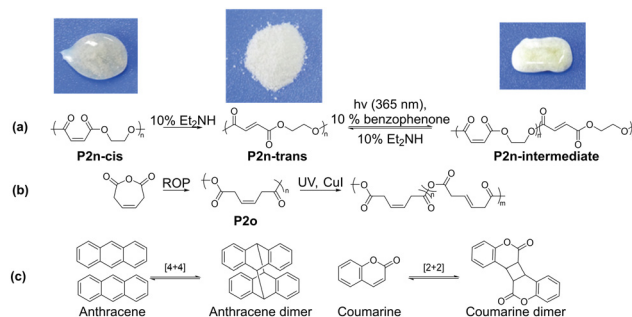
response to pH. This merocyanine form is typically strongly coloured and can absorb light in the visible region.<sup>65</sup> In addition, spiropyrans can also be responsive to redox and temperature changes depending on whether they contain any specific functionality.<sup>66</sup>

Exploiting the difference in molecular volume and charge between the two forms of spiropyran, the light-driven expansion of hydrogels has been explored by Stupp's group.<sup>67</sup> Sulfonate groups were included in spiropyran to increase its water solubility, while the methacrylate group was added to enable free radical polymerization. Subsequently, the spiropyran methacrylate was co-polymerized with oligo(ethylene glycol) methyl ether methacrylate and *N,N'*-methylenebis(acrylamide) as a crosslinker to form **P2I** (Fig. 4b). When irradiated with light, the charge density of the polymer increased, allowing water to enter the polymer network, and then swelled up to 30%. Other examples of spiropyran-based hydrogels demonstrating actuation include the work of Sumaru<sup>68</sup> and Florea.<sup>69</sup>

Spiropyrans have also been explored in drug delivery systems. For instance, Salami-Kalajahi and Roghani-Mamaqani's group prepared a poly(methyl methacrylate)-*b*-poly(*N*-isopropylacrylamide) block copolymer with spiropyran as the end group (**P2m**).<sup>70</sup> Doxorubicin (DOX, a chemotherapy drug) was loaded in the self-assembled **P2m**, and its release was examined under different pH values and UV irradiation. Less than 30% doxorubicin release was observed in neutral conditions, while 60–85% of DOX was found to be released in acidic and elevated temperature conditions (Fig. 4c). Alternatively, under UV irradiation, DOX release was found to be the fastest, with almost 100% release after 2 days, demonstrating the potential of light control for drug release. However, in this case, UV light as the trigger is suboptimal due to its lack of penetrative power, cytotoxicity and mutagenic effects on cells. A more elegant solution is the use of NIR up-conversion to provide stimuli for the ring opening. Some efforts have been reported making use of lanthanides nanoparticles to facilitate the up-conversion.<sup>71,72</sup>

**2.1.4 C=C *cis-trans* photo-isomerisation.** Stereochemical control of polymers is a well-established approach towards controlling their properties. For instance, Hirabayashi prepared a succinic anhydride–propylene oxide polymer comprising predominantly *Z* isomer.<sup>73</sup> When isomerised into the *E* form in the presence of morpholine, the polymer exhibited higher crystallinity, higher bio-degradability and higher *T<sub>g</sub>*. However, unlike the well-documented *cis-trans* photo-isomerism of azobenzene, the corresponding *cis-trans* photo isomerism in C=C bonds is much less common. In this area, the common synthetic approach is co-polymerization and cyclization.<sup>74–76</sup>

In 2019, Lu's group reported an example of *cis-trans* photo isomerism in polymers (Fig. 5).<sup>77</sup> Ethylene oxide and maleic anhydride were co-polymerized to form **P2n** predominantly in the amorphous *cis* form. Upon treatment with diethylamine, the double bond isomerised to the more thermodynamically stable *trans* form, which was crystalline



**Fig. 5** (a) Photo *cis-trans* isomerisation of polymers with corresponding modulation of their crystallinity.<sup>77</sup> (b) Ring-opening polymerisation to form **P2o**, which could be photo-isomerised into the *trans* form. (c) Photodimerisation of anthracene and coumarin moieties. Reproduced from ref. 77 with permission. Copyright 2019, John Wiley and Sons.

in nature. Subsequently, irradiation with UV light in the presence of benzophenone for 5 h resulted in about 30% conversion from the *trans* to *cis* isomer, accompanied by the corresponding loss of crystallinity. Another example in the same year is the work by Buchard's group.<sup>78</sup> Polycarbonate **P2o** was prepared by ring-opening polymerization to obtain the predominantly *cis* form. This was isomerised into the more thermodynamically stable *trans*-form (52% after 68 h) upon exposure to UV light at room temperature in the presence of CuI. The *trans* isomer was a viscoelastic solid, while the *cis* isomer was a powder, demonstrating a practical approach to changing the properties of polymers by exposure to UV light. However, unlike the other polymers discussed, this isomerism has not been reported to be reversible.

**2.1.5 Anthracene and coumarins.** Another mechanism of photo-responsive moieties is photodimerization such as that exhibited by anthracenes [4 + 4], and coumarins [2 + 2] (Fig. 5c). This mechanism is useful for controllable crosslinking of polymeric networks, such as in the work by Saito *et al.*,<sup>79</sup> where they made use of anthracene to reversibly crosslink epoxy networks, enabling light-mediated healability. He's group also achieved similar results using coumarin as a photocrosslinker.<sup>80</sup> Pleasingly, these photodimerization reactions can often be controlled by modulating the wavelength of the incident light, with longwave UV (~355 nm) promoting the dimerization, while shortwave UV (~265 nm) promotes bond cleavage.

**2.1.6 Disulfide linkage.** Disulfides bonds are known to undergo homolytic photocleavage to form sulfenyl radicals, which is commonly exploited in dynamic covalent networks. Kessler's group prepared an epoxy network comprising 4,4-diglycidylazobenzene, sebacic acid and 4,4-dithiodibutyric acid (**P2p**, Fig. 8).<sup>81</sup> The resultant polymer exhibited a smectic liquid crystalline structure. The number of disulfide bonds was limited to just 10% to prevent the polymer from being over-dynamic, which reduced the stability of the liquid crystalline phase. The azobenzene moiety imparted photo-induced shape memory and actuation properties, while the disulfide bonds enabled photo-induced



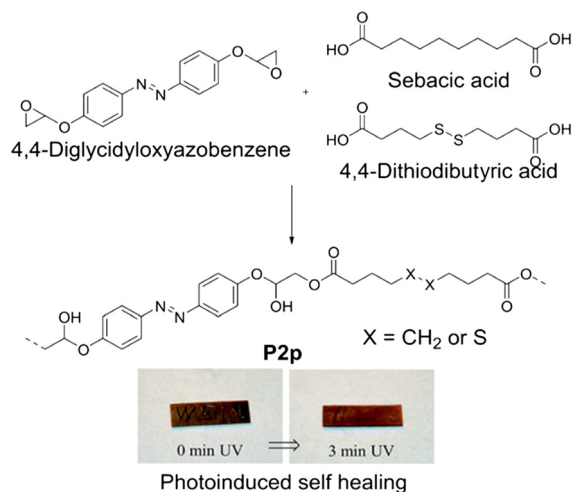


Fig. 6 Disulfide-mediated self-healing of P2m. Reproduced from ref. 81 with permission. Copyright 2017, The Royal Society of Chemistry.

self-healing within 3 min (Fig. 8). In another example reported by Gautrot, disulfide bonds were used as a crosslinker to prepare a hyaluronic acid-based hydrogel.<sup>82</sup> Similar to P2p, the polymer exhibited photo-induced self-healing, showing that the broken sample could be welded by adding a photo-initiator, followed by irradiation with UV light

for 2 min. Some weakening of the material was observed compared to the pristine sample although the polymer was strong enough to be handled without special precautions (Fig. 6).

## 2.2 Force-responsive structure

In recent years, there has been a growing interest in polymers that can transduce mechanical inputs into specific chemical transformations. The resultant chemical responses can be categorised as either scissile (*i.e.*, covalent bond-breaking reactions) or non-scissile (*i.e.*, non-covalent bond disruptions and conformational changes) transformations.<sup>83</sup> By tailoring the composition, types and positions of mechanophores (mechanically activated chemical groups) on the polymer chain, the mechanoresponsive behaviour of these materials can be programmed at a molecular level. In addition, the mechanochromic behaviour displayed by many mechanophores further highlights their potential to be used for the accurate detection of stress.<sup>84</sup> In this section, we elaborate on the force-induced structural transformations of different chemical structures, including pyran derivatives, supramolecular assemblies, and other emerging structures.

**2.2.1 Pyran derivatives.** Pyran derivatives, such as spiropyran and naphthopyran, are some of the most studied mechanophores. Through a 6-electron electrocyclic ring-

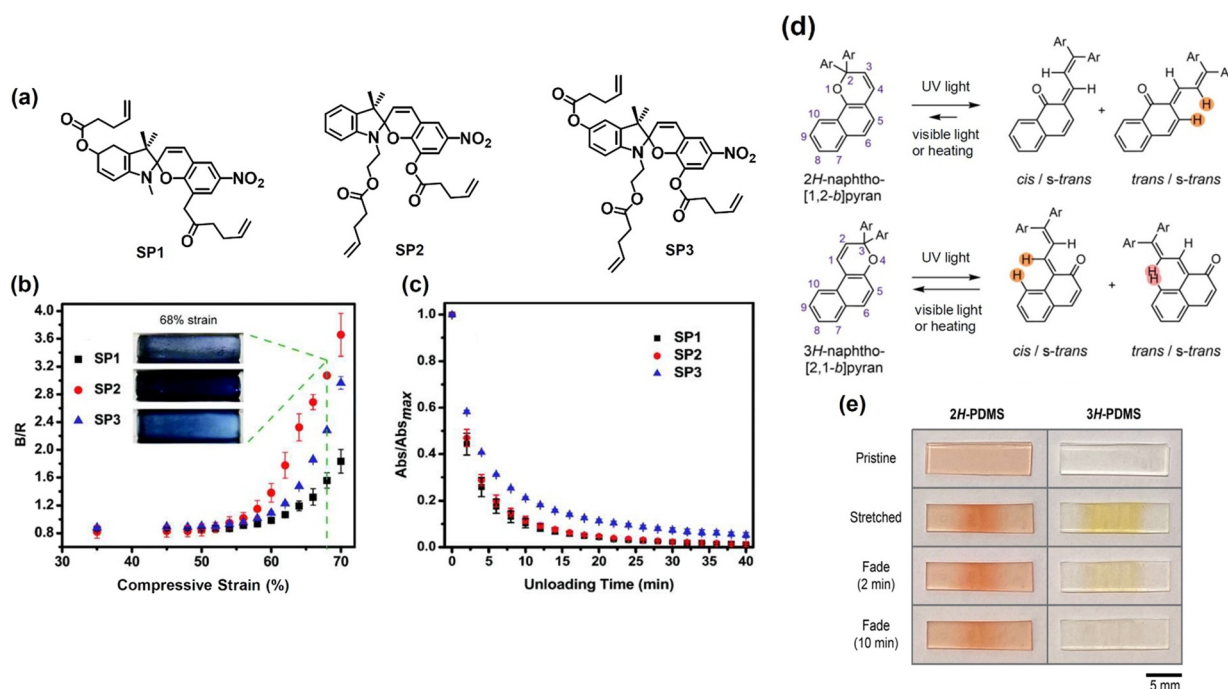
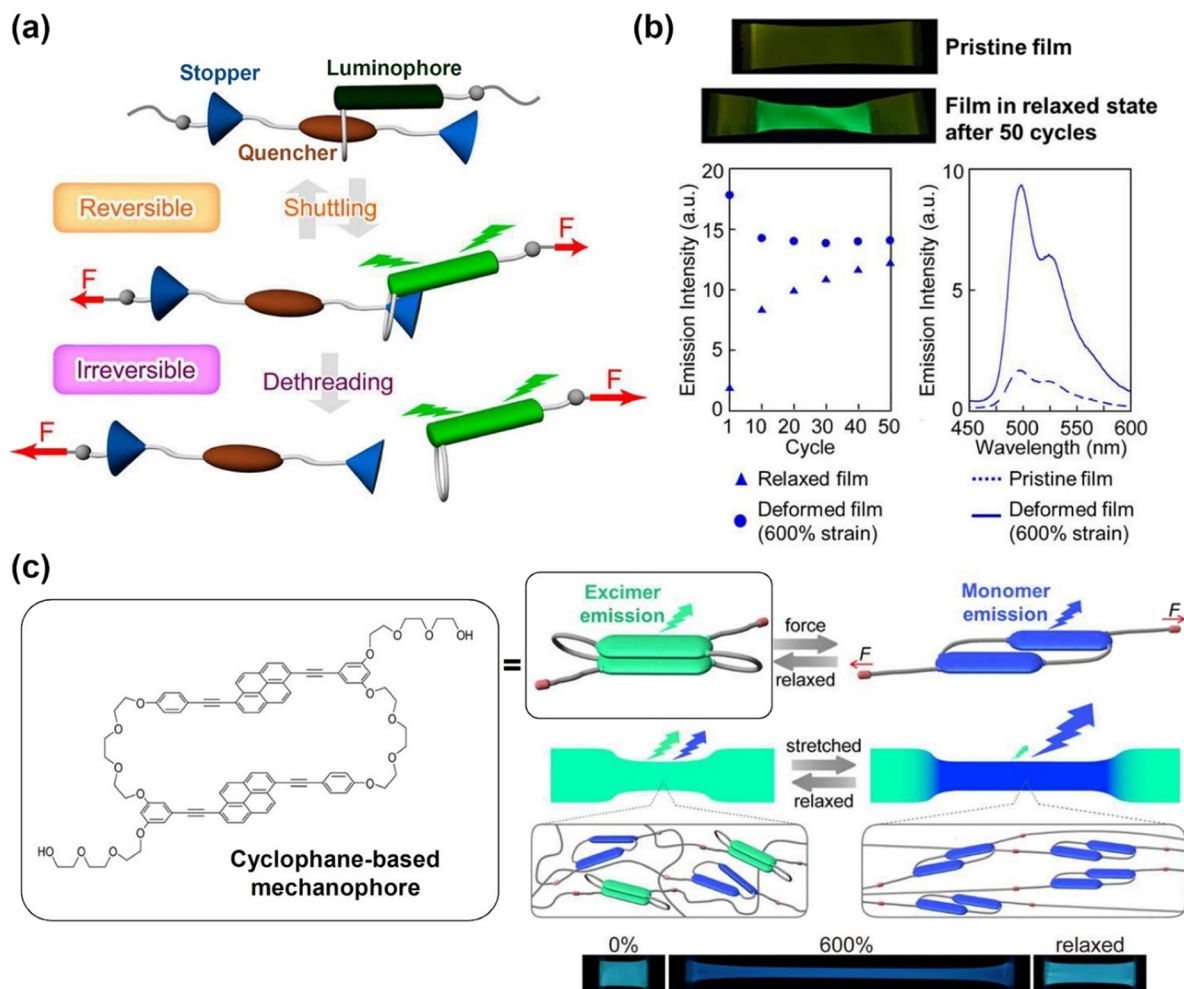


Fig. 7 (a) Chemical structures of the 6-nitro-spiropyran mechanophores with differing attachment points. (b) Graph of B/R (blue channel intensity/red channel intensity) as a function of compressive strain for the various spiropyran samples. Insets: Photographs of the spiropyran samples at 68% strain. (c) Graph of Abs/Abs<sub>max</sub> (absorption intensity/maximum absorption intensity) as a function of unloading time in darkness from 62% compressive strain for the spiropyran samples. (d) Ring-opening reaction of the 2H- and 3H-naphthopyrans, forming merocyanine isomers. (e) Photographs of the 2H- and 3H-naphthopyran PDMS films immediately after being in tension and after subsequent stress relaxation. (a)–(c) are reproduced from ref. 85 with permission. Copyright 2019, The Royal Society of Chemistry. (d) and (e) are reproduced from ref. 86 with permission. Copyright 2021, Wiley.





**Fig. 8** (a) Schematic diagram of the shuttling and dethreading function of rotaxane-based supramolecular mechanophores. (b) Photographs of the rotaxane-based pristine film and the fluorescent deformed film and plots of the emission intensity against cycle and wavelength for the films under the different conditions as specified. (c) Schematic illustration of the conformational changes in the cyclophane mechanophore leading to mechanochromic luminescence. Reproduced from ref. 94 and 95 with permission. Copyright 2021, the American Chemical Society.

opening reaction, the weak C–O bond in the pyran ring can be broken. This transforms the ring-closed pyrans to the ring-opened merocyanine, displaying mechanochromic behaviour in the process.<sup>87</sup> Depending on the combination of the polymer chain attachment points and the nature of the substituents, the threshold force required to induce this transformation can be altered.<sup>88</sup>

Qiu *et al.* fabricated 6-nitro-spiropyran mechanophores with different attachment points (Fig. 7a).<sup>85</sup> The threshold activations were found to occur at ~60% strain and 4–7 MPa stress (Fig. 7b). This activation resulted in the appearance of absorption peaks at 500–650 nm, corresponding to the formation of merocyanine. A rapid decrease in absorption strength was recorded as the unloading of compressive strain gradually increased from 62%, showing that the polymers possessed a reversible mechanochromic response (Fig. 7c). Although both electronic and geometric effects influenced the mechanochromic behaviour of the mechanophores, the latter was found to be the dominant factor. Osler and co-workers investigated the mechanochemical reactivity of isomeric 2*H*-

and 3*H*-naphthopyran mechanophores using solution-phase ultrasonication experiments and in crosslinked polydimethylsiloxane (PDMS) elastomers (Fig. 7d).<sup>89</sup> The ring-opening reaction of the 2*H*-naphthopyran substrate was found to produce a red merocyanine dye ( $\lambda_{\text{max}} = 485$  nm), while the 3*H*-naphthopyran formed a yellow merocyanine ( $\lambda_{\text{max}} = 440$  nm) upon mechanical activation. The yellow dye in the 3*H*-naphthopyran polymer faded completely after 10 min of force removal, returning to the original colourless state. In contrast, the reddish colouration in the 2*H*-naphthopyran polymer was more persistent, taking a longer time to fade after the stress relaxation and still being visible in the pristine film (Fig. 7e), showing the greater stability of the merocyanine compound formed from the 2*H*-naphthopyran.

**2.2.2 Supramolecular assemblies.** Supramolecular assemblies, which consist of self-organising complexes held together by non-covalent bonds, often exhibit superior mechanoresponsive behaviour, with a high level of sensitivity to mechanical forces. In these assemblies, the breakage of the weak non-covalent bonds, *e.g.*, van der Waals



interactions, hydrogen bonding, and  $\pi$ -stacking interactions, between complexes triggers a structural transformation. Compared to other mechanoresponsive polymers, which rely on the breakage of covalent bonds in the mechanophores, supramolecular assemblies are advantageous in being more sensitive due to their lower activation energy as well as having generally higher reversibility.<sup>88,90–93</sup>

Sagara's group investigated the mechanoresponsive behaviour of rotaxane-based supramolecular mechanophores.<sup>94</sup> The rotaxane mechanophores were composed of a luminophore-containing ring, which was threaded onto an axle with a matching quencher and two stoppers (Fig. 8a). Reversible fluorescence changes were observed even after 50 loading and unloading cycles due to the molecular shuttling of the mechanophores. An increase in fluorescent intensity was measured under the uniaxial deformation, but immediately reversed when the deformation was released (Fig. 8b). However, when excessive force was applied at the strain of 600%, the ring with the luminophore slipped past the stoppers, permanently breaking the mechanical bond. This dethreading resulted in an irreversible fluorescence change. The same group recently reported the fabrication of a cyclophane-based mechanophore containing two fluorescent 1,6-bis(phenylethynyl)pyrene moieties (Fig. 8c).<sup>95</sup> The pyrene moieties could form an excimer with an emission around the wavelength of 530 nm, whereas the pyrene monomer emission was at 470 nm, which induced a colour change based on the mechanophore assembly structures. Excimer emission dominated the emission spectra of the dilute solutions with a low composition of cyclophane mechanophore (0.8 wt%) and polyurethane elastomers. Upon deformation, conformational changes occurred in the polymer, leading to a greater monomer emission. This phenomenon was observed when the mechanophore was covalently embedded in a linear, segmented polyurethane elastomer, and the film produced exhibited a distinct colour change from cyan to blue at a strain of 600%.

Imato and co-workers developed mechanoresponsive supramolecular polymers using fluorescent pyrene and naphthalene diimides incorporated in the mid-chain of poly( $\epsilon$ -caprolactone)s.<sup>96</sup> With no mechanical stimuli, fluorescence quenching occurred as the pyrene formed an intramolecular charge transfer complex with the naphthalene diimides. The application of force triggered the dissociation of the complex, leading to strong fluorescent emission.

Tetraarylsuccinonitrile is the another mechanoluminescent moiety that can generate colored radicals using mechanical stimuli. Otsuka's group introduced a tetraarylsuccinonitrile moiety at the crosslinking points of a polymer gel.<sup>97</sup> After freezing the polymer gel, the swelled solvent induced homolytic dissociation of the central carbon-carbon bond of the tetraarylsuccinonitrile skeleton, resulting in not only a color change but also light emission of the gel (Fig. 9b). The structure change and mechanoluminescence were reversible upon heating and freezing the gel. The same

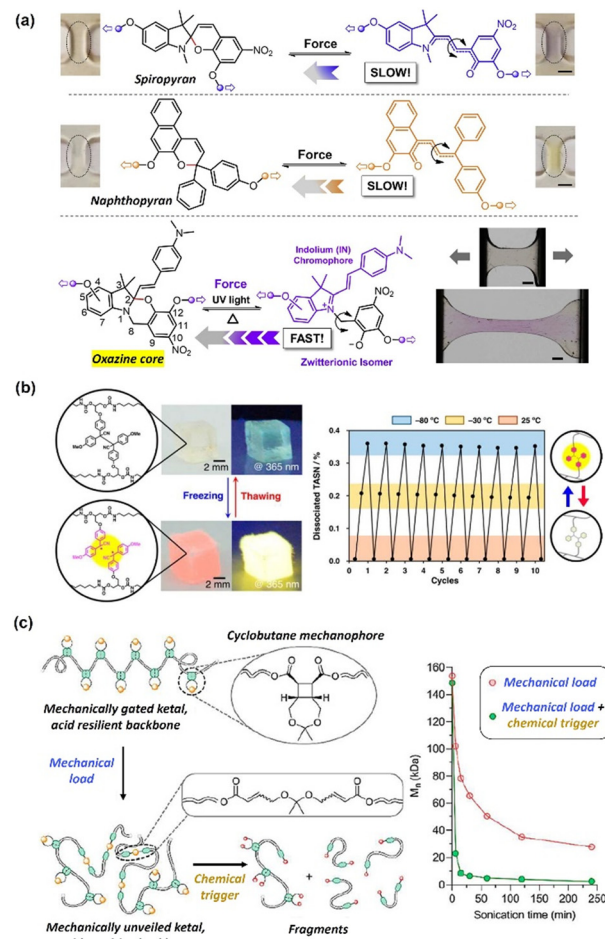
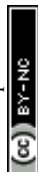


Fig. 9 (a) Force-induced chemical transformations of spiropyran, naphthopyran and oxazine. Inset: Photographs of polymer films before and after the application of force. Reproduced from ref. 101 with permission. Copyright 2021, Elsevier. (b) Reversible color change and light emission of the tetraarylsuccinonitrile-containing gel at ambient temperature (25 °C) and freezing (–80 °C) conditions. (c) Schematic diagram of the mechanically-gated ketal degrading into fragments with the application of both mechanical load and chemical trigger as stimuli and plot of molecular weight ( $M_n$ ) against sonication time for the mechanically gated polymers in the presence of different stimuli. Reproduced from ref. 104 and 107 with permission. Copyright 2018 and 2020, the American Chemical Society, respectively.

group also introduced tetraarylsuccinonitrile functions into polystyrene and silsesquioxane composite elastomers, which allowed the materials to display reversible mechanofluorescence upon grinding.<sup>98,99</sup>

Lin *et al.* incorporated a cyclobutane mechanophore on a polymer backbone as a mechanical gate to regulate an acid-sensitive ketal.<sup>100</sup> Given that both the mechanical load and chemical trigger are required to achieve significant molecular weight degradation, this allowed the polymer to retain its degradable properties, while building resistance to unintended degradation (Fig. 9c). The integrity of the polymer backbone was maintained in the presence of only a chemical trigger using trifluoroacetic acid. However, upon the application of a mechanical load through ultrasonication,



polymer degradation occurred to an apparent limiting molecular weight of 28 kDa. When the two stimuli were combined, an 11-fold decrease in molecular weight to 2.5 kDa was achieved. Although the bond cleavage was not reversible, the design and introduction of a mechanophore enabled the polymer chains to exhibit unique degradation functions.

**2.2.3 Other force-responsive polymers.** Recent developments have led to the emergence of other novel mechanoresponsive structures. Qian *et al.* employed an oxazine-based mechanophore scaffold to create a fast and reversible force-responsive material.<sup>101</sup> Unlike conventional spiropyran and naphthopyran mechanophores, oxazine undergoes a purely ring-opening reaction with no double-bond isomerism involved during its mechanical activation. This process formed coloured zwitterion species, which reverted to the initial state orders of magnitude faster than the merocyanine to spiropyran and naphthopyran transformation (Fig. 9a). The threshold activation strain of the oxazine mechanophore in the bulk polydimethylsiloxane varied in the range of ~90–125%. No phase lag or response fatigue was observed even after 8 continuous loading–unloading cycles.

## 2.3 CO<sub>2</sub>-responsive structure

Carbon dioxide-switchable polymers are stimuli-responsive polymers that employ CO<sub>2</sub> as the primary triggering mechanism to alter and reversibly switch the polymer properties. For instance, controlling the degree of hydrophobicity in the presence of CO<sub>2</sub> (hydrophilic) or the absence of CO<sub>2</sub> (hydrophobic). Incorporating CO<sub>2</sub>-switchable

components has gained much attention in recent years due to their unique advantages including abundance, non-toxic and environmentally friendly nature with no accumulation of chemical species, rapid response, good penetration depth and low cost.<sup>102,103</sup> Most importantly, the excellent precision to control and manipulate the polymer chain structure allows great versatility and autonomy. Generally, this strategy revolves around the design and tailoring of the polymer chain structure of CO<sub>2</sub>-responsive materials in terms of their functionalities, as shown in Fig. 16. The various types of CO<sub>2</sub>-responsive functionalities are composed of copolymers of various compositions, as well as hybridized with functional nanomaterials to form composites.<sup>102,104</sup>

Among the polymerisation strategies, atom transfer radical polymerisation (ATRP) is typically preferred due to its low impurities, simplicity, and controlled polymer growth. Generally, this polymerization involves chemical functionalization of the precursor and polymerization of the CO<sub>2</sub>-responsive monomer to form a CO<sub>2</sub>-responsive copolymer. CO<sub>2</sub>-responsive copolymers have huge potential for application in catalysis, nanoreactors, switchable surfactant/stabilizers, drug delivery, and separation.<sup>105</sup> Alternatively, hypoxia-responsive polymers are also highly relevant in biomedical applications such as tumor treatment.<sup>106</sup> In this section, we discuss the most recent development of CO<sub>2</sub>-responsive polymers, their mechanism, and their applications.

**2.3.1 Guanidine.** Guanidine is an amine derivative that contains three nitrogen groups (two ‘amides’ and one

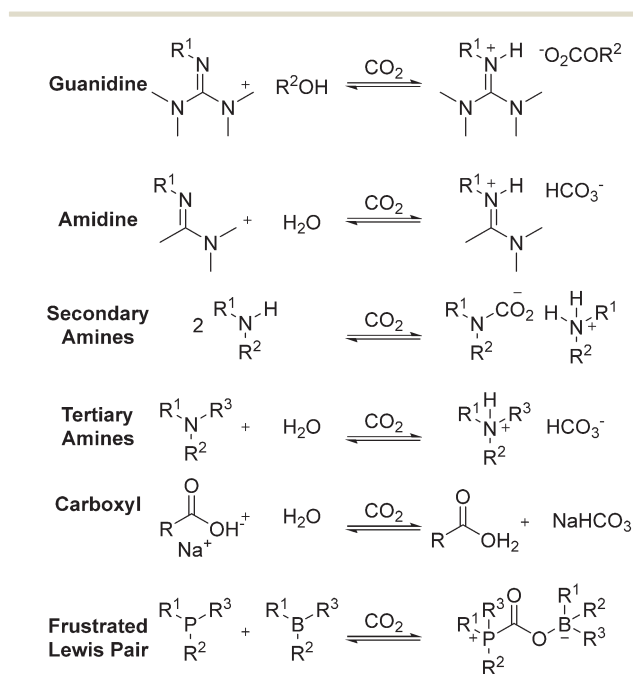


Fig. 10 Functional groups and chemical changes involved in CO<sub>2</sub>-responsive polymers.

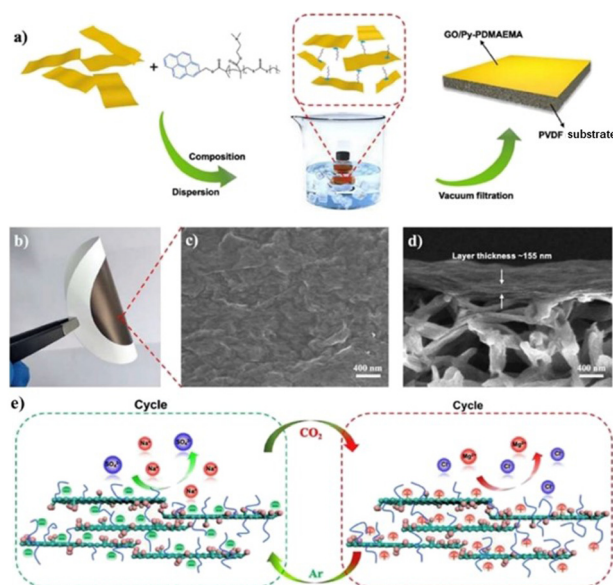
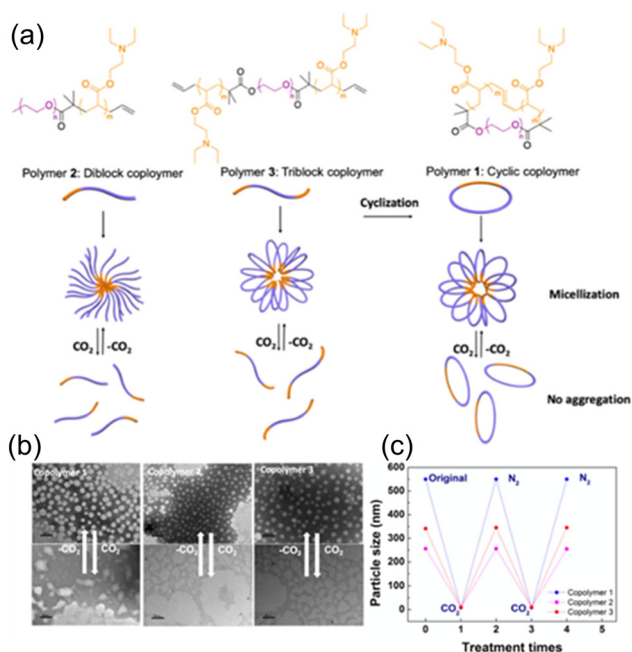


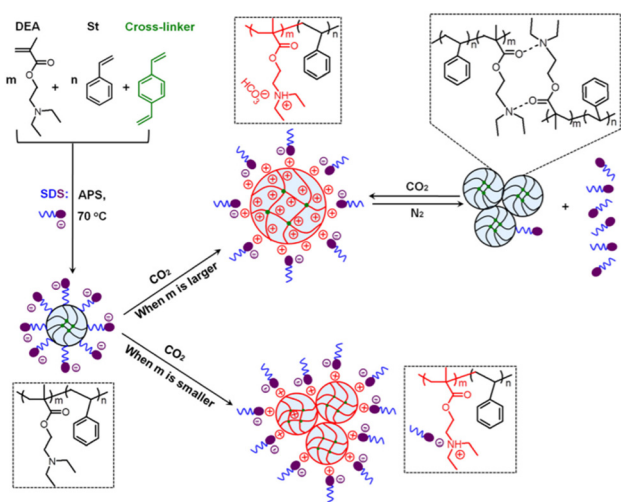
Fig. 11 (a) Schematic illustration of the fabrication process of CO<sub>2</sub>-responsive GO/Py-PDMAEMA nanofiltration membrane. (b) Photo of the resulting membrane. (c) Top and (d) cross-section scanning electron microscopy (SEM) images of the membrane. (e) Mechanism of CO<sub>2</sub>-responsive GO/Py-PDMAEMA composite nanofiltration membrane with gas-induced charge sign reversal on the rejection of salts. Reproduced from ref. 123 with permission. Copyright 2020, Elsevier.



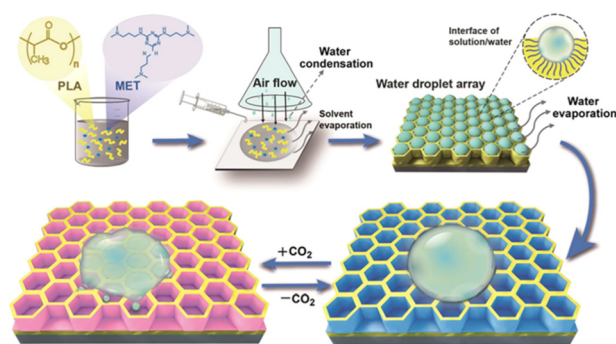


**Fig. 12** (a) Chemical structures of polymer 1 as a cyclic amphiphilic block copolymer, 2 as a di-block copolymer, and 3 as a tri-block copolymer. Schematic representation of the formation of micelles controlled by CO<sub>2</sub>. (b) Transmission electron microscopy (TEM) images (left) and change of hydrodynamic size (right) of the copolymers 1, 2, and 3 (0.2 wt%) in the presence or absence of CO<sub>2</sub>. The scale bars of TEM images in the absence CO<sub>2</sub> (upper) are 1000 nm and that in the presence of CO<sub>2</sub> (lower) are 100 nm. Reproduced from ref. 118 with permission. Copyright 2020, Elsevier.

‘imine’) on one carbon atom, which is also known as a carbon-imidic diamide, as illustrated in Fig. 16. It has an acid dissociation constant (pK<sub>a</sub>) value of ~13.5 and is categorized as an organic superbase, given the resonance



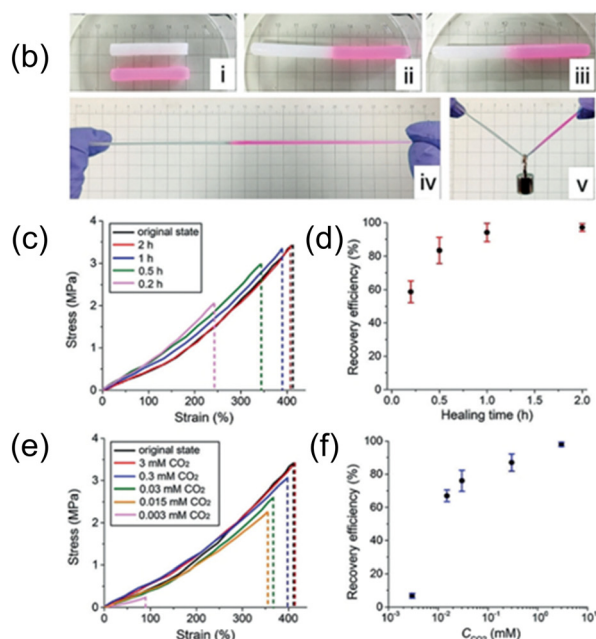
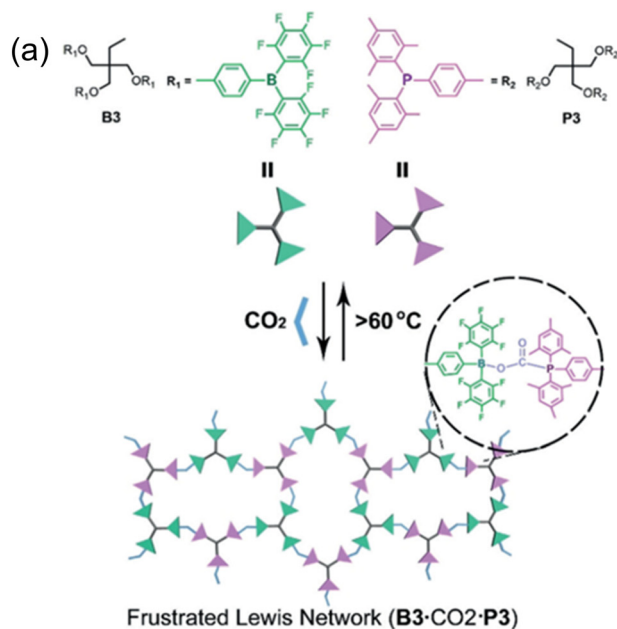
**Fig. 13** Schematic illustration of the fabrication of P(DEA-St) latexes with SDS used as an emulsifier, as well as the mechanism for the responsive destabilization, reversible redispersion, and switchable expansion/collapse transition of the latexes induced by CO<sub>2</sub>/N<sub>2</sub>. Reproduced from ref. 117 with permission. Copyright 2020, Elsevier.



**Fig. 14** Schematic diagram of the honeycomb-like porous film prepared from the PLA/MET complex and its CO<sub>2</sub>-triggered reversible wettability. Reproduced from ref. 125 with permission. Copyright 2021, the American Chemical Society.

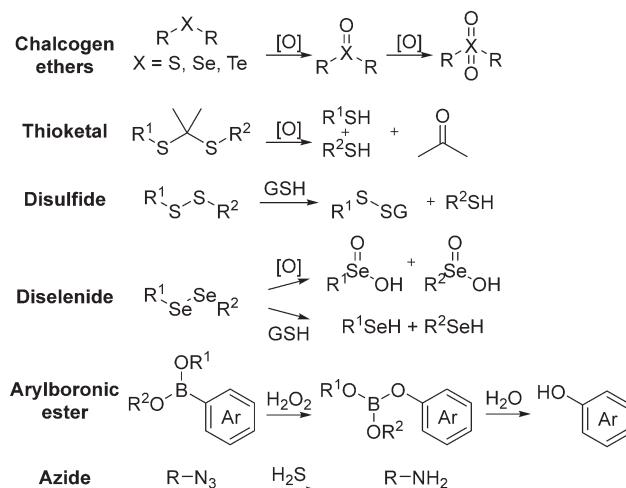
stability of its conjugated acids. Generally, guanidines undergo a protonation reaction upon CO<sub>2</sub> simulation and are converted into guanidinium species. However, the deprotonation reaction can only be achieved by heating instead of inert gas bubbling (Ar or N<sub>2</sub>) due to their high pK<sub>a</sub> value.<sup>107</sup> For instance, Lowe and co-workers developed a polyarginine homopolymer and block copolymer *via* a two-step modification including RAFT polymerization and post-polymerization modification. Interestingly, the copolymer reversibly formed micelles under N<sub>2</sub> and dissociated into a linear chain under CO<sub>2</sub> exposure in an aqueous medium.<sup>108</sup> In another work, Theato and Schattling synthesized a random copolymer of various L-arginine and acrylamide using a similar two-step modification and discovered its dual temperature and CO<sub>2</sub>-responsive behaviors. The copolymer exhibited a reversible hydrophilic/hydrophobic performance under CO<sub>2</sub> or Ar exposure, which can be utilized in drug delivery systems, sensors, and even as “smart” CO<sub>2</sub> trapping surfaces.<sup>109</sup>

**2.3.2 Amidine.** Amidine contains two nitrogen atoms in the ‘amide’ and ‘imine’ functional groups in its structure, which resembles carboxylic acids and has an average pK<sub>a</sub> value of ~9.0 (in the range of 5–12). As shown in Fig. 10, the protonation reaction converts the imino nitrogen to a symmetrical amidinium ion, which can be stabilized by resonance. In general, the stronger basicity of amidine groups causes the equilibrium constant between CO<sub>2</sub> and amidine to be substantial ( $K_{\text{IE}} = 102\text{--}105$ ), leading to higher CO<sub>2</sub> sensitivity and responsivity. Jessop and co-workers first reported the preparation of CO<sub>2</sub>-responsive aliphatic amidine-containing surfactants in 2005.<sup>110</sup> Subsequent work by Yan *et al.* synthesized an amidine-based copolymer *via* ATRP of the difunctional monomer (*N*-amidino)dodecyl acrylamide (AD). These tuneable drug delivery vesicles exhibited smart expansion and contraction cycles upon CO<sub>2</sub> stimulation with controlled-release capability.<sup>111</sup> Guo and co-workers adopted a post-polymerization modification strategy, converting poly(4-chloromethyl styrene) (PCMS) into poly(pazidomethyl styrene) (PAMS) with high amidine functionalities *via* a Cu(I)-catalyzed cycloaddition “click”



**Fig. 15** (a) Trefoil-like frustrated Lewis pair (B3 and P3) as trivalent building blocks to form CO<sub>2</sub>-crosslinked frustrated Lewis networks with reversible CO<sub>2</sub>/thermal responsiveness via CO<sub>2</sub>-bridging dynamic covalent linkages. (b) Self-healing process of the frustrated Lewis network: i) two cut samples (one loaded with red pigment), ii) cut surfaces were treated with CO<sub>2</sub> and brought into contact, iii) self-healed for 30 min under ambient conditions, iv) the healed gel under stretching, and v) on loading. (c) Stress-strain curves of original and healed gel samples after various healing times. (d) Plot of the gel recovery efficiency versus healing time. (e) Stress-strain curves of original and healed gel samples under various levels of CO<sub>2</sub> stimulus. (f) Plot of the gel recovery efficiency versus external CO<sub>2</sub> concentration. Error bars in (d) and (f) denote the standard deviations from at least three experiments. Reproduced from ref. 131 with permission. Copyright 2019, Wiley.

reaction. The resultant homopolymers displayed a reversible hydrophobic-hydrophilic evolution in CHCl<sub>3</sub>/water when



**Fig. 16** Functional groups and chemical changes involved in redox-responsive polymers.

exposed to CO<sub>2</sub> and N<sub>2</sub> in an aqueous medium, showing potential application in sensors, “smart” surfaces, and drug delivery.<sup>111</sup> However, amidine is highly susceptible to hydrolysis in the absence of a CO<sub>2</sub> environment, which disrupts its self-assembly. Moreover, the complex synthesis of amidines makes them a less preferred choice.

**2.3.3 Amine-based copolymers.** All amine-based copolymers can react with CO<sub>2</sub> to form the corresponding bicarbonate salts in water, including the bulky primary and secondary amines, and tertiary amines, as shown in Fig. 10. Among them, tertiary amines possess the best CO<sub>2</sub> reversibility and switchability, which is attributed to their weak alkalinity (pK<sub>a</sub> = 6.7–8.0).<sup>112</sup> The protonation reaction by the bicarbonate anion (pH = 4.0–5.0) can easily occur at ambient temperature, whereas heat is required for primary and secondary amines. Polymers containing tertiary amines can be fully separated in water/THF co-solvent due to their exceptional ionic conversion capability in water. Moreover, the simple manufacturing process and commercial availability of tertiary amines make them the prime choice.<sup>113</sup> Functional monomers with tertiary amines include 2-(dimethylamino)ethyl methacrylate (DMAEMA), 2-(diethylamino)ethyl methacrylate (DEAEMA), and melamine derivative [N<sup>2</sup>,N<sup>4</sup>,N<sup>6</sup>-tris(3-(dimethylamino)propyl)-1,3,5-triazine-2,4,6-triamine] (MET) and others. These monomers offer great possibility to design CO<sub>2</sub>-responsive chain structures by varying their composition/sequence (homopolymers, block, random, alternating, gradient and statistical copolymers), and topologies (graft polymer, hyperbranched, and polymer network). They demonstrated great utilization as catalysts,<sup>114</sup> nanoreactors,<sup>115</sup> switchable surfactants/stabilizers,<sup>104,116–121</sup> and membrane separators.<sup>113,122,123</sup>

**2.3.3.1 Poly(*N,N*-dimethylaminoethyl methacrylate) (PDMAEMA).** To date, poly(*N,N*-dimethylaminoethyl methacrylate) PDMAEMA and poly(*N,N*-diethylaminoethyl methacrylate) PDEAEMA have been labeled as the perfect



CO<sub>2</sub>-switchable moieties and are significantly utilized in many applications. The comparable pK<sub>a</sub> value of the amine copolymers to the aqueous medium allows rapid and reversible protonation/deprotonation under alternating CO<sub>2</sub>/inert gas stimulations.<sup>113</sup> Despite their small structural difference, Zhao and Yin found that the graphene oxide (GO)/pyrene end-functionalized PDMAEMA (Py-PDMAEMA) nanofiltration membrane performed better than the GO/Py-PDEAEMA nanofiltration membrane. They assembled Py-PDMAEMA on GO sheets through  $\pi$ - $\pi$  stacking and electrostatic interaction and fabricated the membranes *via* vacuum filtration on a PVDF microfiltration membrane. The hydrophilic PDMAEMA displayed good solubility and extended chain conformation in an aqueous medium regardless of the alternate CO<sub>2</sub>/Ar bubbling, which maintained an excellent size exclusion effect and charge property, as shown in Fig. 11. On the contrary, the hydrophobic PDEAEMA collapsed after eliminating CO<sub>2</sub> and covered the GO surface, which resulted in a reduction in the charge property and size exclusion effect of the membranes.<sup>123</sup> Zhao and Fan synthesized a random copolymer of poly((*N,N*-dimethyl aminoethylmethacrylate)-*co*-4-methyl-[7-(methacryloyl)oxy-ethyl-oxy]coumarin) (P(DMAEMA-*co*-CMA)) and an amphiphilic diblock copolymer of PS-*b*-P(DMAEMA-*co*-CMA) (PS is hydrophobic polystyrene). The CO<sub>2</sub>-responsive single-chain polymeric nanoparticles aggregated and self-assembled into core-shell micelles in water. The reversible protonation/deprotonation reaction of the tertiary amine groups made the SCNPs swell and shrink reversibly under CO<sub>2</sub>/N<sub>2</sub> stimulation, showing great potential as effective gas-tuneable nanoreactors.<sup>115</sup> Recently, block and random copolymers of DMAEMA and poly(methyl methacrylate) (PMMA) were synthesized through RAFT solution polymerization. The team obtained latexes that could coagulate and re-disperse under alternating N<sub>2</sub> and CO<sub>2</sub> bubbling. They found that the optimum protonation could be achieved by randomizing the MMA content over blocks of MMA. The rapid protonation was contributed by the larger gap between the nitrogen atoms, making them a promising CO<sub>2</sub>-switchable stabilizer.<sup>116</sup>

**2.3.3.2 Poly(*N,N*-diethylaminoethyl methacrylate) (PDEAEMA).** In addition to the typical applications of amine-based copolymers, gas-enabled self-cleaning membranes have gained immense popularity. For instance, Zhang and co-workers<sup>122</sup> developed a blend comprised of the CO<sub>2</sub>-responsive copolymer polyacrylonitrile-*co*-poly(*N,N*-diethylaminoethyl methacrylate) (PAN-*co*-PDEAEMA) with PAN matrix *via* a phase inversion process. The controllable hydrophilicity/hydrophobicity of the membrane surface dictated its self-cleaning efficiency. Upon CO<sub>2</sub> stimulation, the collapsed hydrophobic PDEAEMA segments instantly transformed into a chain-extended state due to the protonation of the tertiary amine groups. The reaction induced hydrophilicity, which deterred the adsorption of proteins on the membrane surface. Deprotonation of the tertiary amine groups by N<sub>2</sub> bubbling returned them to the hydrophobic state. Remarkably, the cleaning efficiency of this

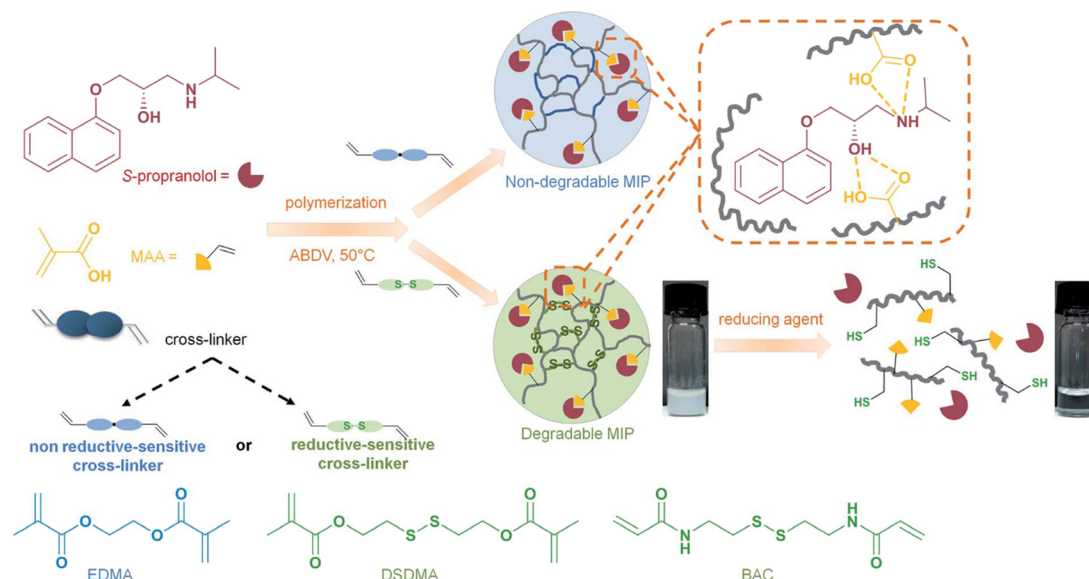
green strategy is comparable to that of the traditional acid and alkaline cleaning.<sup>122</sup>

In their recent work, Feng and Jiang<sup>118</sup> studied the effects of the chemical structure and segment composition on the topological effect and tendency of the CO<sub>2</sub> response by evaluating the properties of self-assembled micelles, as shown in Fig. 12. They synthesized three types of amphiphilic copolymers based on poly(ethylene oxide) (PEO, hydrophilic component) and DEAEMA (hydrophobic component) in the form of di-block, tri-block, and a novel cyclic structure *via* ATRP polymerization. As illustrated in Fig. 12b, the cyclic copolymer (copolymer 1) possessed the largest particle given that it promoted micelle formation and increased the aggregation of the micelles. A plot of particle size for the different copolymers are also depicted in Fig. 12c corresponding to their treatment times showing that copolymer 1 exhibits the largest particle size.

The same group developed a new strategy to generate lightly crosslinked poly(diethylaminoethyl methacrylate-styrene) [P(DEA-St)] latexes with different PDEA contents *via* one-pot emulsion copolymerization, as displayed in Fig. 13.<sup>117</sup> At a high DEA content (98.05 wt%), the latexes switched steadily between swelling and deswelling, which was attributed to the CO<sub>2</sub>-reversible protonation/deprotonation reaction of their PDEA portions. On the contrary, a low DEA content (below 13.74 wt%) made the latexes CO<sub>2</sub>-insensitive due to the insignificant electrostatic interactions. This crosslinked structure proved to be a promising strategy for other common latexes such as PMMA and PS.<sup>120,121</sup>

**2.3.3.3 Melamine derivative [*N*<sup>2</sup>,*N*<sup>4</sup>,*N*<sup>6</sup>-tris(3-(dimethylamino)propyl)-1,3,5-triazine-2,4,6-triamine].** Yin and Feng<sup>124</sup> reported the preparation of a CO<sub>2</sub>-stimulated reversible graphene dispersion by non-covalently functionalizing reduced graphene oxide with a CO<sub>2</sub>-sensitive melamine derivative, *N*<sup>2</sup>, *N*<sup>4</sup>, *N*<sup>6</sup>-tris(3-(dimethylamino)propyl)-1,3,5-triazine-2,4,6-triamine (MET). They found that the excellent graphene dispersion is attributed to the strong van der Waals interaction between MET and the graphene surface. Reversible aggregation/dispersion could be easily realized by interchanging CO<sub>2</sub> and N<sub>2</sub> bubbling, which manipulated the desorption/adsorption of MET on the graphene surface. This novel gas-triggered aggregation/dispersion smart graphene with controllable stimuli-responsive dispersity demonstrates great potential in the medical and biochemical fields. Recently, the same group developed a biocompatible polylactic acid (PLA) bioinspired honeycomb-like porous film with ON/OFF CO<sub>2</sub> gas-triggered switchable wettability.<sup>125-127</sup> This group employed the breath figure method to prepare the non-responsive PLA and CO<sub>2</sub>-sensitive MET. The film displayed noticeable hydrophobic-hydrophilic conversion, as shown in Fig. 14. By tuning the PLA/MET ratio, they could precisely position the hydrophilic CO<sub>2</sub>-sensitive groups in the inner surface and control the water penetration and wettability of the pore. Consequently, the enhanced surface wettability improved the cell-film interaction and the subsequent cell attachment. The combination of a biocompatible polymer and natural gas trigger allows the





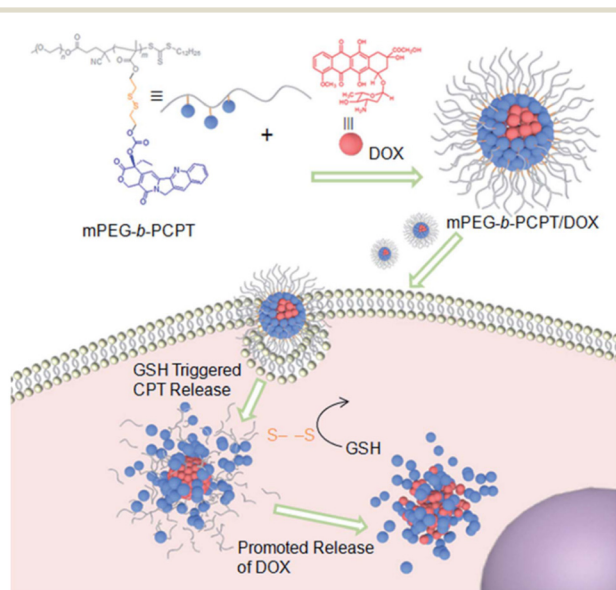
**Fig. 17** Schematic representation of synthesis and reduction-induced degradation of S-propranolol molecularly imprinted polymers for drug delivery. Adapted with permission from ref. 146 Copyright 2020, The Royal Society of Chemistry.

preparation of future intelligent materials for biomedical and bioengineering applications.

**2.3.4 Carboxyl-based copolymers.** Generally, carboxyl has a relatively low  $pK_a$  value of  $\sim 5.0$  to  $9.0$ . It undergoes a protonation reaction upon  $CO_2$  simulation and converts the sodium salt of acid from anionic surfactants to non-ionized erucic acid, as shown in Fig. 10. For instance, Zhang and Feng developed a  $CO_2$ -responsive anionic worm-like micellar system based on sodium erucate.<sup>128</sup> The protonation/

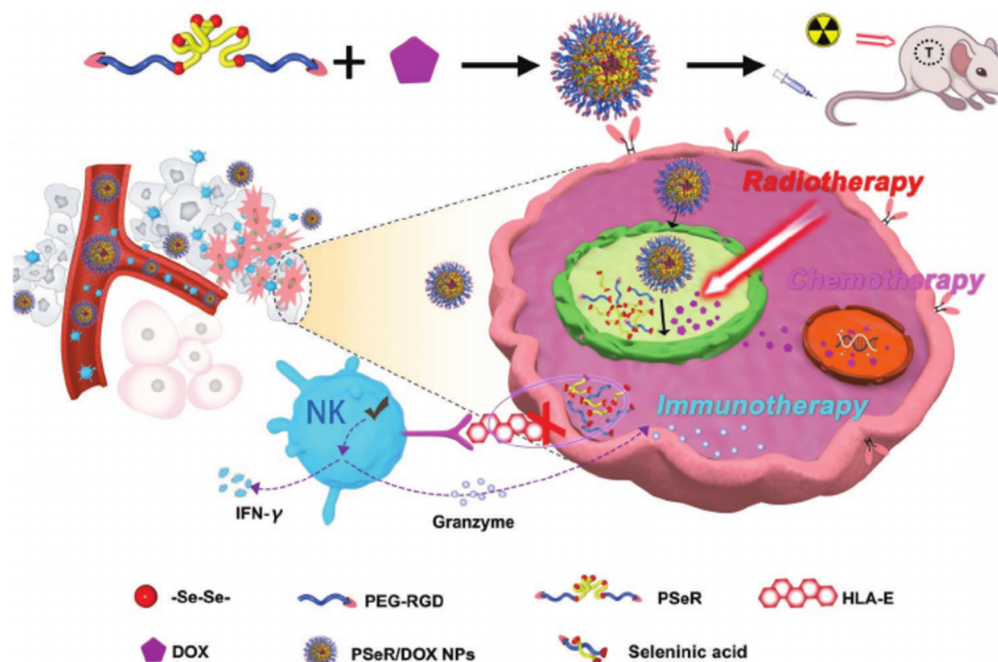
deprotonation process interchanged between the worm-like micelles and low-viscosity emulsion particles, which is attributed to the reversible conversion of the sodium salt of the erucic acid (anionic surfactant) into the non-ionized erucic acid. In another work, Fischer and co-workers reported the preparation of carboxyl functionalized,  $CO_2$ -switchable nanoparticles *via* surfactant-free mini-emulsion polymerization by employing a reactive surfactant known as surfmer, *i.e.*, *N*-methacryloyl-11-aminoundecanoic acid (treated equimolarly with NaOH).<sup>129</sup> The obtained latex had a size of about 100 nm with good dispersion. The protonation reaction was carried out *via*  $CO_2$  bubbling to instantly form carbonic acid, which covalently attached onto the surface of the colloid, and could be deprotonated by ultrasonic treatment. In another work by Wang and Zhu, they fabricated zwitterionic crosslinked polymer particles comprising DEAEMA and sodium methacrylate (SMA).<sup>130</sup> These particles possessed  $CO_2/N_2$ -adjustable isoelectric points in the pH range of 7.5–8.0, and subsequently were used as an emulsifier for Pickering emulsions. The optimization of the cationic amine group and the anionic carboxyl group provides insight for the preparation of future  $CO_2$ -responsive polymer materials.

**2.3.5 Lewis acid–base pair copolymers.** The most common approach and strategy for the preparation of  $CO_2$ -responsive polymers is by modifying the polymer chain functionalities, as shown in the earlier sections. There has been an increase in the development of innovative dual  $CO_2$ -responsive polymer systems based on the frustrated Lewis pair (FLP) theory in recent years. Stephan and co-workers first introduced this theory in 2006,<sup>132</sup> where the Lewis acid and base offer latent interactions to connect small molecules such as dihydrogen ( $H_2$ ) and carbon dioxide ( $CO_2$ ) to create a connecting (bridging) structure that possesses reversible



**Fig. 18** Schematic illustration of the preparation of mPEG-b-PCPT/DOX nanomedicine and the “drug release promoting release strategy” of mPEG-b-PCPT/DOX for synergistic cancer chemotherapy. Adapted with permission from ref. 147 Copyright 2019, The Royal Society of Chemistry.



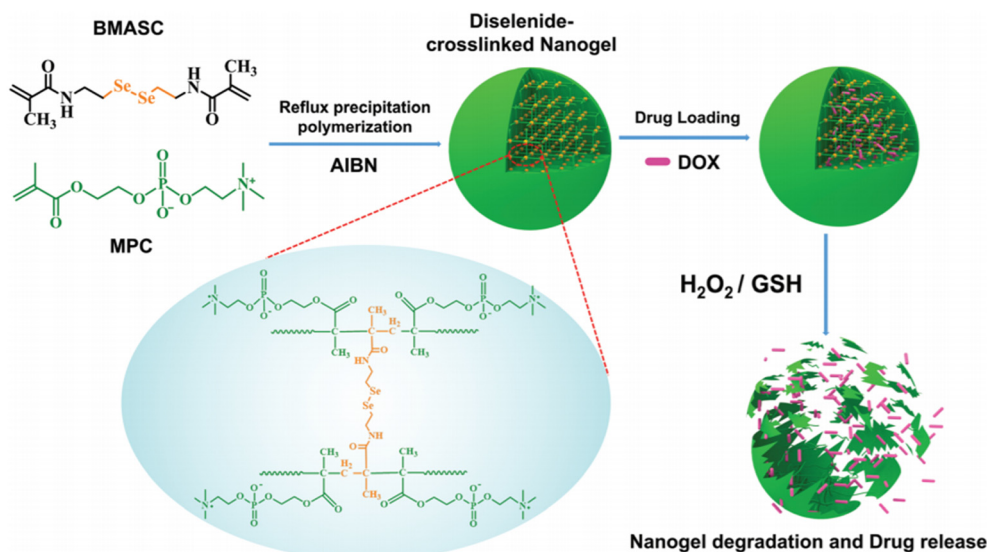


**Fig. 19** Schematic illustration of utilizing selenium-containing nanoparticles to implement combined chemotherapy, radiotherapy, and immunotherapy. Adapted with permission from ref. 155 Copyright 2020, Wiley.

cleavage and re-bonding feature, as illustrated in Fig. 15. For instance, Yan and co-workers demonstrated this theory by adding Lewis acid–base pairs to a polymer, and successfully developed a recyclable nano-catalyst with good activity and recyclability, showing great potential as a wastewater treatment membrane.<sup>133</sup>

Subsequently, they adopted the same theory and developed a novel polymer system exhibiting ultrafast response, self-healing capability, reversibility, and excellent mechanical robustness. As shown in Fig. 15, this is due to

the bridging of CO<sub>2</sub> in the polymer segment, which subsequently induced assembly in organic solvent systems, demonstrating potential in future gas-sensitive smart materials.<sup>131</sup> In their most recent work, they developed a gel material with a double-crosslinked FLP network comprised of dynamic CO<sub>2</sub> gas-bridged connections and permanent chemical crosslinks by reacting triaryl borane (TB), triarylphosphine (TPP), and CO<sub>2</sub>. Notably, the strength and toughness of the gel could be tuned by adjusting the CO<sub>2</sub> content, which dictated the density of supramolecular nodes



**Fig. 20** Illustration of the preparation, biodegradable behavior and dual redox-responsive drug release of P(MPC-Se-Se-MPC) nanogels. Adapted with permission from ref. 160 Copyright 2020, Wiley.



in the network. Furthermore, the excellent self-healing stimulated by CO<sub>2</sub> *via* dynamic covalent network reconstruction allows these innovative soft materials to be potentially applied as sensors, actuators, and biomedical devices.<sup>134</sup>

## 2.4 Redox-induced structure switch

The development of redox-responsive polymeric materials has been dramatically researched over the years to optimize and regulate the delivery and release of encapsulated therapeutic agents, such as doxorubicin (DOX), camptothecin (CPT), and paclitaxel (PTX), especially for tumour treatment. Their environment displays many redox activities involving biological reductants and oxidants, making redox-responsive materials a suitable material for the preparation of drug delivery systems.<sup>135</sup> The typical redox-responsive species include (i) reactive oxygen species (ROS), (ii) glutathione species (GSH), (iii) ROS + GSH species, and the recent (iv) hydrogen sulphide (H<sub>2</sub>S)-based species, as displayed in Fig. 16.<sup>136</sup> Generally, there are two approaches to incorporate drugs in delivery systems. The first approach involves loading a drug in an amphiphilic micelle assembly, where hydrophobic-hydrophilic conversion is the primary responsive mechanism. The second approach involves incorporating the drug in a polymer chain integrated with a responsive species, where bond cleavage is the main responsive mechanism.<sup>137</sup>

ROS is a highly reactive species made up of a group of oxygen-containing molecules. It is categorized into two types, *i.e.*, the radical type comprised of hydroxyl radical (HO<sup>•</sup>) and superoxide (O<sub>2</sub><sup>•-</sup>) and the non-radical type comprised of hydrogen peroxide (H<sub>2</sub>O<sub>2</sub>), HOCl, and singlet oxygen (<sup>1</sup>O<sub>2</sub>). Among them, H<sub>2</sub>O<sub>2</sub> is a popular ROS-responsive material due to its relative stability and longer half-life. A low concentration of these species makes them a useful biological signal in living organisms, while excessive amounts can lead to an imbalance between ROS and antioxidants, which is known as oxidative stress. This oxidative stress damages lipids, proteins, and DNA, adversely leading to physical harm.<sup>138</sup> Examples of ROS-based species include chalcogen ethers, thioketals, aryl boronic esters, and many others.

Alternatively, GSH is a reduction-responsive tripeptide containing cysteine, glycine, and glutamate. The huge redox potential difference between the intracellular (~10 mM) and extracellular environments (~10 μM) at any concentration make GSH a proper biological signal for intracellular delivery. Most importantly, GSH production maintains the redox equilibrium by balancing the oxidative stress produced by ROS.<sup>139</sup> Ideally, the employment of both ROS and GSH will be favourable because of the versatility and performance. Besides the typical species, H<sub>2</sub>S, the simplest gaseous thiol, has gained attention lately. H<sub>2</sub>S exists in deprotonated anion form due to its acidic nature and has demonstrated positive physiological and

pathological effects, especially in encapsulated therapeutics.<sup>140–142</sup>

**2.4.1 Disulfide linkage.** A widely used GSH-responsive species, disulfide, is comprised of a sulfur-sulfur (S-S) linkage with a bond energy of 240 kJ mol<sup>-1</sup>. In the presence of GSH, the disulfide linkage undergoes oxidative cleavage to form thiols, as shown in Fig. 16, contributing to successive drug release. The similarity between the thiol-disulfide exchange reaction to the biological system makes it an ideal drug delivery capsule.<sup>139</sup> Generally, the disulfide linkage is incorporated *via* various strategies. The first strategy is integrating the disulfide linkage into the main chain, as demonstrated in the recent studies by Ghosh and co-workers.<sup>143</sup> Their group incorporated a disulfide group into the supramolecular assembly of a protein, bovine serum albumin (BSA), which underwent disulfide linkage cleavage upon GSH exposure. Subsequently, the protein was released, leading to enzymatic activity. In another work, Ju and He designed and fabricated a reduction-sensitive amphiphilic triblock copolymer poly(ethyl ethylene phosphate)-*b*-poly(disulfide)-*b*-poly(ethyl ethylene phosphate) (PEEP-PDS-PEEP) through thiol-disulfide polycondensation and ring-opening polymerization (ROP).<sup>144</sup> The copolymer demonstrated good self-assembly and profoundly released the DOX hydrophobic drug upon reduction-trigger *via* poly(disulfide) scission and dissociation. Recently, Wang *et al.* introduced a disulfide bond into the conjugates of oxaliplatin(IV) and oleic acid (OA) to form a reduction-responsive nanoscale assembly.<sup>145</sup> Similar to previous work, the self-assembly structure underwent disulfide bond cleavage and displayed high anticancer potency and drug efficiency.

The second strategy is by pendant group integration, where a disulfide-containing component is attached to the main backbone of the polymer. For instance, Shen *et al.* attached the disulfide-containing cleavable prodrug monomer camptothecin (CPT) to a methoxy poly(ethylene glycol) (mPEG)-based polymer chain by RAFT living polymerization and developed an amphiphilic copolymer.<sup>147</sup> Besides CPT, doxorubicin (DOX) was encapsulated *via* hydrophobic and π-π stacking interactions. In their work, the co-release of both anticancer drugs was well controlled and demonstrated a synergetic effect with enhanced anticancer efficacy, as illustrated in Fig. 18.

The last strategy is by crosslinking with a cleavable disulfide-containing crosslinker. Bhattacharya and co-workers covalently crosslinked the disulfide group on a polymer chain and reported an excellent drug release profile.<sup>148</sup> In 2020, Zhao *et al.* directly polymerized methacrylic acid with the reductive-sensitive crosslinker bis(2-methacryloyloxyethyl) disulfide (DSDMA) or *N,N'*-bis(acryloyl) cystamine (BAC) using *S*-propranolol as a model template to form a degradable molecularly imprinted polymer (MIP).<sup>146</sup> As shown in Fig. 17, the team found that the MIP-disulfide could readily degrade *via* bond cleavage in a reductive environment and had a better release performance than the traditional ethylene



glycol dimethacrylate (EDMA)-based MIP. This approach can be effectively adopted as an intracellular controlled drug delivery system.

**2.4.2 Chalcogen linkage.** Chalcogens are chemical elements found in group XIV of the periodic table, which are comprised of sulfur (S), selenium (Se), and tellurium (Te). These three common chalcogens possess similar chemical reactivities and readily undergo oxidation, as illustrated in Fig. 16. However, the difference in their electronegativity and atomic radius influences their oxidation sensitivity and reactivity. The one with the lowest electronegativity, tellurium, has the highest sensitivity, followed by selenium (Se), and lastly sulfur (S). These elements are typically integrated into the main chain and/or within the pendant groups to form various ether-based copolymers such as thioether (S-based), selenoether (Se-based), and telluroether (Te-based), which are activated based on the hydrophilicity of the ether group.

Similarly, telluroether has the highest sensitivity, followed by selenoether, and lastly thioether. For instance, Lee *et al.* developed three ROS-responsive amphiphilic block copolymers based on polycaprolactone (PCL) with selenide and sulfide pendent.<sup>149</sup> As expected, PCL-*co*-selenide demonstrated faster oxidation compared to PCL-*co*-sulfide due to the high sensitivity of selenide. However, it transformed back to its amphiphilic nature after the  $\beta$ -elimination reaction, leading to a poor disassociation and drug release performance. Their result showed that  $\alpha$ -ethylthio caprolactone displayed an excellent H<sub>2</sub>O<sub>2</sub>-induced hydrophobic-hydrophilic transition from ethyl thioether to its sulfoxide. This event resulted in excellent disassembly, demonstrating a promising vesicle for photodynamic therapy.<sup>150</sup>

Xu and group intensively researched selenoether-based copolymers. In their recent high-impact work, they successfully developed selenium-containing nanoparticles combining various cancer treatments (radiotherapy, immunotherapy, and chemotherapy), as illustrated in Fig. 19. Seleninic acid was formed upon the cleavage of the diselenide bonds under  $\gamma$ -radiation, which exhibited anticancer activity by upregulating the reROS levels in cancer cells, paving a promising path for simultaneous cancer treatment.<sup>113,151</sup> The tumor-targeting peptide-modified nanoparticles could actively accumulate in cancer cells through systemic administration. Following radiotherapy, the diselenide portion in the polymer was oxidized to seleninic acid, and the loaded drug DOX was released in the nucleus, realizing its chemotherapy function. The seleninic acid blocked HLA-E expression, and further enhanced the NK cell-mediated immunotherapy by releasing cytokines and lytic molecule (granzyme). Recently, Xu and team employed the hydrothermal process to fabricate carbon-dots with selenium-sulfur dynamic covalent bonds. The Se-S-CDs increased the thioredoxin reductase (TrxR) activity and enhanced the cell viability, demonstrating promising biological applications such as cell culturing.<sup>27,152,153</sup>

**2.4.3 Thioketal linkage.** Thioketal is a sulfur-based ROS-responsive group that undergoes an oxidative backbone cleavage mechanism to produce two thiols and a ketone product. Hence, polymers containing this linkage will degrade and dissociate in the presence of ROS, as shown in Fig. 16, and are widely used in drug delivery systems.<sup>154–157</sup> Wang *et al.* employed the thioketal linkage to develop a pathologically responsive mitochondrial gene delivery vector. Their recent work demonstrated the thioketal-based polymer dissociation by high mitochondrial ROS exposure to release functional DNA genes that improve the gene transfection efficiency and correct genetic abnormalities, showing great discovery in *in situ* mitochondrial gene therapy.<sup>154</sup> In a recent study, Li and Chen developed a thioketal-gated mesoporous silica nanoparticle by grafting ROS-sensitive mPEG on the particle surface. The vancomycin-loaded MSP displayed an excellent controlled release profile through thioketal cleavage. Besides, the antibacterial properties and non-cytotoxicity show its capability as an antibacterial material for wound treatment.<sup>157</sup>

**2.4.4 Aryl boronic ester.** Aryl boronic ester is an ROS-responsive functional group, which is widely utilized in the preparation of H<sub>2</sub>O<sub>2</sub>-responsive materials due to its selectivity and sensitivity towards H<sub>2</sub>O<sub>2</sub>. The linkage is usually attached as a pendant group and reacts with H<sub>2</sub>O<sub>2</sub> by the backbone breakage or hydrophilicity switch. For instance, Hsu and co-workers synthesized a PCL bearing pendant aryl boronic esters. Exposure to H<sub>2</sub>O<sub>2</sub> induced the migration of the aryl group to the oxygen atom, known as nucleophilic addition, followed by the hydrolysis of the borate ester to release phenol, which underwent 1,6-rearrangement. Subsequently, this rearrangement exposed the active phenol group. The copolymer showed high sensitivity to H<sub>2</sub>O<sub>2</sub> and good hydrolytic stability, allowing it to be used as a drug delivery carrier. Garcia *et al.* synthesized a diblock copolymer based on a hydrophilic PEG segment and an aryl boronic ester-functionalized hydrophobic polycarbonate segment. They systematically studied the oxidation of nanoparticles and found that the dissociation of aryl boronic ester was highly dependent on the polymer concentration, while the amount of H<sub>2</sub>O<sub>2</sub> could control the drug release amount.<sup>158</sup> In recent work, Jager prepared a novel ROS-responsive amphiphilic block copolymer comprised of a hydrophobic boronic ester-based ROS in the hydrophilic backbone. The copolymer yielded either the hydrophilic carboxylic acid or an amphiphilic phenol upon exposure to H<sub>2</sub>O<sub>2</sub> and displayed a hydrophilic switch before the controlled drug release.<sup>159</sup>

**2.4.5 Diselenide linkage.** Both oxidation responsiveness and reduction responsiveness can be found in diselenide-based copolymers due to the similar chemical properties of selenium and sulfur. The dual-responsive capability allows diverse applications in both physiological and pathological environments. In addition, the bond energy of diselenide (Se-Se 172 kJ mol<sup>-1</sup>) is much lower than that of the carbon-selenium bond, C-Se (244 kJ mol<sup>-1</sup>), and disulfide bonds (S-S, 240 kJ mol<sup>-1</sup>), making it more reactive to an external



stimulus. These findings were evinced in the work by Luo and Zhang, where (mPEG-PCL-Se)<sub>2</sub> tri-block copolymer micelles showed faster DOX release than the (mPEG-PCL-S)<sub>2</sub> tri-block copolymer micelles.<sup>161</sup> In another work, Tsai and co-workers developed a diselenide-linked polymeric nanogel (PEG-Se-Se). They performed the redox-responsive drug release study using 0.1% H<sub>2</sub>O<sub>2</sub> and 0.1 mg mL<sup>-1</sup> of GSH in PBS buffer with pH of 7.4 at 37 °C. The drug-loaded diselenide nanogel underwent bond cleavage under stimuli (H<sub>2</sub>O<sub>2</sub> and GSH), resulting in the release of the encapsulated DOX. The nanogel exhibited good DOX release profiles in the presence of both GSH (reductive) and H<sub>2</sub>O<sub>2</sub> (oxidative).<sup>162</sup>

Recently, Tian and co-workers designed 2-methacryloyloxyethyl phosphorylcholine (MPC) with a diselenide bond-containing crosslinker (*N,N'*-bis(methacryloyl) selenocystamine (BMASC)). Copolymerization resulted in the formation of a novel zwitterionic nanogel with an exceptional dual redox-labile property. As illustrated in Fig. 20, the diselenide linkage of the drug-loaded nanogel cleaved and dissociated in the reducing (GSH) and oxidative (H<sub>2</sub>O<sub>2</sub>) environments. Subsequently, the disintegrated nanogel released the drug effectively. In addition to its excellent release profile, the low leakage and non-cytotoxicity of the nanogel make it a suitable drug delivery carrier.<sup>160</sup>

**2.4.6 Azide-based linkage.** Currently, the bio-orthogonal azido group has been identified as a potential H<sub>2</sub>S-responsive copolymer due to its high H<sub>2</sub>S-responses, where azide reduction is the primary mechanism. For instance, Zhang and Lin prepared a series of H<sub>2</sub>S-trigger *N*-(2-hydroxyethyl)-4-azide-1,8-naphthalimide-ended amphiphilic diblock copolymers, poly(2-hydroxyethyl methacrylate)-*block*-poly(methyl methacrylate) (N<sub>3</sub>-Nap-PHEMA-*b*-PMMA-N<sub>3</sub>). Upon the introduction of H<sub>2</sub>S, the DOX-loaded micelles underwent charge reversal from negative to positive as the

azido functional group reduced. The cellular uptake of DOX-loaded micelles was improved by employing an electrostatic attraction, contributing to the fast DOX release rate for potential tumor diagnosis and therapy.<sup>140</sup>

In another work, Yan and Sang created a novel *O*-azido methyl benzoate (AzMB)-containing block copolymer that is highly responsive to H<sub>2</sub>S stimulus. As shown in Fig. 21, the cleavage of the AzMB functional group changed the amphiphilicity, leading to controlled dissociation of the self-assembled nanocapsule.<sup>141</sup> Similarly, Almutairi and Kawasaki developed a self-assembled H<sub>2</sub>S-responsive cholesterol-modified dextran (SC-Dex) nanogel in their recent work. In the presence of H<sub>2</sub>S, cholesterol dissociated from the main dextran chain *via* reduction and arrangement of the aryl azide functional group. Subsequently, the nanogel swelled and released the encapsulated protein controllably.<sup>142</sup>

**2.4.7 Other redox-responsive polymers.** Besides the several linkages mentioned above, other redox-sensitive bonds such as ferrocene-based and polyoxalate-based bonds were incorporated to create redox-responsive polymer delivery systems. Ferrocene is an organometallic chemical compound that is comprised of two coplanar cyclopentadienyl rings bound on opposite sides of a central iron (Fe) atom. These metallocenes are usually ROS responsive, stable, and have an excellent reversible redox property. Hydrophobic-hydrophilic conversion is the primary responsive mechanism, where the hydrophobic ferrocene groups are oxidized into hydrophilic ferricenium upon exposure to ROS. For instance, Xu and co-workers designed a ferrocene-containing amphiphilic block polymer (PACMO-*b*-PAEFC) *via* ATRP, with poly(2-acryloyl oxyethyl ferrocenecarboxylate) (PAEFC) as the hydrophobic component and poly(*N*-acryloyl morpholine) (PACMO) as the hydrophilic component. Under ROS triggering, the reductive ferrocene groups of the PACMO-*b*-PAEFC micelles were converted into the hydrophilic ferricenium, resulting in swelling and releasing the encapsulated drugs. In addition, the oxidative micelles could reversibly convert back upon

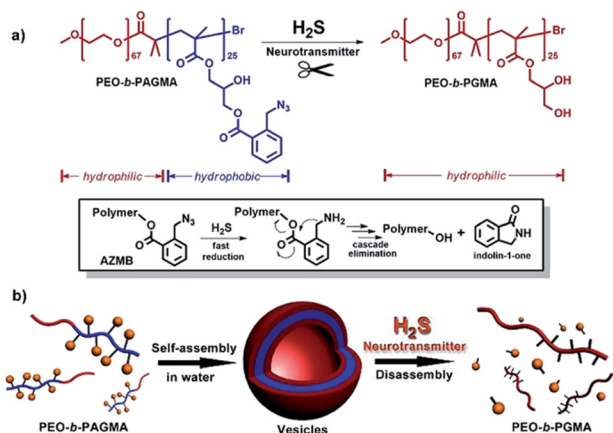


Fig. 21 (a) H<sub>2</sub>S-responsive cleavage of *O*-azido methyl benzoate (AzMB)-containing diblock copolymer (PEO-*b*-PAGMA) and H<sub>2</sub>S-induced cascade reaction mechanism. (b) Schematic illustration of polymer self-assembly into vesicles and H<sub>2</sub>S-responsive controlled disassembly process. Copyright (2016) adapted with permission from ref. 141 Copyright, 2020 Wiley.

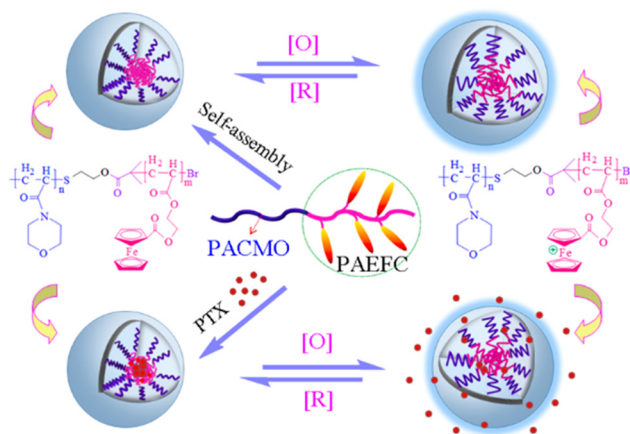


Fig. 22 Schematic diagram of the loading and *in vitro* release of drug from the copolymer micelles upon triggering by oxidation and reduction stimuli. Adapted with permission from ref. 163 Copyright 2017, the American Chemical Society.



reduction by vitamin C, as shown in Fig. 22.<sup>163</sup> In another work, Höcherl and Jäger<sup>164</sup> synthesized a novel self-immolating  $\text{H}_2\text{O}_2$ -sensitive biodegradable polyoxalate prodrug *via* a simple one-pot synthesis. The drug molecules were integrated into the backbone of the polymer with responsive polyoxalate bonds. The linkage underwent rapid chain-cleavage in an oxidative environment and effectively released the drugs as required.

## 2.5 pH-responsive polymers

pH-responsive polymers have great potential to be applied in fields such as drug delivery, although at present, significant limitations in polymer encapsulation-based delivery systems have been observed in clinical trials.<sup>90,165,166</sup> By carefully strategizing and tailoring the side chains of the polymer, the pH-responsive behaviours of these polymers can be manipulated *via* the bottom-up approach, achieving the appropriate response from the polymer at the chemical environment of the active site.<sup>9,90,167–171</sup> In this section, the pH-induced structural transformation of several responsive polymers including acid-labile polymers, crosslinking polymers, and zwitterionic polymers will be discussed. Given that there are a myriad of examples of pH-responsive polymers, we aim to highlight a few works and applications. The interested reader is referred to other comprehensive reviews in the literature regarding these polymers.<sup>172,173</sup>

**2.5.1 Boronic acid linkage.** Boronic acid-functionalised polymers pose a great advantage of structural reversibility in detection and sensor applications due to their reversible dynamic covalent bonds formed upon complexation with diol/catechol moieties.<sup>174</sup> The pH sensitivity of the complexation and dissociation from crosslinking of the polymer chains allows adverse changes in the physical properties of the polymer, resulting in a response to a change in the chemical environment.<sup>175</sup> In the following section, several examples of boronic acid polymers are highlighted to emphasize their efficiency as pH-responsive polymers for several loading and release responses on various substrates.

Ju *et al.* prepared a pH-responsive cellulose/4-vinyl-phenylboronic acid (VPBA) composite bio-hydrogel using electron-beam irradiation at room temperature for the polymerisation of VPBA to poly VPBA.<sup>176</sup> The novel composite bio-hydrogel was believed to have potential application in the biomedical field due to the incorporation of the biocompatible cellulose matrix.<sup>177</sup> They made use of the concept of reversibility of the complex formed between glucose monomers in cellulose and the phenylboronic acid in VPBA.<sup>178</sup> They also highlighted that the equilibrium established in aqueous medium between the neutral and anionic form of the borate was a crucial factor for the formation of covalent complexes, as shown in Fig. 23a. The complex formed between anionic boronic acid and glucose was stable, whereas the complex of neutral phenylboronic acid and glucose was unstable. The resulting ionisation equilibrium shifted towards the anionic phenylboronic acid.

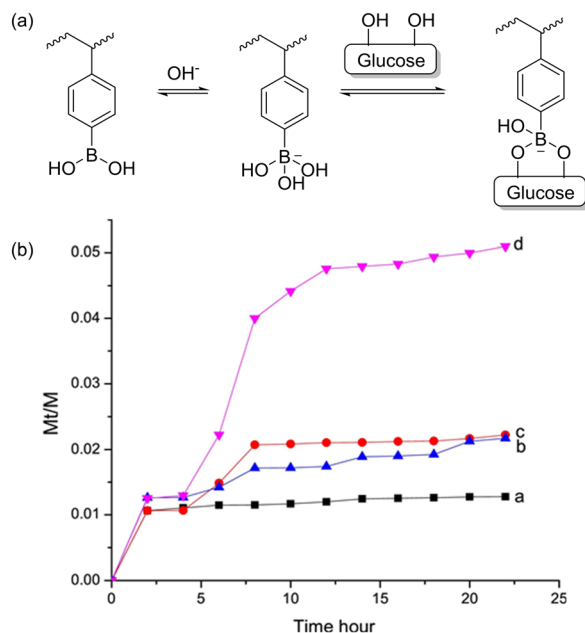
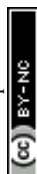


Fig. 23 (a) Equilibria of poly-4-vinyl-phenylboronic acid between neutral and anionic form and complexation with glucose. (b) Release profiles of FITC-insulin from cellulose/VPBA hydrogels at 28 °C, pH = 9.0, under various glucose concentrations: 0 g L<sup>-1</sup> (a), 1.0 g L<sup>-1</sup> (b), 3.0 g L<sup>-1</sup> (c) and 5.0 g L<sup>-1</sup> (d). Reproduced from ref. 176 with permission. Copyright 2018, Elsevier.

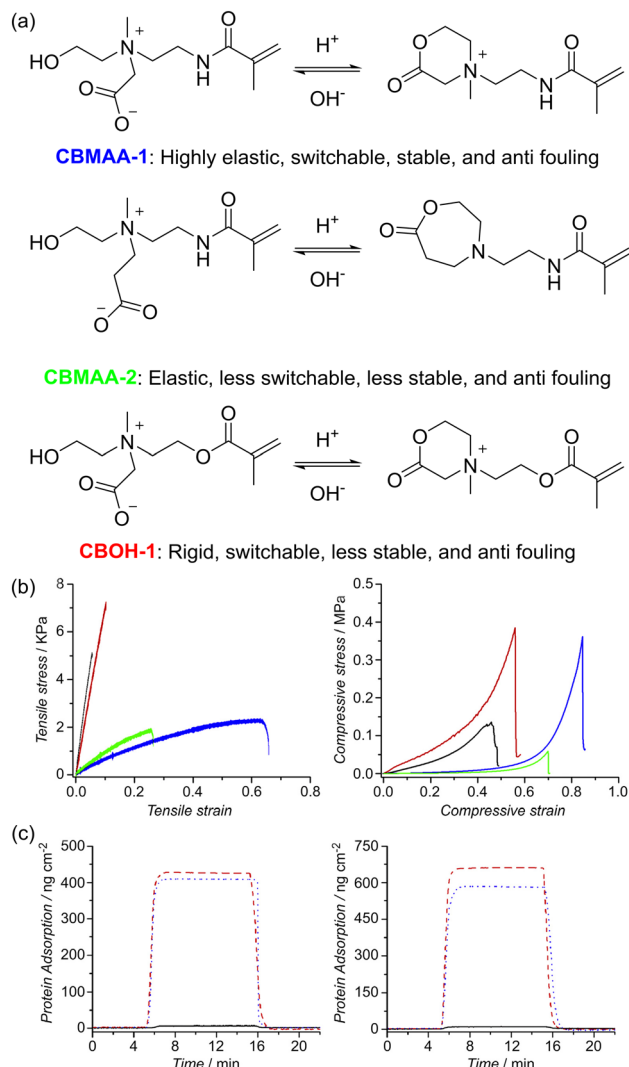
This demonstrates that two factors, *i.e.*, pH and glucose concentration, affect the equilibrium position between the charged and uncharged phenylboronic acid. Thus, the polymer characteristics such as hydrophilicity can be drastically affected upon regulation of the glucose level. Lastly, they demonstrated the responsive properties of the novel composite bio-hydrogel through the self-regulated release of insulin from the composite hydrogel through various concentrations of glucose solution. The release of the insulin was labelled *via* fluorescein isothiocyanate (FITC) for the tracking of fluorescence intensity of the external milieu. It was believed that a threshold concentration of glucose was responsible for triggering the spike in the release between 3.0–5.0 g L<sup>-1</sup>, as shown in Fig. 23b.

**2.5.2 Zwitterionic polymers.** Zwitterionic polymeric materials have attracted great interest due to their outstanding anti-fouling properties such as protein resistance<sup>179,180</sup> and slowing the growth of microorganisms.<sup>181,182</sup> However, currently, several limitations of zwitterionic materials such as their fragile and rigid nature, which limit their biocompatibility and utility in flexible medical devices,<sup>183,184</sup> need to be circumvented before the potentials of these materials can be fully realised. The examples illustrated in this section aim to address the limitations of zwitterionic polymers and highlight their potential as biomedical materials.

Cheng's group designed and synthesized an all-in-one tunable zwitterionic material (poly2-((2-hydroxyethyl)(2-methacrylamidoethyl)(methyl)ammonio)acetate (pCBMAA-1))

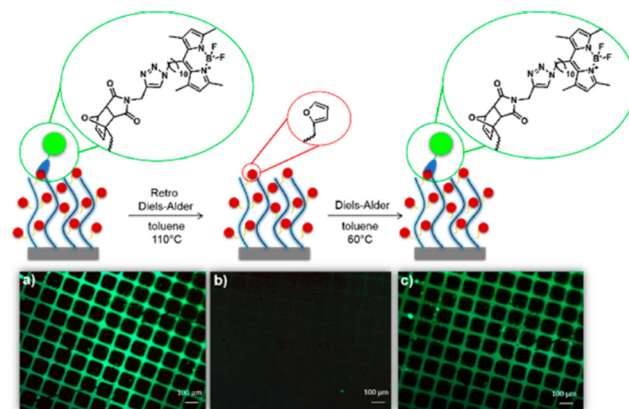


## Review



**Fig. 24** (a) Chemical structure and characteristics of carboxybetaine derivatives. All listed carboxybetaine derivatives show excellent antifouling properties. (b) Tensile (left) and compression (right) results for pCBMAA-1 (blue), pCBMAA-2 (green), pCBOH-1 (red), and pCBMA-2 (black) hydrogels prepared at 1.5 M (c) SPR sensorgrams showing ultralow fouling properties of zwitterionic pCBMAA-1 (left) and pCBMAA-2 (right) polymer brushes against the adsorption of 1 mg mL<sup>-1</sup> fibrinogen (black solid line), undiluted human plasma (red dash line) and undiluted human blood serum (blue dotted line). Reproduced from ref. 185 with permission. Copyright 2013, Elsevier.

encompassing elasticity, switchable antimicrobial-antifouling properties and stability.<sup>185</sup> In their design, a hydroxy group was introduced on one of the side chains of the quaternary ammonium to enable switchability from the cationic antimicrobial form to the zwitterionic antifouling form, as shown in Fig. 24a. CBMAA-2 is a variation of their original zwitterionic polymer CBMAA-1, with a seven-membered ring structure in the cationic form rather than the six-membered ring in CBMAA-1. The initial synthesis of the two polymers is illustrated in Fig. 24b. The physical properties of the two polymers were examined. As shown in Fig. 24c, both PCMAA-1 (blue) and PCMAA-2 (green) could



**Fig. 25** Fluorescence images of polymer brushes functionalized with BODIPY-maleimide (a) after Diels-Alder, (b) after retro-Diels-Alder and (c) after a second Diels-Alder reaction. Reproduced from ref. 203 with permission. Copyright 2017, the American Chemical Society.

withstand higher tensile and compressive strain than the methacrylate-based polymer pCBMOH-H. This was attributed to the higher hydrophilicity and stronger hydrogen bonds of methacrylamide compared to methacrylate, resulting in a softer and more elastic material. Surface plasmon resonance (SPR) results also showed that both pCBMAA-1 and pCBMAA-2 displayed excellent antifouling properties as the amount of protein adsorbed was below the detection limit (0.3 ng cm<sup>-2</sup>) of the SPR sensor.

## 2.6 Thermal-induced structure switch

Heat is a common stimulus that changes the physical properties of polymers,<sup>186</sup> in some cases due to the change in chemical structure *via* breaking or forming bonds, leading to even more significant changes such as changes in polymer solubility. These polymers are useful in some applications such as drug delivery,<sup>187,188</sup> thermoelectric generators,<sup>189,190</sup> thermal energy storage<sup>191–193</sup> and liquid chromatography.<sup>194,195</sup> In this section, we discuss polymers with thermal-induced chemical structural changes, with particular focus on reversible chemical transformation and phase transitions, which can act as a new type of phase-change material.<sup>196,197</sup> Also, we only give a brief overview of this topic, and the interested reader is referred to other comprehensive reviews.<sup>198,199</sup>

**2.6.1 Diels-Alder cycloaddition.** One of the most well-established reversible temperature-dependent reactions is the Diels-Alder (DA) cycloaddition. Briefly, cycloaddition typically occurs between electron-rich dienes, such as furans and pyrroles, with electron-deficient dienophiles, such as maleimides. These classical building blocks have been widely utilized in the synthesis of a variety of self-healing polymeric materials<sup>200,201</sup> and nanogels.<sup>202</sup> Some examples of these polymers that are capable of undergoing reversible DA and retro-DA reactions will be discussed.

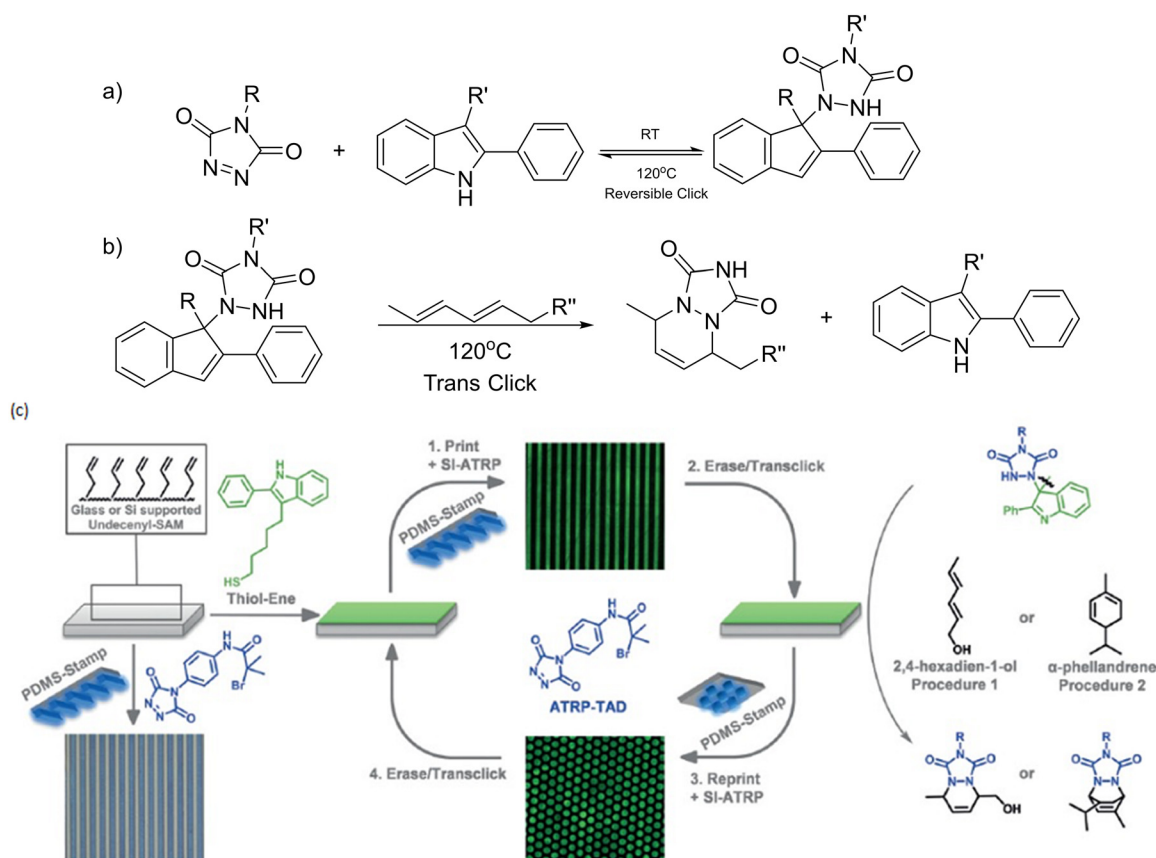


Sanyal and co-workers reported the first example of utilizing DA cycloaddition to conjugate maleimide-containing molecules on furan-containing polymer brushes under mild and reagent-free conditions.<sup>203</sup> The reaction was found to be highly efficient, functionalising all the polymer brushes at 60 °C (Fig. 25). The reaction was also found to be reversible at 110 °C *via* the retro-DA pathway. As a proof of concept, a fluorescent boron-dipyrromethene (BODIPY)-maleimide dye and a protein binding ligand were prepared and conjugated on the polymer brush. Green fluorescence was clearly observed after the reaction (Fig. 25b), which was completely quenched after the retro-DA (Fig. 25c).

Another example of reversible DA reaction was demonstrated by Du Prez and co-workers.<sup>204</sup> Triazolinodione (TAD) reversible click chemistry was combined with microcontact interactions to print, erase and reprint polymer brushes on a surface. The polymer brushes were first fabricated *via* ATRP of a TAD bearing-initiator on the surface of an alkene-modified substrate; in this case, glass or silicone-supported 10-undecenyl trichlorosilane self-assembled membrane (SAM) was used. Subsequent surface-induced ATRP produced substrates functionalised with micropatterned polymethylacrylate brushes. The indole-TAD

click reaction occurred at room temperature, while the reverse reaction was observed at a higher temperature of 120 °C. Upon covalent immobilization of the indole derivative on the substrate *via* ATRP, the desired imprinted micropattern could be observed by introducing fluorophores and examined using fluorescence microscopy. Erasure of TAD from the substrate could be achieved through an irreversible *trans*-click reaction by immersing the substrate in a solution of 2,4-hexadien-1-ol, regenerating the indole on the substrate. Fig. 26 illustrates the general rewritable process of the polymer brush and the substrate.

**2.6.2 Lower critical solution temperature (LCST)/upper critical solution temperature (UCST) polymers.** Reversibility in chemical bonds can also translate into drastic physical changes in the properties of polymers, such as solubility and miscibility of the polymer in aqueous medium. LCST refers to temperature below which polymers are fully miscible, while UCST refers to the temperature above which they are fully miscible. The presence of an LCST is often driven by unfavorable entropy changes upon mixing due to strong solvent-solute interactions. To date, the most explored polymer exhibiting LCST is poly(*N*-isopropylacrylamide) (PNIPAM), which exhibits an LCST with water of around 32



**Fig. 26** (a) TAD click reaction with an indole derivative, which is reversible at higher temperatures. (b) Example of a *trans*-click reaction: after the TAD-indole adduct is cleaved, the indole derivative is regenerated. (c) Functionalization of alkene-modified substrates by TAD click chemistry and generation of rewritable surfaces employing the *trans*-click approach using either 2,4-hexadien-1-ol (procedure 1) or  $\alpha$ -phellandrene (procedure 2). Reproduced from ref. 204 with permission. Copyright 2017, Wiley.



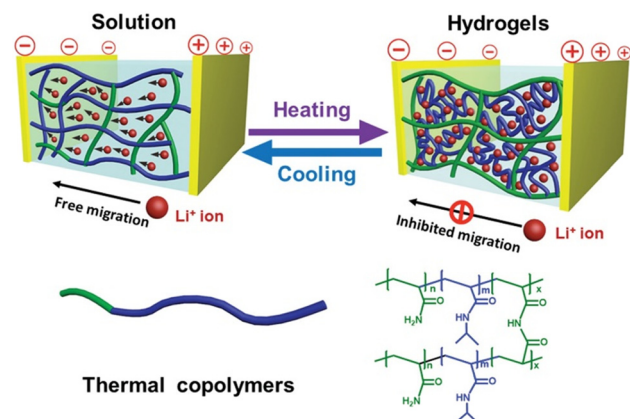


Fig. 27 Illustration of sol-gel transition of electrolyte that slows the migration of conductive ions between the electrodes. Upon increasing the temperature, the electrolyte solution transforms to a hydrogel through hydrophobic association. Reproduced from ref. 215 with permission. Copyright 2015, Wiley.

°C depending on the conditions. This thermal-responsive polymer is used to efficiently inhibit thermal runaways in devices such as lithium-ion batteries or supercapacitors<sup>205–210</sup> and building applications.<sup>211</sup> Some further examples of the applications of LCST/UCST polymers are presented in this section, although a full discussion is beyond the scope of this review, which has been thoroughly discussed elsewhere.<sup>212–214</sup>

In 2015, Chen and co-workers fabricated a thermal copolymer, poly(*N*-isopropylacrylamide-*co*-acrylamide) (PNIPAM/AM), using free radical polymerization with *N*-isopropylacrylamide (NIPAM) and acrylamide (AM) as monomers and bisacrylamide as a crosslinking reagent and AIBN as the polymerization initiator.<sup>215</sup> The copolymer was soluble in aqueous solutions below 32–34 °C given that it was hydrophilic.<sup>216,217</sup> The PNIPAM/AM solution was transformed into white hydrogels due to the disruption of the hydrogen bonds between the *N*-isopropyl groups and water, as shown in Fig. 27. Interestingly, the transition temperature for the phase change of the sol-gel process could be controlled by the adjusting the ratio of the monomers, *i.e.*, PNIPAM and AM, in the copolymer mix. They utilized the polymer as an electrolyte in supercapacitors and showcased the sol-gel process of the polymer to allow suppression or migration of conductive ions in the device upon an increase or reduction of the temperature, hence regulating the overall specific capacitance and impedance of the device.

Another example of a PNIPAM-based thermo-responsive polymer was reported by Chen and co-workers.<sup>218</sup> PNIPAM was dissolved in an ionic liquid solvent (1-methyl-3-methylimidazolium-bis(trifluoromethylsulfonyl)imide) to form an ionogel. At room temperature, this ionogel was plastic-like and rigid with an elastic modulus of 62.5 MPa. However, when heated above the UCST (~60.5 °C), the ionogel became transparent and soft with an elastic modulus of 0.66 kPa, representing a change in stiffness ratio by a

factor of  $10^5$  with a mild temperature change. The use of the phase transition to improve mechanical properties was also demonstrated by Marcellan's group.<sup>219</sup> Hong and Wu's group further exploited PNIPAM to prepare muscle-like hydrogels, which could be steered by light.<sup>220</sup> This was achieved by incorporating gold nanoparticles in the polymer to enhance the photo-thermal effect. Consequently, the robot could be driven by using green laser irradiation.

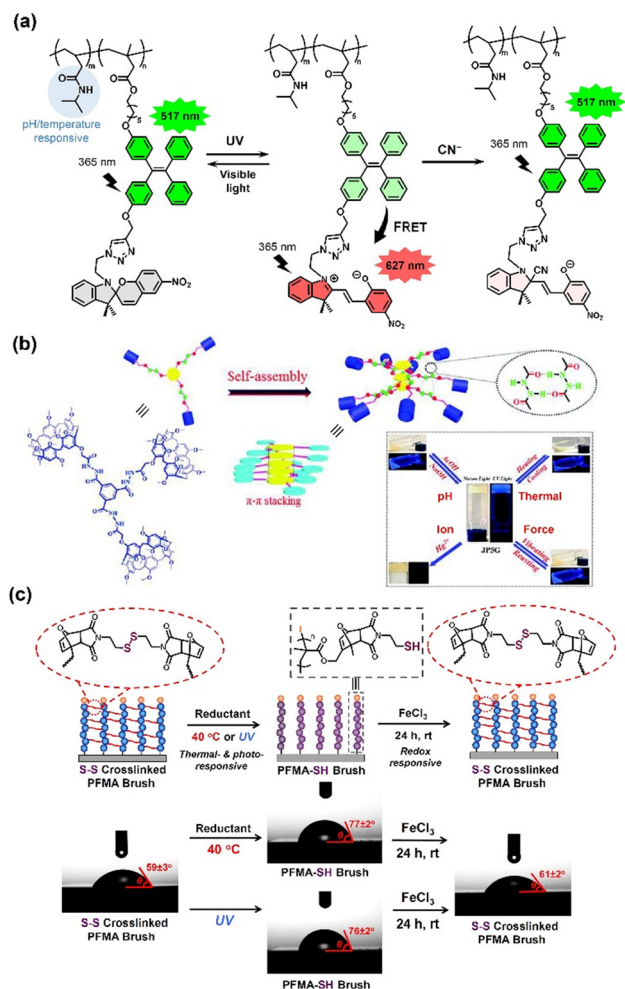
## 2.7 Multi-stimuli-responsive structure switch

The abovementioned functional groups can be incorporated into a polymer chain to achieve dual or multi-stimuli-responsive polymer materials.<sup>7,8,221</sup> These polymer materials enable reversible switching of their structures and properties *via* different stimuli for drug release, molecule sensing, healable materials, and smart surface applications. In this section, a few examples of polymer materials with a single type of multi-stimuli-responsive group or with multiple functional groups will be introduced.

Spiropyran is one of the most widely used photochromic compounds for multi-stimuli applications, boasting high responsivity to a multitude of environmental factors, such as light, pH, temperature and the presence of ions. As a distinct color change occurs during the reversible ring-opening formation of merocyanine from spiropyran, this makes it ideal to be used in the development of optical sensors.<sup>222</sup> Zhang *et al.* fabricated spiropyran-modified poly(*N*-isopropylacrylamide)-based multi-stimuli responsive microgels.<sup>223</sup> The microgel-based optical devices (etalons) showed reversible responsiveness to light, pH, temperature and copper(II) cation ( $\text{Cu}^{2+}$ ) concentrations. The microgels also exhibited two-photon fluorescence, highlighting their potential for applications in bioimaging. Similarly, Nhien and coworkers synthesized a novel multi-stimuli responsive amphiphilic aggregation-induced emission (AIE) copolymer using tetraphenylethylene-spiropyran monomers.<sup>224</sup> The polymer exhibited photo-switchable properties, with ratiometric fluorescence between the green tetraphenylethylene (517 nm) and red merocyanine emissions (627 nm) the Förster resonance energy transfer (FRET) process. In the ring-opened merocyanine form, the emission of the material showed a strong dependence on pH, temperature, and cyanide anion ( $\text{CN}^-$ ) concentration. Furthermore, due to its good biocompatibility coupled with low limit of detection (LOD = 0.26  $\mu\text{M}$ ) for aqueous  $\text{CN}^-$ , this material is a promising FRET sensor for the detection of  $\text{CN}^-$  in living cells.

Supramolecular polymer systems are popular components in the design of multi-stimuli responsive polymers. Through the use of multiple non-covalent binding motifs, these polymers are often capable of exhibiting reversible responsiveness to a myriad of stimuli.<sup>227–229</sup> For example, Jiang *et al.* reported the preparation of a stable supramolecular polymer containing tripodal pillar[5]arene tails. This supramolecular polymer could undergo a





**Fig. 28** (a) Chemical structures of AIE-containing copolymers and their reversible energy transfer *via* the FRET process. The structure switch can be quenched by adding  $\text{CN}^-$  ions. Adapted from ref. 224 with permission. Copyright 2020, the American Chemical Society. (b) Chemical structure and illustration of tripodal pillar[5]arene-based multi-stimuli-responsive supramolecular polymers. Adapted from ref. 225 with permission. Copyright 2018, the American Chemical Society. (c) Crosslinking and decrosslinking reactions of PFMA brush *via* thermal-, photo- and redox stimuli. The multi-stimuli responsive surfaces exhibited reversible and precise control of surface wettability, with images of the water contact angle measurement shown. Adapted from ref. 226 with permission. Copyright 2020, the American Chemical Society.

reversible gel-sol transition *via* pH, thermal, and force stimuli and demonstrated strong AIE after gelation (Fig. 28b).<sup>225</sup> Moreover, the polymer also displayed strong interaction with mercuric cation ( $\text{Hg}^{2+}$ ) to form a gel, indicating its potential application to remove  $\text{Hg}^{2+}$  from water. Hatai and coworkers used coumarin moieties together with a central 1,3,5-trisubstituted benzene core and poly(ethylene glycol) linkers to create a multi-stimuli responsive supramolecular polymer.<sup>230,231</sup> The material was found to be light and pH sensitive, owing to the photodimerization of coumarin and the cleavage of the hydrazone bonds, respectively. The addition of  $\text{Cu}^{2+}$  ions was

found to induce disassembly of the nanoaggregates. By controlling the 3 stimuli (light, pH and  $\text{Cu}^{2+}$  concentration), the aggregation behavior of the polymer could be controlled. This allowed the polymer to successfully achieve the encapsulation and targeted release of hydrophobic molecules, such as drugs and dyes. Xiong and coworkers employed a novel AIE luminogen to design an organic multi-stimuli-responsive fluorescent material.<sup>228,232</sup> Consisting of vinylpyridine motifs on a tetraphenylethene backbone, the AIE luminogen displayed reversible fluorescence under varying force, pH, and temperature stimuli. Due to the supramolecular intermolecular interactions and presence of a shrinkable space in the packing structure of the polymer, this material could sustain fluorescence emission even under external pressure as high as 11.25 GPa.

The Diels-Alder mechanism conjugates double-bond systems by reacting diene bonds with a single double bond, which is typically reversible by light and heat. This multi-stimulus-responsive conjugation has been used to impart reversibility to functional polymers. Yamamoto and coworkers demonstrated a multi-responsive reversible topologically converting polymers using anthracene and coumarin derivatives.<sup>233</sup> Exploiting the Diels-Alder mechanism, the polymers reversibly dimerized from a linear to cyclic structure and cleaved the anthryl groups by light or heat stimuli. Poly(ethylene oxide) with electron-donating and electron-withdrawing substituted anthryl end groups was irradiated at 365 nm for photo-dimerisation. Afterwards, linearization of the polymers was successfully achieved by heating at 150 °C. Sim *et al.* also employed the Diels-Alder mechanism and disulfide linkage to create multi-stimuli-responsive polymer brushes.<sup>226</sup> The authors uniquely applied bis(2-maleimidoethyl) disulfide to form a crosslinked poly(furfuryl methacrylate) (PFMA) brush gel *via* a Diels-Alder reaction. The disulfide bond (S-S) could cleave upon thermal or photo stimulus and rebridge under oxidative stimulus. The combination of Diels-Alder moieties and disulfide bonds allowed the polymer brush gels to be crosslinked and decrosslinked with thermal, photo and oxidative stimuli. The surface wettability and patterns could be precisely and spatially modulated and potentially applied for adsorptive/desorptive interfaces and rewritable interfaces.

The combination of functional groups and/or polymers with different stimuli-responsive properties also provide an effective method to prepare multi-stimuli responsive polymers. For example, Gebeyehu *et al.* developed a dual thermo- and photo-responsive supramolecular polymer based on uracil and oligomeric polypropylene glycol.<sup>234</sup> The thermo-sensitive polypropylene backbone was end-capped with photo-sensitive uracil moieties using a one-step Michael addition reaction and self-assembly of the oligomers was initiated by double hydrogen bonding interactions between the uracil moieties upon immersion in aqueous conditions. This polymer could self-assemble to form micelles and exhibit reversible phase transition behavior in aqueous solutions. By manipulating the concentration and duration of



**Table 1** Summary of working principals of stimuli-responsive polymers and their corresponding structures

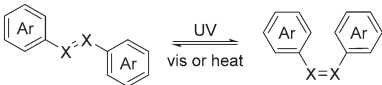
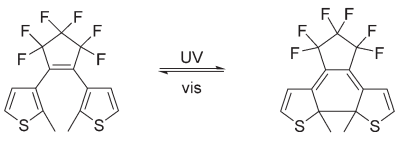
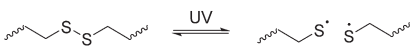
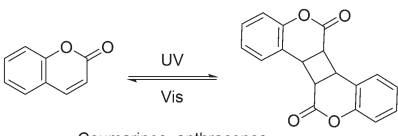
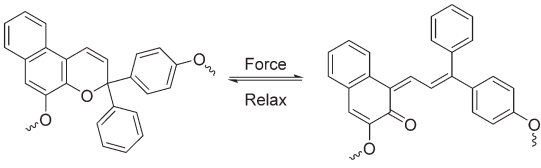

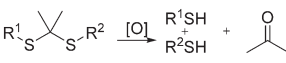
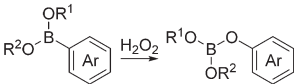
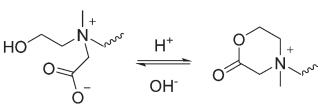
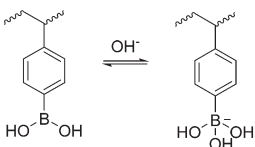
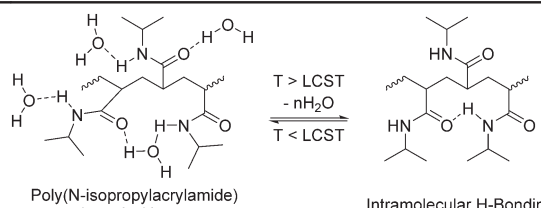
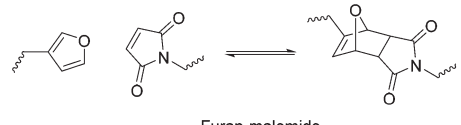
Type of stimuli	Working principal	Typical structures
Light	<i>Cis-Trans</i> isomerism	 <p>Azobenzenes, Stilbenes, Aliphatic ethylenes</p>
	Ring opening/closure	 <p>Spiroprans, dithienylethenes</p>
	Homolytic cleavage	 <p>Disulfides</p>
	Cycloaddition	 <p>Coumarines, anthracenes</p>
	Ring opening/closure	 <p>Spiroprans and naphthopyrans</p>
CO <sub>2</sub>	Macromolecular conformational change	 <p>Macromolecular Assemblies</p>
	Ionic incorporation (acid/base reaction)	$\begin{matrix} R^1 & & R^3 \\ & \diagdown & / \\ & N^+ & \\ & / & \diagdown \\ R^2 & & R^2 \end{matrix} + H_2O \xrightleftharpoons{CO_2} \begin{matrix} R^1 & & R^3 \\ & \diagdown & / \\ & N^+ & \\ & / & \diagdown \\ R^2 & & R^2 \end{matrix} + HCO_3^-$ <p>Guanidines, amidines, amines, carboxyls</p>
	Covalent incorporation	$\begin{matrix} R^1 & & R^3 \\ & \diagdown & / \\ & P^+ & \\ & / & \diagdown \\ R^2 & & R^2 \end{matrix} + \begin{matrix} R^1 & & R^3 \\ & \diagdown & / \\ & B^- & \\ & / & \diagdown \\ R^2 & & R^2 \end{matrix} \xrightleftharpoons{CO_2} \begin{matrix} R^1 & & R^3 \\ & \diagdown & / \\ & P^+ & \\ & / & \diagdown \\ R^2 & & R^2 \end{matrix} - O - \begin{matrix} R^1 & & R^3 \\ & \diagdown & / \\ & B^- & \\ & / & \diagdown \\ R^2 & & R^2 \end{matrix}$ <p>Amines, Frustrated Lewis pairs</p>
Redox	Oxidative cleavage	 <p>Thioether, disulfide, diselenide</p>
	Addition of oxygen	$\begin{matrix} R & & X & & R \\ & \diagdown & & / & \\ & C & & C & \\ & / & & \diagdown & \\ X & & S, Se, Te & & X \end{matrix} \xrightarrow{[O]} \begin{matrix} O & & O \\    & &    \\ R & & C & & R \end{matrix} \xrightarrow{[O]} \begin{matrix} O & & O \\    & &    \\ R & & C & & R \end{matrix}$ <p>Chalcogen ethers</p>
	Rearrangement	 <p>Boronic esters</p>
	Ring opening/closure	 <p>Lactones</p>
pH	Brønsted acid/base reaction	 <p>Boronic esters</p>



Table 1 (continued)

Type of stimuli	Working principal	Typical structures
Thermal	Change in solvation above and below LCST/UCST	 <p>Poly(N-isopropylacrylamide) solvated with water</p> <p>Intramolecular H-Bonding</p>
	Diels-Alder reaction	 <p>Furan-maleimide</p>

UV irradiation and aqueous solution temperature, these micelles displayed tunable and reversible hydrophilic/hydrophobic properties, which could potentially mimic biological processes for applications in drug delivery and gene transport. Jiang and the co-workers reported the preparation of triple-stimuli-responsive polymers by incorporating a redox-responsive ferrocene unit and a pH/CO<sub>2</sub>-responsive *N,N*-diethylamino ethyl group.<sup>235</sup> These polymers exhibited unique reversible phase transition behavior in an aqueous solution. For example, in an acidic environment, the polymers formed spherical particles, where the size and morphology of their aggregates changed upon oxidative stimuli given that the ferrocene segment switches their hydrophobic/hydrophilic properties.

### 3 Conclusions and outlook

The field of stimuli-responsive switchable polymers has progressed tremendously in the past two decades. Many of the stimuli-responsive moieties such as azobenzenes, spiropyranes, disulfide groups, and amidine groups have seen new applications, focusing on tuning their properties and their incorporation in new polymers. The fundamental understanding of the chemistry, structure, geometry and conformation of stimuli-responsive moieties as well as how these factors modulate the switchable functions and properties of the corresponding switchable stimuli-responsive polymers have also been significantly realized, allowing us to appropriately predict the properties of the polymers based on their chemical structure (as summarized in Table 1). Besides these well-known stimuli-responsive moieties, new stimuli-responsive structures have also been designed and developed, such as rotaxanes and some supramolecular polymers. The discovery of these stimuli-responsive species opens new opportunities for the development of advanced materials with desirable properties. Multi-stimuli-responsive polymer materials consisting of different stimuli-responsive moieties or a single stimuli-responsive moiety and capable of responding to different stimuli represent another interesting area to be explored. With the advancement of stimuli-

responsive polymers, we envision that they will continue to find new applications beyond the drug delivery, molecular sensing and self-healing functions emphasized in this review, while other applications such as artificial muscles and chameleon-like materials have also seen significant advances. We also believe that their current limitations such as rate of response, reversibility, and selectivity will be overcome with further research. Overall, we believe that the field of stimuli-responsive polymer materials will continue to advance and play an important role in future emerging smart materials.

### Conflicts of interest

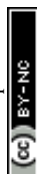
There are no conflicts to declare.

### Acknowledgements

This work was supported and acknowledged by the Agency of Science, Technology, and Research (A\*STAR) Advanced Manufacturing & Engineering – Young Individual Research Grant (AME-YIRG-A2084c0165).

### Notes and references

- 1 M. A. Stuart, W. T. Huck, J. Genzer, M. Muller, C. Ober, M. Stamm, G. B. Sukhorukov, I. Szleifer, V. V. Tsukruk and M. Urban, *et al.*, Emerging applications of stimuli-responsive polymer materials, *Nat. Mater.*, 2010, 9(2), 101.
- 2 M. Yoshida and J. Lahann, Smart Nanomaterials, *ACS Nano*, 2008, 2(6), 1101.
- 3 O. Sato, Dynamic molecular crystals with switchable physical properties, *Nat. Chem.*, 2016, 8(7), 644.
- 4 F. Guo and Z. Guo, Inspired smart materials with external stimuli responsive wettability: a review, *RSC Adv.*, 2016, 6(43), 36623.
- 5 J. Zhuang, M. R. Gordon, J. Ventura, L. Li and S. Thayumanavan, Multi-stimuli responsive macromolecules and their assemblies, *Chem. Soc. Rev.*, 2013, 42(17), 7421.
- 6 F. Liu and M. W. Urban, Recent advances and challenges in designing stimuli-responsive polymers, *Prog. Polym. Sci.*, 2010, 35(1–2), 3.



- 7 K. M. Herbert, S. Schrettl, S. J. Rowan and C. Weder, 50th Anniversary Perspective: Solid-State Multistimuli, Multiresponsive Polymeric Materials, *Macromolecules*, 2017, **50**(22), 8845.
- 8 X. Fu, L. Hosta-Rigau, R. Chandrawati and J. Cui, Multi-Stimuli-Responsive Polymer Particles, Films, and Hydrogels for Drug Delivery, *Chem*, 2018, **4**(9), 2084.
- 9 T. Wei, Z. Tang, Q. Yu and H. Chen, Smart Antibacterial Surfaces with Switchable Bacteria-Killing and Bacteria-Releasing Capabilities, *ACS Appl. Mater. Interfaces*, 2017, **9**(43), 37511.
- 10 R. Liang, L. Wang, H. Yu, A. Khan, B. Ul Amin and R. U. Khan, Molecular design, synthesis and biomedical applications of stimuli-responsive shape memory hydrogels, *Eur. Polym. J.*, 2019, **114**, 380.
- 11 J. Cao, X. Y. Tan, N. Jia, J. Zheng, S. W. Chien, H. K. Ng, C. K. I. Tan, H. Liu, Q. Zhu and S. Wang, *et al.*, Designing good compatibility factor in segmented Bi<sub>0.5</sub>Sb<sub>1.5</sub>Te<sub>3</sub> – GeTe thermoelectrics for high power conversion efficiency, *Nano Energy*, 2022, **96**, 107147.
- 12 J. Cao, J. Zheng, H. Liu, C. K. I. Tan, X. Wang, W. Wang, Q. Zhu, Z. Li, G. Zhang and J. Wu, Flexible elemental thermoelectrics with ultra-high power density, *Mater. Today Energy*, 2022, **25**, 100964.
- 13 M. H. Chua, X. Y. D. Soo, W. P. Goh, Z. M. Png, Q. Zhu and J. Xu, Thioxanthylum Cations: Highly Reversible Hydrochromic Materials with Tunable Color and Moisture Sensitivity, *Chem. – Eur. J.*, 2022, e202201975.
- 14 S. Wang, P. J. Ong, S. Liu, W. Thitsartarn, M. J. B. H. Tan, A. Suwardi, Q. Zhu and X. J. Loh, Recent Advances in Host-Guest Supramolecular Hydrogels for Biomedical Applications, *Chem. – Asian J.*, 2022, **17**(18), e202200608.
- 15 M. Ilčíková, J. Tkáč and P. Kasák, Switchable Materials Containing Polyzwitterion Moieties, *Polymers*, 2015, **7**(11), 2344.
- 16 H. Sun, C. P. Kabb, M. B. Sims and B. S. Sumerlin, Architecture-transformable polymers: Reshaping the future of stimuli-responsive polymers, *Prog. Polym. Sci.*, 2019, **89**, 61.
- 17 R. C. Duarte, A. A. V. Flores and M. Stevens, Camouflage through colour change: mechanisms, adaptive value and ecological significance, *Philos. Trans. R. Soc., B*, 2017, **372**, 1724.
- 18 L. M. Mathger, E. J. Denton, N. J. Marshall and R. T. Hanlon, Mechanisms and behavioural functions of structural coloration in cephalopods, *J. R. Soc., Interface*, 2009, **6**(Suppl 2), S149.
- 19 H. Nilsson Skold, S. Aspögren and M. Wallin, Rapid color change in fish and amphibians - function, regulation, and emerging applications, *Pigm. Cell Melanoma Res.*, 2013, **26**(1), 29.
- 20 J. K. Muiruri, J. C. C. Yeo, Q. Zhu, E. Y. Ye, X. J. Loh and Z. B. Li, Poly(hydroxyalkanoates): Production, Applications and End-of-Life Strategies-Life Cycle Assessment Nexus, *ACS Sustainable Chem. Eng.*, 2022, **10**(11), 3387.
- 21 H. J. Zhu, J. M. J. Qiang, C. G. Wang, C. Y. Chan, Q. Zhu, E. Y. Ye, Z. B. Li and X. J. Loh, Flexible polymeric patch based nanotherapeutics against non-cancer therapy, *Bioact. Mater.*, 2022, **18**, 471.
- 22 S. Sugiarto, R. R. Pong, Y. C. Tan, Y. Leow, T. Sathasivam, Q. Zhu, X. J. Loh and D. Kai, Advances in sustainable polymeric materials from lignocellulosic biomass, *Mater. Today Energy*, 2022, **26**, 101022.
- 23 E. Moulin, L. Faour, C. C. Carmona-Vargas and N. Giuseppone, From Molecular Machines to Stimuli-Responsive Materials, *Adv. Mater.*, 2020, **32**(20), e1906036.
- 24 X. Cao, A. Gao, J.-t. Hou and T. Yi, Fluorescent supramolecular self-assembly gels and their application as sensors: A review, *Coord. Chem. Rev.*, 2021, **434**, 213792.
- 25 H. Lambert, A. C. Bonillo, Q. Zhu, Y. W. Zhang and T. C. Lee, Supramolecular gating of guest release from cucurbit 7 uril using de novo design, *npj Comput. Mater.*, 2022, **8**(1), 471–491.
- 26 X. J. Loh, V. P. N. Nguyen, N. Kuo and J. Li, Encapsulation of basic fibroblast growth factor in thermogelling copolymers preserves its bioactivity, *J. Mater. Chem.*, 2011, **21**(7), 2246.
- 27 X. J. Loh, W. Guerin and S. M. Guillaume, Sustained delivery of doxorubicin from thermogelling poly (PEG/PPG/PTMC urethane)s for effective eradication of cancer cells, *J. Mater. Chem.*, 2012, **22**(39), 21249.
- 28 X. J. Loh, Poly (DMAEMA-co-PPGMA): Dual-responsive “reversible” micelles, *J. Appl. Polym. Sci.*, 2013, **127**(2), 992.
- 29 S. Wang, J. K. Muiruri, X. Y. D. Soo, S. Liu, W. Thitsartarn, B. H. Tan, A. Suwardi, Z. Li, Q. Zhu and X. J. Loh, Bio-PP and PP-based Biocomposites: Solutions for a Sustainable Future, *Chem. – Asian J.*, 2022, e202200972.
- 30 S. Sugiarto, R. Pong, Y. Tan, Y. Leow, T. Sathasivam, Q. Zhu, X. Loh and D. Kai, Advances in sustainable polymeric materials from lignocellulosic biomass, *Mater. Today Energy*, 2022, **26**, 101022.
- 31 G. S. Hartley, The Cis-form of Azobenzene, *Nature*, 1937, **140**(3537), 281.
- 32 H. M. D. Bandara and S. C. Burdette, Photoisomerization in different classes of azobenzene, *Chem. Soc. Rev.*, 2012, **41**(5), 1809.
- 33 M. Koch, M. Saphiannikova, S. Santer and O. Guskova, Photoisomers of Azobenzene Star with a Flat Core: Theoretical Insights into Multiple States from DFT and MD Perspective, *J. Phys. Chem. B*, 2017, **121**(37), 8854.
- 34 T. Fujino, S. Y. Arzhantsev and T. Tahara, Femtosecond Time-Resolved Fluorescence Study of Photoisomerization of trans-Azobenzene, *J. Phys. Chem. A*, 2001, **105**(35), 8123.
- 35 J. Volarić, J. Buter, A. M. Schulte, K.-O. van den Berg, E. Santamaría-Aranda, W. Szymanski and B. L. Feringa, Design and Synthesis of Visible-Light-Responsive Azobenzene Building Blocks for Chemical Biology, *J. Org. Chem.*, 2022, **87**(21), 14319.
- 36 A. A. Beharry, O. Sadoski and G. A. Woolley, Azobenzene Photoswitching without Ultraviolet Light, *J. Am. Chem. Soc.*, 2011, **133**(49), 19684.
- 37 F. Cheng, Y. Zhang, R. Yin and Y. Yu, Visible light induced bending and unbending behavior of crosslinked liquid-



- crystalline polymer films containing azotolane moieties, *J. Mater. Chem.*, 2010, **20**(23), 4888.
- 38 Z. Jiang, M. Xu, F. Li and Y. Yu, Red-Light-Controllable Liquid-Crystal Soft Actuators via Low-Power Excited Upconversion Based on Triplet-Triplet Annihilation, *J. Am. Chem. Soc.*, 2013, **135**(44), 16446.
  - 39 G. S. Kumar and D. C. Neckers, Photochemistry of azobenzene-containing polymers, *Chem. Rev.*, 1989, **89**(8), 1915.
  - 40 N. Anwar, T. Willms, B. Grimme and A. J. C. Kuehne, Light-Switchable and Monodisperse Conjugated Polymer Particles, *ACS Macro Lett.*, 2013, **2**(9), 766.
  - 41 H. Satzger, S. Spörlein, C. Root, J. Wachtveitl, W. Zinth and P. Gilch, Fluorescence spectra of trans- and cis-azobenzene – emission from the Franck-Condon state, *Chem. Phys. Lett.*, 2003, **372**(1), 216.
  - 42 H. Ren, D. Chen, Y. Shi, H. Yu and Z. Fu, Multi-responsive fluorescence of amphiphilic diblock copolymer containing carboxylate azobenzene and N-isopropylacrylamide, *Polymer*, 2016, **97**, 533.
  - 43 T. Morizo and K. Kenji, Isomerization of cis-Azobenzene in the Solid Phase, *Bull. Chem. Soc. Jpn.*, 1964, **37**(9), 1284.
  - 44 T. Yamamoto, Y. Norikane and H. Akiyama, Photochemical liquefaction and softening in molecular materials, polymers, and related compounds, *Polym. J.*, 2018, **50**(8), 551.
  - 45 H. S. Blair, H. I. Pague and J. E. Riordan, Photoresponsive effects in azo polymers, *Polymer*, 1980, **21**(10), 1195.
  - 46 H. Zhou, C. Xue, P. Weis, Y. Suzuki, S. Huang, K. Koynov, G. K. Auernhammer, R. Berger, H.-J. Butt and S. Wu, Photoswitching of glass transition temperatures of azobenzene-containing polymers induces reversible solid-to-liquid transitions, *Nat. Chem.*, 2017, **9**(2), 145.
  - 47 T. Yoshino, M. Kondo, J.-i. Mamiya, M. Kinoshita, Y. Yu and T. Ikeda, Three-Dimensional Photomobility of Crosslinked Azobenzene Liquid-Crystalline Polymer Fibers, *Adv. Mater.*, 2010, **22**(12), 1361.
  - 48 M. Chen, B. Yao, M. Kappl, S. Liu, J. Yuan, R. Berger, F. Zhang, H. J. Butt, Y. Liu and S. Wu, Entangled Azobenzene-Containing Polymers with Photoinduced Reversible Solid-to-Liquid Transitions for Healable and Reprocessable Photoactuators, *Adv. Funct. Mater.*, 2019, **30**(4), 1906752.
  - 49 Y. Yue, Y. Norikane, R. Azumi and E. Koyama, Light-induced mechanical response in crosslinked liquid-crystalline polymers with photoswitchable glass transition temperatures, *Nat. Commun.*, 2018, **9**(1), 3234.
  - 50 X. Lu, S. Guo, X. Tong, H. Xia and Y. Zhao, Tunable Photocontrolled Motions Using Stored Strain Energy in Malleable Azobenzene Liquid Crystalline Polymer Actuators, *Adv. Mater.*, 2017, **29**(28), 1606467.
  - 51 J. Zheng, Z. M. Png, S. H. Ng, G. X. Tham, E. Ye, S. S. Goh, X. J. Loh and Z. Li, Vitrimers: Current research trends and their emerging applications, *Mater. Today*, 2021, **51**, 586.
  - 52 A. S. Kuenstler, K. D. Clark, J. Read de Alaniz and R. C. Hayward, Reversible Actuation via Photoisomerization-Induced Melting of a Semicrystalline Poly(Azobenzene), *ACS Macro Lett.*, 2020, **9**(6), 902.
  - 53 Q.-T. Fu, X. Yan, T. Li, X.-Y. Zhang, Y. He, W.-D. Zhang, Y. Liu, Y. Li and Z.-G. Gu, Diarylethene-based conjugated polymer networks for ultrafast photochromic films, *New J. Chem.*, 2019, **43**(39), 15797.
  - 54 T. Fukushima, K. Tamaki, A. Isobe, T. Hirose, N. Shimizu, H. Takagi, R. Haruki, S.-i. Adachi, M. J. Hollamby and S. Yagai, Diarylethene-Powered Light-Induced Folding of Supramolecular Polymers, *J. Am. Chem. Soc.*, 2021, **143**(15), 5845.
  - 55 M. Irie and M. Mohri, Thermally irreversible photochromic systems. Reversible photocyclization of diarylethene derivatives, *J. Org. Chem.*, 1988, **53**(4), 803.
  - 56 M. Irie, T. Fukaminato, K. Matsuda and S. Kobatake, Photochromism of Diarylethene Molecules and Crystals: Memories, Switches, and Actuators, *Chem. Rev.*, 2014, **114**(24), 12174.
  - 57 K. Matsuda and M. Irie, Diarylethene as a photoswitching unit, *J. Photochem. Photobiol., C*, 2004, **5**(2), 169.
  - 58 J. Zhang and H. Tian, The Endeavor of Diarylethenes: New Structures, High Performance, and Bright Future, *Adv. Opt. Mater.*, 2018, **6**(6), 1701278.
  - 59 A. M. Asadirad, S. Boutault, Z. Erno and N. R. Branda, Controlling a polymer adhesive using light and a molecular switch, *J. Am. Chem. Soc.*, 2014, **136**(8), 3024.
  - 60 L. Oggioni, C. Toccafondi, G. Pariani, L. Colella, M. Canepa, C. Bertarelli and A. Bianco, Photochromic Polyurethanes Showing a Strong Change of Transparency and Refractive Index, *Polymers*, 2017, **9**(9), 462.
  - 61 S. Ikejiri, Y. Takashima, M. Osaki, H. Yamaguchi and A. Harada, Solvent-Free Photoresponsive Artificial Muscles Rapidly Driven by Molecular Machines, *J. Am. Chem. Soc.*, 2018, **140**(49), 17308.
  - 62 Y. Hirshberg and E. Fischer, Multiple Reversible Color Changes Initiated by Irradiation at Low Temperature, *J. Chem. Phys.*, 1953, **21**(9), 1619.
  - 63 V. I. Minkin, Photo-, Thermo-, Solvato-, and Electrochromic Spiroheterocyclic Compounds, *Chem. Rev.*, 2004, **104**(5), 2751.
  - 64 R. Klajn, Spiropyran-based dynamic materials, *Chem. Soc. Rev.*, 2014, **43**(1), 148.
  - 65 L. Wang and Q. Li, Photochromism into nanosystems: towards lighting up the future nanoworld, *Chem. Soc. Rev.*, 2018, **47**(3), 1044.
  - 66 L. Kortekaas and W. R. Browne, The evolution of spiropyran: fundamentals and progress of an extraordinarily versatile photochrome, *Chem. Soc. Rev.*, 2019, **48**(12), 3406.
  - 67 C. Li, A. Iscen, L. C. Palmer, G. C. Schatz and S. I. Stupp, Light-Driven Expansion of Spiropyran Hydrogels, *J. Am. Chem. Soc.*, 2020, **142**(18), 8447.
  - 68 T. Satoh, K. Sumaru, T. Takagi and T. Kanamori, Fast-reversible light-driven hydrogels consisting of spirobenzopyran-functionalized poly(N-isopropylacrylamide), *Soft Matter*, 2011, **7**(18), 8030.



- 69 W. Francis, A. Dunne, C. Delaney, L. Florea and D. Diamond, Spiropyran based hydrogels actuators—Walking in the light, *Sens. Actuators, B*, 2017, **250**, 608.
- 70 B. Razavi, A. Abdollahi, H. Roghani-Mamaqani and M. Salami-Kalajahi, Light- and temperature-responsive micellar carriers prepared by spiropyran-initiated atom transfer polymerization: Investigation of photochromism kinetics, responsivities, and controlled release of doxorubicin, *Polymer*, 2020, **187**, 122046.
- 71 L. Zhou, Z. Chen, K. Dong, M. Yin, J. Ren and X. Qu, DNA-mediated Construction of Hollow Upconversion Nanoparticles for Protein Harvesting and Near-Infrared Light Triggered Release, *Adv. Mater.*, 2014, **26**(15), 2424.
- 72 S. Chen, Y. Gao, Z. Cao, B. Wu, L. Wang, H. Wang, Z. Dang and G. Wang, Nanocomposites of Spiropyran-Functionalized Polymers and Upconversion Nanoparticles for Controlled Release Stimulated by Near-Infrared Light and pH, *Macromolecules*, 2016, **49**(19), 7490.
- 73 S. Takenouchi, A. Takasu, Y. Inai and T. Hirabayashi, Effects of Geometrical Difference of Unsaturated Aliphatic Polyesters on Their Biodegradability II. Isomerization of Poly(maleic anhydride-co-propylene oxide) in the Presence of Morpholine, *Polym. J.*, 2002, **34**(1), 36.
- 74 Q. A. Zhu and Y. X. Lu, Facile Synthesis of Bicyclic Amidines and Imidazolines from 1,2-Diamines, *Org. Lett.*, 2010, **12**(18), 4156.
- 75 W. T. Neo, Q. Ye, M. H. Chua, Q. Zhu and J. Xu, Solution-Processable Copolymers Based on Triphenylamine and 3, 4-Ethylenedioxythiophene: Facile Synthesis and Multielectrochromism, *Macromol. Rapid Commun.*, 2020, **41**(21), 2000156.
- 76 Q. Zhu, S. Wang, X. Wang, A. Suwardi, M. H. Chua, X. Y. D. Soo and J. Xu, Bottom-up engineering strategies for high-performance thermoelectric materials, *Nano-Micro Lett.*, 2021, **13**(1), 1.
- 77 Z. Q. Wan, W. M. Ren, S. Yang, M. R. Li, G. G. Gu and X. B. Lu, Reversible Transformation between Amorphous and Crystalline States of Unsaturated Polyesters by Cis-Trans Isomerization, *Angew. Chem., Int. Ed.*, 2019, **58**(49), 17636.
- 78 T. M. McGuire, C. Pérale, R. Castaing, G. Kociok-Köhn and A. Buchard, Divergent Catalytic Strategies for the Cis/Trans Stereoselective Ring-Opening Polymerization of a Dual Cyclic Carbonate/Olefin Monomer, *J. Am. Chem. Soc.*, 2019, **141**(34), 13301.
- 79 T. Hughes, G. P. Simon and K. Saito, Light-Healable Epoxy Polymer Networks via Anthracene Dimer Scission of Diamine Crosslinker, *ACS Appl. Mater. Interfaces*, 2019, **11**(21), 19429.
- 80 Q. Chen, Q. Yang, P. Gao, B. Chi, J. Nie and Y. He, Photopolymerization of Coumarin-Containing Reversible Photoresponsive Materials Based on Wavelength Selectivity, *Ind. Eng. Chem. Res.*, 2019, **58**(8), 2970.
- 81 Y. Li, Y. Zhang, O. Rios, J. K. Keum and M. R. Kessler, Photo-responsive liquid crystalline epoxy networks with exchangeable disulfide bonds, *RSC Adv.*, 2017, **7**(59), 37248.
- 82 L. Wu, S. Di Cio, H. S. Azevedo and J. E. Gautrot, Photoconfigurable, Cell-Remodelable Disulfide Cross-linked Hyaluronic Acid Hydrogels, *Biomacromolecules*, 2020, **21**(12), 4663.
- 83 K. M. Wiggins, J. N. Brantley and C. W. Bielawski, Methods for activating and characterizing mechanically responsive polymers, *Chem. Soc. Rev.*, 2013, **42**(17), 7130.
- 84 H. Traeger, D. J. Kiebal, C. Weder and S. Schrettl, From Molecules to Polymers—Harnessing Inter- and Intramolecular Interactions to Create Mechanochromic Materials, *Macromol. Rapid Commun.*, 2021, **42**(1), 2000573.
- 85 W. Qiu, P. A. Gurr, G. da Silva and G. G. Qiao, Insights into the mechanochromism of spiropyran elastomers, *Polym. Chem.*, 2019, **10**(13), 1650.
- 86 S. K. Osler, M. E. McFadden and M. J. Robb, Comparison of the reactivity of isomeric 2H- and 3H-naphthopyran mechanophores, *J. Polym. Sci.*, 2021, **59**(21), 2537.
- 87 E. Izak-Nau, D. Campagna, C. Baumann and R. Göstl, Polymer mechanochemistry-enabled pericyclic reactions, *Polym. Chem.*, 2020, **11**(13), 2274.
- 88 Y. Chen, G. Mellot, D. van Luijk, C. Creton and R. P. Sijbesma, Mechanochemical tools for polymer materials, *Chem. Soc. Rev.*, 2021, **50**(6), 4100.
- 89 S. K. Osler, M. E. McFadden and M. J. Robb, Comparison of the reactivity of isomeric 2H- and 3H-naphthopyran mechanophores, *J. Polym. Sci.*, 2021, 2537–2544.
- 90 X. J. Loh, Z.-X. Zhang, K. Y. Mya, Y.-I. Wu, C. B. He and J. Li, Efficient gene delivery with paclitaxel-loaded DNA-hybrid polyplexes based on cationic polyhedral oligomeric silsesquioxanes, *J. Mater. Chem.*, 2010, **20**(47), 10634.
- 91 J. Y. Lim, S. S. Goh, S. S. Liow, K. Xue and X. J. Loh, Molecular gel sorbent materials for environmental remediation and wastewater treatment, *J. Mater. Chem. A*, 2019, **7**(32), 18759.
- 92 X. Fan, B. H. Tan, Z. Li and X. J. Loh, Control of PLA stereoisomers-based polyurethane elastomers as highly efficient shape memory materials, *ACS Sustainable Chem. Eng.*, 2017, **5**(1), 1217.
- 93 X. J. Loh, J. Gong, M. Sakuragi, T. Kitajima, M. Liu, J. Li and Y. Ito, Surface coating with a thermoresponsive copolymer for the culture and non-enzymatic recovery of mouse embryonic stem cells, *Macromol. Biosci.*, 2009, **9**(11), 1069.
- 94 T. Muramatsu, Y. Okado, H. Traeger, S. Schrettl, N. Tamaoki, C. Weder and Y. Sagara, Rotaxane-Based Dual Function Mechanophores Exhibiting Reversible and Irreversible Responses, *J. Am. Chem. Soc.*, 2021, **143**(26), 9884.
- 95 Y. Sagara, H. Traeger, J. Li, Y. Okado, S. Schrettl, N. Tamaoki and C. Weder, Mechanically Responsive Luminescent Polymers Based on Supramolecular Cyclophane Mechanophores, *J. Am. Chem. Soc.*, 2021, **143**(14), 5519.
- 96 K. Imato, R. Yamanaka, H. Nakajima and N. Takeda, Fluorescent supramolecular mechanophores based on



- charge-transfer interactions, *Chem. Commun.*, 2020, **56**(57), 7937.
- 97 S. Kato, K. Ishizuki, D. Aoki, R. Goseki and H. Otsuka, Freezing-Induced Mechanoluminescence of Polymer Gels, *ACS Macro Lett.*, 2018, **7**(9), 1087.
  - 98 T. Sumi, R. Goseki and H. Otsuka, Tetraarylsuccinonitriles as mechanochromophores to generate highly stable luminescent carbon-centered radicals, *Chem. Commun.*, 2017, **53**(87), 11885.
  - 99 F. Hoshino, T. Kosuge, D. Aoki and H. Otsuka, Mechanofluorescent polymer/silsesquioxane composites based on tetraarylsuccinonitrile, *Mater. Chem. Front.*, 2019, **3**(12), 2681.
  - 100 Y. Lin, T. B. Kouznetsova and S. L. Craig, Mechanically Gated Degradable Polymers, *J. Am. Chem. Soc.*, 2020, **142**(5), 2105.
  - 101 H. Qian, N. S. Purwanto, D. G. Ivanoff, A. J. Halmes, N. R. Sottos and J. S. Moore, Fast, reversible mechanochromism of regioisomeric oxazine mechanophores: Developing in situ responsive force probes for polymeric materials, *Chem.*, 2021, **7**(4), 1080.
  - 102 M. F. Cunningham and P. G. Jessop, Carbon Dioxide-Switchable Polymers: Where Are the Future Opportunities?, *Macromolecules*, 2019, **52**, 6801.
  - 103 S. Lin and P. Theato, CO<sub>2</sub> - Responsive Polymers, *Macromol. Rapid Commun.*, 2013, **34**, 1118.
  - 104 B. Jiang, Y. Zhang, X. Huang, T. Kang, S. J. Severtson, W.-J. Wang and L. Pingwei, Tailoring CO<sub>2</sub>-Responsive Polymers and Nanohybrids for Green Chemistry and Processes, *Ind. Eng. Chem. Res.*, 2019, **58**, 15088.
  - 105 P. G. Jessop and M. F. Cunningham, in *CO<sub>2</sub>-switchable Materials*, Royal Society of Chemistry, 2020, DOI: [10.1039/9781788012850-00001](https://doi.org/10.1039/9781788012850-00001).
  - 106 T. Thambi, V. G. Deepagan, H. Y. Yoon, H. S. Han, S.-H. Kim, S. Son, D.-G. Jo, C.-H. Ahn, Y. D. Suh and K. Kim, *et al.*, Hypoxia-responsive polymeric nanoparticles for tumor-targeted drug delivery, *Biomaterials*, 2014, **35**(5), 1735.
  - 107 L. Phan, D. Chiu, D. J. Heldebrant, H. Huttenhower, E. John, X. Li, P. Pollet, R. Wang, C. A. Eckert and C. L. Liotta, *et al.*, Switchable Solvents Consisting of Amidine/Alcohol or Guanidine/Alcohol Mixtures, *Ind. Eng. Chem. Res.*, 2008, **47**, 539.
  - 108 J. Y. Quek, P. J. Roth, R. A. Evans, T. P. Davis and A. B. Lowe, Reversible addition-fragmentation chain transfer synthesis of amidine-based, CO<sub>2</sub>-responsive homo and AB diblock (Co)polymers comprised of histamine and their gas-triggered self-assembly in water, *J. Polym. Sci., Part A: Polym. Chem.*, 2013, **51**(2), 394.
  - 109 P. Schattling, I. Pollmann and P. Theato, Synthesis of CO<sub>2</sub>-responsive polymers by post-polymerization modification, *React. Funct. Polym.*, 2014, **75**, 16.
  - 110 Y. Liu, P. G. Jessop, M. Cunningham, C. A. Eckert and C. L. Liotta, Switchable Surfactants, *Science*, 2006, **313**, 958–960.
  - 111 Q. Yan, R. Zhou, C. Fu, H. Zhang, Y. Yin and J. Yuan, CO<sub>2</sub>-responsive polymeric vesicles that breathe, *Angew. Chem., Int. Ed.*, 2011, **50**(21), 4923.
  - 112 H. Liu, S. Lin, Y. Feng and P. Theato, CO<sub>2</sub>-Responsive polymer materials, *Polym. Chem.*, 2017, **8**(1), 12.
  - 113 L. Dong and Y. Zhao, CO<sub>2</sub>-switchable membranes: structures, functions, and separation applications in aqueous medium, *J. Mater. Chem. A*, 2020, **8**(33), 16738.
  - 114 S. Chen, X. Lin, Z. Zhai, R. Lan, J. Li, Y. Wang, S. Zhou, Z. H. Farooqi and W. Wu, Synthesis and characterization of CO<sub>2</sub>-sensitive temperature-responsive catalytic poly(ionic liquid) microgels, *Polym. Chem.*, 2018, **9**(21), 2887.
  - 115 W. Fan, X. Tong, F. Farnia, B. Yu and Y. Zhao, CO<sub>2</sub>-Responsive Polymer Single-Chain Nanoparticles and Self-Assembly for Gas-Tunable Nanoreactors, *Chem. Mater.*, 2017, **29**(13), 5693.
  - 116 M. Ramezanpour and A. Rezaee Shirin-Abadi, Emulsion polymerization using three types of RAFT prepared well-defined polymeric stabilizers based on 2-dimethylaminoethyl methacrylate (DMAEMA) under CO<sub>2</sub> atmosphere: a comparative study, *J. Polym. Res.*, 2021, **28**(7), 1189–1198.
  - 117 M. Mu, R. Yuan, G. Zhang, D. Wu, H. Quan, P. Han and Y. Feng, Tuning CO<sub>2</sub>-induced reversible redispersion or irreversible destabilisation for latex separation, *J. Colloid Interface Sci.*, 2020, **573**, 250.
  - 118 Y. Jiang, T. Zhang, Z. Yi, Y. Han, X. Su and Y. Feng, Diblock, Triblock and Cyclic Amphiphilic Copolymers with CO<sub>2</sub> Switchability: Effects of Topology, *Polymers*, 2020, **12**(4), 984.
  - 119 A. Rezaee Shirin-Abadi, A. Darabi, P. G. Jessop and M. F. Cunningham, Tuning the aggregation and redispersion behavior of CO<sub>2</sub>-switchable latexes by a combination of DMAEMA and PDMAEMA-b-PMMA as stabilizing moieties, *Polymer*, 2016, **106**, 303–312.
  - 120 A. R. Shirin-Abadi, P. G. Jessop and M. F. Cunningham, In Situ Use of Aqueous RAFT Prepared Poly(2-(diethylamino) ethyl methacrylate) as a Stabilizer for Preparation of CO<sub>2</sub> Switchable Latexes, *Macromol. React. Eng.*, 2017, **11**(1), 1600035.
  - 121 A. Rezaee Shirin-Abadi, A. Darabi, P. G. Jessop and M. F. Cunningham, Tuning the aggregation and redispersion behavior of CO<sub>2</sub>-switchable latexes by a combination of DMAEMA and PDMAEMA-b-PMMA as stabilizing moieties, *Polymer*, 2016, **106**, 303.
  - 122 J. Zhang, Y. Liu, J. Guo, Y. Yu, Y. Li and X. Zhang, A CO<sub>2</sub>-responsive PAN/PAN-co-PDEAEMA membrane capable of cleaning protein foulant without the aid of chemical agents, *React. Funct. Polym.*, 2020, **149**, 104503.
  - 123 C. Yin, L. Dong, Z. Wang, M. Chen, Y. Wang and Y. Zhao, CO<sub>2</sub>-responsive graphene oxide nanofiltration membranes for switchable rejection to cations and anions, *J. Membr. Sci.*, 2019, **592**, 117374.
  - 124 H. Yin, H. Liu, W. Wang and Y. Feng, CO<sub>2</sub>-Induced Reversible Dispersion of Graphene by a Melamine Derivative, *Langmuir*, 2015, **31**(44), 12260.
  - 125 H. Yin, F. Zhan, Z. Li, H. Huang, P. Marcasuzaa, X. Luo, Y. Feng and L. Billon, CO<sub>2</sub>-Triggered ON/OFF Wettability Switching on Bioinspired Polylactic Acid Porous Films for Controllable Bioadhesion, *Biomacromolecules*, 2021, **22**(4), 1721.



- 126 R. Liang, X. Yang, P. Y. M. Yew, S. Sugiarto, Q. Zhu, J. Zhao, X. J. Loh, L. Zheng and D. Kai, PLA-lignin nanofibers as antioxidant biomaterials for cartilage regeneration and osteoarthritis treatment, *J. Nanobiotechnol.*, 2022, 327.
- 127 X. Y. D. Soo, S. Wang, C. C. J. Yeo, J. Li, X. P. Ni, L. Jiang, K. Xue, Z. Li, X. Fei and Q. Zhu, Polylactic acid face masks: Are these the sustainable solutions in times of COVID-19 pandemic?, *Sci. Total Environ.*, 2022, **807**, 151084.
- 128 Y. Zhang, H. Yin and Y. Feng, CO<sub>2</sub>-responsive anionic wormlike micelles based on natural erucic acid, *Green Mater.*, 2014, **2**(2), 95.
- 129 V. Fischer, K. Landfester and R. Muñoz-Espí, Molecularly Controlled Coagulation of Carboxyl-Functionalized Nanoparticles Prepared by Surfactant-Free Miniemulsion Polymerization, *ACS Macro Lett.*, 2012, **1**(12), 1371.
- 130 P. Liu, W. Lu, W. J. Wang, B. G. Li and S. Zhu, Highly CO<sub>2</sub>/N<sub>2</sub>-switchable zwitterionic surfactant for pickering emulsions at ambient temperature, *Langmuir*, 2014, **30**(34), 10248.
- 131 L. Chen, R. Liu, X. Hao and Q. Yan, CO<sub>2</sub> - Cross-Linked Frustrated Lewis Networks as Gas-Regulated Dynamic Covalent Materials, *Angew. Chem., Int. Ed.*, 2019, **58**(1), 264.
- 132 G. C. Welch, R. R. San Juan, J. D. Masuda and D. W. Stephan, Reversible, Metal-Free Hydrogen Activation, *Science*, 2006, **314**, 1124–1126.
- 133 L. Chen, R. Liu and Q. Yan, Polymer Meets Frustrated Lewis Pair: Second-Generation CO<sub>2</sub> -Responsive Nanosystem for Sustainable CO<sub>2</sub> Conversion, *Angew. Chem., Int. Ed.*, 2018, **57**(30), 9336.
- 134 R. Liu, Y. Wang and Q. Yan, CO<sub>2</sub> - Strengthened Double-Cross-Linked Polymer Gels from Frustrated Lewis Pair Networks, *Macromol. Rapid Commun.*, 2021, **42**(6), e2000699.
- 135 Z. Fan and H. Xu, Recent Progress in the Biological Applications of Reactive Oxygen Species-Responsive Polymers, *Polym. Rev.*, 2020, **60**(1), 114.
- 136 P.-H. Hsu and A. Almutairi, Recent progress of redox-responsive polymeric nanomaterials for controlled release, *J. Mater. Chem. B*, 2021, **9**, 2179.
- 137 X. Zhang, L. Han, M. Liu, K. Wang, L. Tao, Q. Wan and Y. Wei, Recent progress and advances in redox-responsive polymers as controlled delivery nanoplateforms, *Mater. Chem. Front.*, 2017, **1**(5), 807.
- 138 F. Gao and Z. Xiong, Reactive Oxygen Species Responsive Polymers for Drug Delivery Systems, *Front. Chem.*, 2021, **9**, 649048.
- 139 J. K. Oh, Disassembly and tumor-targeting drug delivery of reduction-responsive degradable block copolymer nanoassemblies, *Polym. Chem.*, 2019, **10**(13), 1554.
- 140 H. Zhang, X. Kong, Y. Tang and W. Lin, Hydrogen Sulfide Triggered Charge-Reversal Micelles for Cancer-Targeted Drug Delivery and Imaging, *ACS Appl. Mater. Interfaces*, 2016, **8**(25), 16227.
- 141 Q. Yan and W. Sang, H<sub>2</sub>S gasotransmitter-responsive polymer vesicles, *Chem. Sci.*, 2016, **7**(3), 2100.
- 142 P.-H. Hsu, R. Kawasaki, K. Yamana, H. Isozaki, S. Kawamura, A. Ikeda and A. Almutairi, Hydrogen Sulfide-Responsive Self-Assembled Nanogel, *ACS Appl. Polym. Mater.*, 2020, **2**(9), 3756.
- 143 S. Chakraborty, R. Khamrui and S. Ghosh, Redox responsive activity regulation in exceptionally stable supramolecular assembly and co-assembly of a protein, *Chem. Sci.*, 2020, **12**(3), 1101.
- 144 P. Ju, J. Hu, F. Li, Y. Cao, L. Li, D. Shi, Y. Hao, M. Zhang, J. He and P. Ni, A biodegradable polyphosphoester-functionalized poly(disulfide) nanocarrier for reduction-triggered intracellular drug delivery, *J. Mater. Chem. B*, 2018, **6**(44), 7263.
- 145 X. Kuang, D. Chi, J. Li, C. Guo, Y. Yang, S. Zhou, C. Luo, H. Liu, Z. He and Y. Wang, Disulfide bond based cascade reduction-responsive Pt(IV) nanoassemblies for improved anti-tumor efficiency and biosafety, *Colloids Surf., B*, 2021, **203**, 111766.
- 146 Y. Zhao, C. Simon, M. Daoud Attieh, K. Haupt and A. Falcimaigne-Cordin, Reduction-responsive molecularly imprinted nanogels for drug delivery applications, *RSC Adv.*, 2020, **10**(10), 5978.
- 147 J. Shen, Q. Wang, J. Fang, W. Shen, D. Wu, G. Tang and J. Yang, Therapeutic polymeric nanomedicine: GSH-responsive release promotes drug release for cancer synergistic chemotherapy, *RSC Adv.*, 2019, **9**(64), 37232.
- 148 K. Bhattacharya, S. L. Banerjee, S. Das, S. Samanta, M. Mandal and N. K. Singha, REDOX Responsive Fluorescence Active Glycopolymer Based Nanogel: A Potential Material for Targeted Anticancer Drug Delivery, *ACS Appl. Bio Mater.*, 2019, **2**(6), 2587.
- 149 J. J. C. Lee, S. Sugiarto, P. J. Ong, X. Y. D. Soo, X. Ni, P. Luo, Y. Y. K. Hnin, J. S. Y. See, F. Wei and R. Zheng, Lignin-g-polycaprolactone as a form-stable phase change material for thermal energy storage application, *J. Energy Storage*, 2022, **56**, 106118.
- 150 L. Yu, M. Zhang, F.-S. Du and Z.-C. Li, ROS-responsive poly( $\epsilon$ -caprolactone) with pendent thioether and selenide motifs, *Polym. Chem.*, 2018, **9**(27), 3762.
- 151 S. Gao, T. Li, Y. Guo, C. Sun, B. Xianyu and H. Xu, Selenium-Containing Nanoparticles Combine the NK Cells Mediated Immunotherapy with Radiotherapy and Chemotherapy, *Adv. Mater.*, 2020, **32**(12), e1907568.
- 152 L. Zhang, C. Sun, Y. Tan and H. Xu, Selenium-sulfur-doped carbon dots with thioredoxin reductase activity, *CCS Chem.*, 2022, **4**, 2239–2248.
- 153 X. J. Loh, S. H. Goh and J. Li, Biodegradable thermogelling poly [(R)-3-hydroxybutyrate]-based block copolymers: Micellization, gelation, and cytotoxicity and cell culture studies, *J. Phys. Chem. B*, 2009, **113**(35), 11822.
- 154 Y. Wang, L. F. Hu, P. F. Cui, L. Y. Qi, L. Xing and H. L. Jiang, Pathologically Responsive Mitochondrial Gene Therapy in an Allotopic Expression-Independent Manner Cures Leber's Hereditary Optic Neuropathy, *Adv. Mater.*, 2021, **33**, 2103307.



- 155 L. Xu, M. Zhao, W. Gao, Y. Yang, J. Zhang, Y. Pu and B. He, Polymeric nanoparticles responsive to intracellular ROS for anticancer drug delivery, *Colloids Surf., B*, 2019, **181**, 252.
- 156 W. Zhang, X. Hu, Q. Shen and D. Xing, Mitochondria-specific drug release and reactive oxygen species burst induced by polyprodrug nanoreactors can enhance chemotherapy, *Nat. Commun.*, 2019, **10**(1), 1704.
- 157 J. Li, Z. Ding, Y. Li, J. Miao, W. Wang, K. Nundlall and S. Chen, Reactive oxygen species-sensitive thioketal-linked mesoporous silica nanoparticles as drug carrier for effective antibacterial activity, *Mater. Des.*, 2020, **195**, 109021.
- 158 E. A. Garcia, D. Pessoa and M. Herrera-Alonso, Oxidative instability of boronic acid-installed polycarbonate nanoparticles, *Soft Matter*, 2020, **16**(10), 2473.
- 159 E. Jager, V. Sincari, L. J. C. Albuquerque, A. Jager, J. Humajova, J. Kucka, J. Pankrac, P. Paral, T. Heizer and O. Janouskova, *et al.*, Reactive Oxygen Species (ROS)-Responsive Polymersomes with Site-Specific Chemotherapeutic Delivery into Tumors via Spacer Design Chemistry, *Biomacromolecules*, 2020, **21**(4), 1437.
- 160 Y. Tian, M. Lei, L. Yan and F. An, Diselenide-crosslinked zwitterionic nanogels with dual redox-labile properties for controlled drug release, *Polym. Chem.*, 2020, **11**(13), 2360.
- 161 L. Zhang, Y. Liu, K. Zhang, Y. Chen and X. Luo, Redox-responsive comparison of diselenide micelles with disulfide micelles, *Colloid Polym. Sci.*, 2019, **297**(2), 225.
- 162 B. Z. Hailemeskel, K. D. Addisu, A. Prasannan, S. L. Mekuria, C.-Y. Kao and H.-C. Tsai, Synthesis and characterization of diselenide linked poly(ethylene glycol) nanogel as multi-responsive drug carrier, *Appl. Surf. Sci.*, 2018, **449**, 15.
- 163 F. Xu, H. Li, Y. L. Luo and W. Tang, Redox-Responsive Self-Assembly Micelles from Poly(N-acryloylmorpholine-block-2-acryloyloxyethyl ferrocenecarboxylate) Amphiphilic Block Copolymers as Drug Release Carriers, *ACS Appl. Mater. Interfaces*, 2017, **9**(6), 5181.
- 164 A. Höcherl, E. Jäger, A. Jäger, M. Hrubý, R. Konefal, O. Janoušková, J. Spěváček, Y. Jiang, P. W. Schmidt and T. P. Lodge, *et al.*, One-pot synthesis of reactive oxygen species (ROS)-self-immolative polyoxalate prodrug nanoparticles for hormone dependent cancer therapy with minimized side effects, *Polym. Chem.*, 2017, **8**(13), 1999.
- 165 D. Bobo, K. J. Robinson, J. Islam, K. J. Thurecht and S. R. Corrie, Nanoparticle-Based Medicines: A Review of FDA-Approved Materials and Clinical Trials to Date, *Pharm. Res.*, 2016, **33**(10), 2373.
- 166 V. P. N. Nguyen, N. Kuo and X. J. Loh, New biocompatible thermogelling copolymers containing ethylene-butylene segments exhibiting very low gelation concentrations, *Soft Matter*, 2011, **7**(5), 2150.
- 167 R. Cheng, F. Meng, C. Deng, H.-A. Klok and Z. Zhong, Dual and multi-stimuli responsive polymeric nanoparticles for programmed site-specific drug delivery, *Biomaterials*, 2013, **34**(14), 3647.
- 168 M. Karimi, A. Ghasemi, P. Sahandi Zangabad, R. Rahighi, S. M. Moosavi Basri, H. Mirshekari, M. Amiri, Z. Shafaei Pishabad, A. Aslani and M. Bozorgomid, *et al.*, Smart micro/nanoparticles in stimulus-responsive drug/gene delivery systems, *Chem. Soc. Rev.*, 2016, **45**(5), 1457.
- 169 L. Gan, G. R. Deen, X. Loh and Y. Gan, New stimuli-responsive copolymers of N-acryloyl-N'-alkyl piperazine and methyl methacrylate and their hydrogels, *Polymer*, 2001, **42**(1), 65.
- 170 X. J. Loh, B. J. H. Yee and F. S. Chia, Sustained delivery of paclitaxel using thermogelling poly (PEG/PPG/PCL urethane) s for enhanced toxicity against cancer cells, *J. Biomed. Mater. Res., Part A*, 2012, **100**(10), 2686.
- 171 E. A. Appel, M. J. Rowland, X. J. Loh, R. M. Heywood, C. Watts and O. A. Scherman, Enhanced stability and activity of temozolomide in primary glioblastoma multiforme cells with cucurbit [n] uril, *Chem. Commun.*, 2012, **48**(79), 9843.
- 172 S. Dai, P. Ravi and K. C. Tam, pH-Responsive polymers: synthesis, properties and applications, *Soft Matter*, 2008, **4**(3), 435.
- 173 G. Kocak, C. Tuncer and V. Bütün, pH-Responsive polymers, *Polym. Chem.*, 2017, **8**(1), 144.
- 174 G. Springsteen and B. Wang, A detailed examination of boronic acid-diol complexation, *Tetrahedron*, 2002, **58**(26), 5291.
- 175 K. Kataoka, H. Miyazaki, M. Bunya, T. Okano and Y. Sakurai, Totally synthetic polymer gels responding to external glucose concentration: their preparation and application to on-off regulation of insulin release, *J. Am. Chem. Soc.*, 1998, **120**(48), 12694.
- 176 H. Peng, X. Ning, G. Wei, S. Wang, G. Dai and A. Ju, The preparations of novel cellulose/phenylboronic acid composite intelligent bio-hydrogel and its glucose, pH-responsive behaviors, *Carbohydr. Polym.*, 2018, **195**, 349.
- 177 D. Klemm, B. Heublein, H. P. Fink and A. Bohn, Cellulose: fascinating biopolymer and sustainable raw material, *Angew. Chem., Int. Ed.*, 2005, **44**(22), 3358.
- 178 S. Kitano, Y. Koyama, K. Kataoka, T. Okano and Y. Sakurai, A novel drug delivery system utilizing a glucose responsive polymer complex between poly (vinyl alcohol) and poly (N-vinyl-2-pyrrolidone) with a phenylboronic acid moiety, *J. Controlled Release*, 1992, **19**(1), 161.
- 179 Z. Zhang, T. Chao, S. Chen and S. Jiang, Superlow Fouling Sulfobetaine and Carboxybetaine Polymers on Glass Slides, *Langmuir*, 2006, **22**(24), 10072.
- 180 A. J. Keefe and S. Jiang, Poly(zwitterionic)protein conjugates offer increased stability without sacrificing binding affinity or bioactivity, *Nat. Chem.*, 2012, **4**(1), 59.
- 181 G. Cheng, G. Li, H. Xue, S. Chen, J. D. Bryers and S. Jiang, Zwitterionic carboxybetaine polymer surfaces and their resistance to long-term biofilm formation, *Biomaterials*, 2009, **30**(28), 5234.
- 182 G. Cheng, H. Xue, Z. Zhang, S. Chen and S. Jiang, A Switchable Biocompatible Polymer Surface with Self-Sterilizing and Nonfouling Capabilities, *Angew. Chem., Int. Ed.*, 2008, **47**(46), 8831.
- 183 L. R. Carr, H. Xue and S. Jiang, Functionalizable and nonfouling zwitterionic carboxybetaine hydrogels with a



- carboxybetaine dimethacrylate crosslinker, *Biomaterials*, 2011, **32**(4), 961.
- 184 Z. Zhang, T. Chao and S. Jiang, Physical, Chemical, and Chemical-Physical Double Network of Zwitterionic Hydrogels, *J. Phys. Chem. B*, 2008, **112**(17), 5327.
  - 185 B. Cao, L. Li, Q. Tang and G. Cheng, The impact of structure on elasticity, switchability, stability and functionality of an all-in-one carboxybetaine elastomer, *Biomaterials*, 2013, **34**(31), 7592.
  - 186 A. S. Hoffman, "Intelligent" Polymers in Medicine and Biotechnology, *Artif. Organs*, 1995, **19**(5), 458.
  - 187 M. A. Ward and T. K. Georgiou, Thermoresponsive Polymers for Biomedical Applications, *Polymers*, 2011, **3**(3), 1215–1242.
  - 188 A. K. Bajpai, S. K. Shukla, S. Bhanu and S. Kankane, Responsive polymers in controlled drug delivery, *Prog. Polym. Sci.*, 2008, **33**(11), 1088.
  - 189 T. A. Yemata, A. K. K. Kyaw, Y. Zheng, X. Z. Wang, Q. Zhu, W. S. Chin and J. W. Xu, Enhanced thermoelectric performance of poly(3,4-ethylenedioxythiophene):poly(4-styrenesulfonate) (PEDOT:PSS) with long-term humidity stability via sequential treatment with trifluoroacetic acid, *Polym. Int.*, 2020, **69**(1), 84.
  - 190 H. Zhou, M. H. Chua, Q. Zhu and J. W. Xu, High-performance PEDOT:PSS-based thermoelectric composites, *Compos. Commun.*, 2021, **27**, 100877.
  - 191 Z. M. Png, X. Y. D. Soo, M. H. Chua, P. J. Ong, A. Suwardi, C. K. I. Tan, J. W. Xu and Q. Zhu, Strategies to reduce the flammability of organic phase change Materials: A review, *Sol. Energy*, 2022, **231**, 115.
  - 192 Z. M. Png, X. Y. D. Soo, M. H. Chua, P. J. Ong, J. W. Xu and Q. Zhu, Triazine derivatives as organic phase change materials with inherently low flammability, *J. Mater. Chem. A*, 2022, **10**(7), 3633.
  - 193 K. W. Shah, P. J. Ong, M. H. Chua, S. H. G. Toh, J. J. C. Lee, X. Y. D. Soo, Z. M. Png, R. Ji, J. Xu and Q. Zhu, Application of Phase Change Materials in Building Components and the use of Nanotechnology for its improvement, *Energy Build.*, 2022, 112018.
  - 194 I. Tan, F. Roohi and M.-M. Titirici, Thermoresponsive polymers in liquid chromatography, *Anal. Methods*, 2012, **4**(1), 34.
  - 195 P. Maharjan, B. W. Woonton, L. E. Bennett, G. W. Smithers, K. DeSilva and M. T. W. Hearn, Novel chromatographic separation — The potential of smart polymers, *Innovative Food Sci. Emerging Technol.*, 2008, **9**(2), 232.
  - 196 Q. Zhu, M. H. Chua, P. J. Ong, J. J. Cheng Lee, K. Le Osmund Chin, S. Wang, D. Kai, R. Ji, J. Kong and Z. Dong, *et al.*, Recent advances in nanotechnology-based functional coatings for the built environment, *Mater. Today Adv.*, 2022, **15**, 100270.
  - 197 X. Y. D. Soo, Z. M. Png, M. H. Chua, J. C. C. Yeo, P. J. Ong, S. Wang, X. Wang, A. Suwardi, J. Cao and Y. Chen, A highly flexible form-stable silicone-octadecane PCM composite for heat harvesting, *Mater. Today Adv.*, 2022, **14**, 100227.
  - 198 M. Sponchioni, U. Capasso Palmiero and D. Moscatelli, Thermo-responsive polymers: Applications of smart materials in drug delivery and tissue engineering, *Mater. Sci. Eng., C*, 2019, **102**, 589.
  - 199 J. Liu, L. Jiang, S. He, J. Zhang and W. Shao, Recent progress in PNIPAM-based multi-responsive actuators: A mini-review, *Chem. Eng. J.*, 2022, **433**, 133496.
  - 200 Y.-L. Liu and T.-W. Chuo, Self-healing polymers based on thermally reversible Diels-Alder chemistry, *Polym. Chem.*, 2013, **4**(7), 2194.
  - 201 C. Zeng, H. Seino, J. Ren, K. Hatanaka and N. Yoshie, Self-healing bio-based furan polymers cross-linked with various bis-maleimides, *Polymer*, 2013, **54**(20), 5351.
  - 202 C. M. Nimmo, S. C. Owen and M. S. Shoichet, Diels-Alder Click Cross-Linked Hyaluronic Acid Hydrogels for Tissue Engineering, *Biomacromolecules*, 2011, **12**(3), 824.
  - 203 Y. N. Yuksekdog, T. N. Gevrek and A. Sanyal, Diels-Alder "Clickable" Polymer Brushes: A Versatile Catalyst-Free Conjugation Platform, *ACS Macro Lett.*, 2017, **6**(4), 415.
  - 204 O. Roling, K. De Bruycker, B. Vonhoren, L. Stricker, M. Korsgen, H. F. Arlinghaus, B. J. Ravoo and F. E. Du Prez, Rewritable Polymer Brush Micropatterns Grafted by Triazolinone Click Chemistry, *Angew. Chem., Int. Ed.*, 2015, **54**(44), 13126.
  - 205 X. Feng, J. Sun, M. Ouyang, F. Wang, X. He, L. Lu and H. Peng, Characterization of penetration induced thermal runaway propagation process within a large format lithium ion battery module, *J. Power Sources*, 2015, **275**, 261.
  - 206 B. Dunn, H. Kamath and J.-M. Tarascon, Electrical Energy Storage for the Grid: A Battery of Choices, *Science*, 2011, **334**(6058), 928.
  - 207 N.-S. Choi, Z. Chen, S. A. Freunberger, X. Ji, Y.-K. Sun, K. Amine, G. Yushin, L. F. Nazar, J. Cho and P. G. Bruce, Challenges Facing Lithium Batteries and Electrical Double-Layer Capacitors, *Angew. Chem., Int. Ed.*, 2012, **51**(40), 9994.
  - 208 Y. Tang, J. Deng, W. Li, O. I. Malyi, Y. Zhang, X. Zhou, S. Pan, J. Wei, Y. Cai and Z. Chen, *et al.*, Water-Soluble Sericin Protein Enabling Stable Solid-Electrolyte Interphase for Fast Charging High Voltage Battery Electrode, *Adv. Mater.*, 2017, **29**(33), 1701828.
  - 209 Y. Shi, C. Lee, X. Tan, L. Yang, Q. Zhu, X. Loh, J. Xu and Q. Yan, Atomic-Level Metal Electrodeposition: Synthetic Strategies, Applications, and Catalytic Mechanism in Electrochemical Energy Conversion, *Small Struct.*, 2022, **3**(3), 2100185.
  - 210 B.-E. Jia, A. Q. Thang, C. Yan, C. Liu, C. Lv, Q. Zhu, J. Xu, J. Chen, H. Pan and Q. Yan, Rechargeable Aqueous Aluminum-Ion Battery: Progress and Outlook, *Small*, 2022, 2107773.
  - 211 V. P. Bui, H. Z. Liu, Y. Y. Low, T. Tang, Q. Zhu, K. W. Shah, E. Shidoji, Y. M. Lim and W. S. Koh, Evaluation of building glass performance metrics for the tropical climate, *Energy Build.*, 2017, **157**, 195.
  - 212 S.-L. Qiao, M. Mamuti, H.-W. An and H. Wang, Thermoresponsive Polymer Assemblies: From Molecular



- Design to Theranostics Application, *Prog. Polym. Sci.*, 2022, **131**, 101578.
- 213 S. Bharadwaj, B.-J. Niebuur, K. Nothdurft, W. Richtering, N. F. A. van der Vegt and C. M. Papadakis, Cononsolvency of thermoresponsive polymers: where we are now and where we are going, *Soft Matter*, 2022, **18**(15), 2884.
  - 214 R. Hoogenboom and H. Schlaad, Thermoresponsive poly(2-oxazoline)s, polypeptoids, and polypeptides, *Polym. Chem.*, 2017, **8**(1), 24.
  - 215 H. Yang, Z. Liu, B. K. Chandran, J. Deng, J. Yu, D. Qi, W. Li, Y. Tang, C. Zhang and X. Chen, Self-Protection of Electrochemical Storage Devices via a Thermal Reversible Sol–Gel Transition, *Adv. Mater.*, 2015, **27**(37), 5593.
  - 216 T. Tang, A. K. K. Kyaw, Q. Zhu and J. W. Xu, Water-dispersible conducting polyazulene and its application in thermoelectrics, *Chem. Commun.*, 2020, **56**(65), 9388.
  - 217 Q. Zhu, E. Yildirim, X. Z. Wang, A. K. K. Kyaw, T. Tang, X. Y. D. Soo, Z. M. Wong, G. Wu, S. W. Yang and J. W. Xu, Effect of substituents in sulfoxides on the enhancement of thermoelectric properties of PEDOT:PSS: experimental and modelling evidence, *Mol. Syst. Des. Eng.*, 2020, **5**(5), 976.
  - 218 L. Chen, C. Zhao, J. Huang, J. Zhou and M. Liu, Enormous-stiffness-changing polymer networks by glass transition mediated microphase separation, *Nat. Commun.*, 2022, **13**(1), 6821.
  - 219 H. Guo, N. Sanson, D. Hourdet and A. Marcellan, Thermoresponsive Toughening with Crack Bifurcation in Phase-Separated Hydrogels under Isochoric Conditions, *Adv. Mater.*, 2016, **28**(28), 5857.
  - 220 Q. L. Zhu, C. Du, Y. Dai, M. Daab, M. Matejdes, J. Breu, W. Hong, Q. Zheng and Z. L. Wu, Light-steered locomotion of muscle-like hydrogel by self-coordinated shape change and friction modulation, *Nat. Commun.*, 2020, **11**(1), 5166.
  - 221 P. Schattling, F. D. Jochum and P. Theato, Multi-stimuli responsive polymers – the all-in-one talents, *Polym. Chem.*, 2014, **5**(1), 25.
  - 222 A. Abdollahi, H. Roghani-Mamaqani, B. Razavi and M. Salami-Kalajahi, The light-controlling of temperature-responsivity in stimuli-responsive polymers, *Polym. Chem.*, 2019, **10**(42), 5686.
  - 223 Q. M. Zhang, W. Wang, Y.-Q. Su, E. J. M. Hensen and M. J. Serpe, Biological Imaging and Sensing with Multiresponsive Microgels, *Chem. Mater.*, 2016, **28**(1), 259.
  - 224 P. Q. Nhien, W.-L. Chou, T. T. K. Cuc, T. M. Khang, C.-H. Wu, N. Thirumalaivasan, B. T. B. Hue, J. I. Wu, S.-P. Wu and H.-C. Lin, Multi-Stimuli Responsive FRET Processes of Bifluorophoric AIEgens in an Amphiphilic Copolymer and Its Application to Cyanide Detection in Aqueous Media, *ACS Appl. Mater. Interfaces*, 2020, **12**(9), 10959.
  - 225 X.-M. Jiang, X.-J. Huang, S.-S. Song, X.-Q. Ma, Y.-M. Zhang, H. Yao, T.-B. Wei and Q. Lin, Tri-pillar[5]arene-based multi-stimuli-responsive supramolecular polymers for fluorescence detection and separation of Hg<sup>2+</sup>, *Polym. Chem.*, 2018, **9**(37), 4625.
  - 226 X. M. Sim, C. G. Wang, X. Liu and A. Goto, Multistimuli Responsive Reversible Cross-Linking-Decross-Linking of Concentrated Polymer Brushes, *ACS Appl. Mater. Interfaces*, 2020, **12**(25), 28711.
  - 227 E. Yildirim, Q. Zhu, G. Wu, T. L. Tan, J. W. Xu and S. W. Yang, Self-Organization of PEDOT:PSS Induced by Green and Water-Soluble Organic Molecules, *J. Phys. Chem. C*, 2019, **123**(15), 9745.
  - 228 M. H. Chua, K. L. O. Chin, S. J. Ang, X. Y. D. Soo, Z. M. Png, Q. Zhu and J. Xu, Aggregation Induced Emission (AIE)-Active Poly (acrylates) for Electrofluorochromic Detection of Nitroaromatic Compounds, *ChemPhotoChem*, 2022, **6**(11), e202200168.
  - 229 P. J. Ong, Z. M. Png, X. Y. D. Soo, X. Wang, A. Suwardi, M. H. Chua, J. W. Xu and Q. Zhu, Surface modification of microencapsulated phase change materials with nanostructures for enhancement of their thermal conductivity, *Mater. Chem. Phys.*, 2022, **277**, 125438.
  - 230 J. Hatai, C. Hirschhäuser, J. Niemeyer and C. Schmuck, Multi-Stimuli-Responsive Supramolecular Polymers Based on Noncovalent and Dynamic Covalent Bonds, *ACS Appl. Mater. Interfaces*, 2020, **12**(2), 2107.
  - 231 X. Y. D. Soo, Z. M. Png, X. Z. Wang, M. H. Chua, P. J. Ong, S. X. Wang, Z. B. Li, D. Z. Chi, J. W. Xu and X. J. Loh, *et al.*, Rapid UV-Curable Form-Stable Polyethylene-Glycol-Based Phase Change Material, *ACS Appl. Polym. Mater.*, 2022, **4**(4), 2747.
  - 232 J. Xiong, K. Wang, Z. Yao, B. Zou, J. Xu and X. H. Bu, Multi-Stimuli-Responsive Fluorescence Switching from a Pyridine-Functionalized Tetraphenylethene AIEgen, *ACS Appl. Mater. Interfaces*, 2018, **10**(6), 5819.
  - 233 T. Yamamoto, S. Yagyu and Y. Tezuka, Light- and Heat-Triggered Reversible Linear-Cyclic Topological Conversion of Telechelic Polymers with Anthryl End Groups, *J. Am. Chem. Soc.*, 2016, **138**(11), 3904.
  - 234 B. T. Gebeyehu, S.-Y. Huang, A.-W. Lee, J.-K. Chen, J.-Y. Lai, D.-J. Lee and C.-C. Cheng, Dual Stimuli-Responsive Nucleobase-Functionalized Polymeric Systems as Efficient Tools for Manipulating Micellar Self-Assembly Behavior, *Macromolecules*, 2018, **51**(3), 1189.
  - 235 X. Jiang, R. Li, C. Feng, G. Lu and X. Huang, Triple-stimuli-responsive ferrocene-containing homopolymers by RAFT polymerization, *Polym. Chem.*, 2017, **8**(18), 2773.

